Chapter 6
Spectral and Pseudospectral Methods of Solution of the Fokker-Planck and Schrödinger Equations

Abstract Spectral and pseudospectral methods based on classical and nonclassical polynomial basis sets are used for the solution of the Fokker-Planck and Schrödinger equations. Fokker-Planck equations describe many different processes in chemistry and physics, and their study has attracted considerable attention by researchers in many different fields including astrophysics, finance and biology. Pseudospectral methods of solution of the Fokker-Planck equation are presented for several systems such as the Ornstein-Uhlenbeck model for Brownian motion, electron thermalization in atomic moderators, charged particle relaxation in plasmas and models for chemical reactions based on Kramers' equation. A Fokker-Planck equation can be transformed to a Schrödinger equation with a potential that belongs to the class of potentials in supersymmetric quantum mechanics and expressed in terms of the superpotential. The quantum harmonic oscillator and the Morse potential belong to this class of Schrödinger equations. The pseudospectral methods developed for the solution of the Fokker-Planck equation based on nonclassical basis sets are also applied to a large number of the Schrödinger equations including the Henon-Heles potential. Fundamental aspects of different pseudospectral methods such as the Discrete Variable Representation, the Quadrature Discretization method, the Lagrange mesh method and Fourier grid methods are discussed.

6.1 The Fokker-Planck Equation in Chemistry, Physics, Astrophysics and Other Fields

The Fokker-Planck equation is a partial differential equation for a probability density function, $P(\mathbf{v}, \mathbf{r}, t)$, analogous to a distribution function of kinetic theory discussed in Chap. 5. The linear integral Boltzmann equation for a binary gas of test particles of mass m dilutely dispersed in bath particles of mass M at T_b can be approximated by Fokker-Planck equations in the disparate mass limits ($\gamma = M/m \to 0$ or $\gamma \to \infty$) as a consequence of the small energy transfers in particle collisions (Andersen and Shuler 1964). A similar approximation is used in plasma physics for which charged particle Coulomb collisions involve predominantly large impact parameter grazing collisions (Rosenbluth et al. 1957; Spitzer 1962; Mitchner and Kruger 1973; Hinton 1983). These approximations are examples of a large class of Master equations for

B. Shizgal, *Spectral Methods in Chemistry and Physics*, Scientific Computation,
DOI 10.1007/978-94-017-9454-1_6

which a Fokker-Planck equation can be derived with the Kramers-Moyal expansion (Gillespie 1980; Knessl et al. 1984; Kuczka et al. 1995; Risken 1996; Frank 2007; van Kampen 2007).

An alternate derivation of the Fokker-Planck equation is based on stochastic differential equations such as the Langevin equation to model "Brownian" motion as discussed in the next section and in greater detail in several references (Chandrasekhar 1949; Risken 1996; Gardiner 2003; van Kampen 2007; Reif 2008; Paul and Baschnagel 2013). For most of the applications in this chapter, we will consider a Fokker-Planck equation in two variables and a probability density function, $P(x, t)$, where t is the time and x is an independent variable that represents the reduced speed or energy of a particle, the particle position or some other independent variable.

The equation is named after Adrian Fokker[1] and Max Planck.[2] Fokker (1914) studied the relationship between the fluctuations of the rotational motion of dipoles in an electric field and the steady state probability density function. Planck (1917) developed the time dependent equation and provided the relationship between the drift and diffusion coefficients and the random fluctuations inherent in the system.

Fokker-Planck equations are used to model numerous systems in physics, astrophysics, chemistry, biology, engineering, finance and other research fields. Fokker-Planck equations have also been used to model processes in space science, notably the solar and polar wind expansions (Lie-Svendsen and Rees 1996; Pierrard and Lemaire 1998; Marsch 2006; Echim et al. 2011). A large number of chemically reactive systems can be modelled with a Fokker-Planck equation proposed by Kramers (1940). Many aspects of turbulence are modelled as stochastic processes leading to a Fokker-Planck equation (Pope 2000). The applications of the Fokker-Planck equation to stellar dynamics and astrophysics (Chandrasekhar 1942; Spitzer 1998; Chavanis 2006; Binney and Tremaine 2008) overlap applications to plasma physics (Rosenbluth et al. 1957; Spitzer 1962; Boyd and Sanderson 2003). The set of coupled rate equations for the growth of a cluster in nucleation theory is often modelled with a Fokker-Planck equation (Shizgal and Barrett 1989; Demeio and Shizgal 1993a). The Black-Scholes model in mathematical finance (Black and Scholes 1973; Paul and Baschnagel 2013) is based on a Fokker-Planck equation. These are just a few examples of the many different Fokker-Planck equations that arise in diverse applications. Additional discussion of these topics can be found in several textbooks (Risken 1996; Gardiner 2003; Reif 2008) and review papers (Chandrasekhar 1949; Lightman and Shapiro 1978).

---

[1] Adrian Fokker (1887–1972) was a Dutch physicist who made contributions to relativity and statistical mechanics in collaboration with Albert Einstein. The Fokker-Planck equation used to model numerous processes in physics, astrophysics, chemistry, finance and biology bears his name. He also made numerous contributions to music theory.

[2] Max Planck (1858–1947) was a German physicist and the 1918 Nobel laureate for his contributions to the explanation of the photoelectric effect, energy quantization and the introduction of the Planck constant. The basis for this work was his doctoral work on thermodynamics as related to black body radiation at equilibrium. Planck and Fokker independently derived the Fokker-Planck equation of statistical physics.

In Chap. 5, we expressed the solutions of the linearized and linear Boltzmann equations in terms of the eigenvalues of the collision operators involved. For the linearized collision operator and the linear collision operator with unit mass ratio ($\gamma = 1$), the integral operator can be transformed to a Schrödinger equation (Kuščer and Williams 1967; Bobylev and Mossberg 2008). The Fokker-Planck equations discussed in the sections that follow can be transformed to Schrödinger equations with well defined potential functions (Risken 1996). The potentials belong to the class of Schrödinger equations in supersymmetric quantum mechanics (Bernstein and Brown 1984; Comtet et al. 1985; Dutt et al. 1988; Cooper et al. 1995).

6.1.1 From the Langevin Equation to the Fokker-Planck Equation; Brownian Motion

We begin the discussion with the classic treatment of Brownian motion. We consider a subsystem of particles of mass m that interact solely with the particles of a background medium at equilibrium at temperature T_b. The origin of this approach is the work of the botanist Robert Brown[3] who observed the random movement of a pollen grain in a fluid at some temperature T_b. The movement of the so-called "Brownian" particle is random owing to the multitude of collisions of the molecules of the background fluid with the grain. Thus the scalar force, $F(t)$, on the Brownian particle is random in time. However, there is also a steady component that corresponds to the friction involved in the steady movement of the Brownian particle through the fluid. Thus we write $F(t) = F_s(t) + F_r(t)$ where $F_s(t)$ is the steady component related to the viscosity of the fluid and $F_r(t)$ is a largely unknown random or "stochastic" force. The steady component of the force is $F_s(t) = -\alpha v(t)$ where v is the particle velocity in one dimension and α is the friction coefficient that slows the particle as it moves through the fluid. We write the "stochastic" differential equation of motion for the Brownian particle as Newton's law with a random force, that is,

$$m\frac{dv}{dt} = -\alpha v(t) + F_r(t). \tag{6.1}$$

Equation (6.1) is known as the Langevin[4] equation for Brownian motion that was treated previously by Einstein (1906). The main difficulty with Eq. (6.1) is that the detailed time variation of $F_r(t)$ is largely unknown. What is remarkable with this approach is that the friction coefficient α in Eq. (6.1) is related to the properties of

[3] Robert Brown (1773–1858) was a Scottish botanist who made important contributions to botany and statistical physics from his use of a microscope to observe the random motion of pollen grains which was later referred to as Brownian motion.

[4] Paul Langevin (1872–1946) was a French physicist and doctoral student with J.J. Thompson at the Cavendish Laboratory and Pierre Curie in Paris. He worked extensively on paramagnetism and diamagnetism as well as in kinetic theory and theory of Brownian motion following on Einstein's work.

$F_r(t)$ (Reif 2008). Alternative methods are based on computer simulations that follow the time history of the particle positions and velocities (Gunther and Weaver 1978; Gillespie 1996). Monte Carlo simulations have become common in statistical physics and chemistry for the study of multidimensional complex systems in equilibrium and nonequilibrium situations (Bird 1994; Landau and Binder 2009).

An alternative approach to computer simulations is one based on the probability density of the random variable leading to a deterministic Fokker-Planck equation. The stochastic force, $F_r(t)$, is assumed to satisfy two important relations, (1) that the time (or "ensemble") average is zero and (2) the correlation in time has a definite strength, that is

$$\begin{aligned} \overline{F_r(t)} &= 0, \\ \overline{F_r(t)F_r(t')} &= 2\alpha k_B T_b \delta(t-t'), \end{aligned} \tag{6.2}$$

where k_B is the Boltzmann constant and T_b is the temperature of the background. The overbars indicate time or ensemble averages; see Sect. 15.5 in Reif (2008). In addition to the textbooks referenced earlier, excellent discussions of the historical development of stochastic processes are available (Uhlenbeck and Ornstein 1930; Hänggi et al. 1990; Risken 1996; Abbott 2001; Gardiner 2003; van Kampen 2007; Dunkel and Hänggi 2009; Paul and Baschnagel 2013).

Brownian motion and other stochastic processes are modelled with a probability density, $P(v,t)$, corresponding to the values of $v(t)$ sampled in a sufficiently long sequences of realizations of $v(t)$. Thus $P(v,t)$ is similar to the velocity distribution function $f(v,t)$ in kinetic theory in Chap. 5. It has been shown (Uhlenbeck and Ornstein 1930; Chandrasekhar 1949; Reif 2008) that the Fokker-Planck equation for the probability density (equivalently the velocity distribution) of the Brownian particle is given by the Ornstein–Uhlenbeck equation,

$$\frac{\partial P(v,t)}{\partial t} = \nu \frac{\partial}{\partial v}\left[vP(v,t) + \frac{k_B T_b}{m}\frac{\partial P(v,t)}{\partial v}\right], \qquad v \in (-\infty, \infty), \tag{6.3}$$

where the drift and diffusion coefficients, defined in what follows are νv and $\nu k_B T_b/m$, respectively, and $\nu = \alpha/m$ is a collision frequency.

A stochastic process which includes multiplicative as well as additive noise (Chandrasekhar 1949; Lax 1966; Brey et al. 1987; Gitterman 1999; Biró and Jakovác 2005) yields a Fokker-Planck equation with a velocity dependent diffusion coefficient. For this more general stochastic process we have the Langevin equation of the form

$$\frac{dv}{dt} = f(v) + g(v)\xi(t) + \eta(t), \tag{6.4}$$

with $f(v)$ and $g(v)$ are known but unspecified functions. The additive and multiplicative Gaussian random variables, $\eta(t)$ and $\xi(t)$ have zero mean,

$$\overline{\eta(t)} = 0 \qquad \text{and} \qquad \overline{\xi(t)} = 0, \tag{6.5}$$

and correlations given by,

$$\overline{\eta(t)\eta(t')} = 2D\delta(t-t') \qquad \overline{\xi(t)\xi(t')} = 2\beta\delta(t-t'). \tag{6.6}$$

The Fokker-Planck equation for $P(v,t)$ corresponding to this stochastic process is of the form

$$\frac{\partial P(v,t)}{\partial t} = \frac{\partial}{\partial v}\left[A(v)P(v,t) + \frac{\partial B(v)P(v,t)}{\partial v}\right], \tag{6.7}$$

where $A(v)$ and $B(v)$ are the time-independent drift and diffusion coefficients, respectively, given by,

$$\begin{aligned} A(v) &= f(v) + \beta g(v)\frac{dg(v)}{dv}, \\ B(v) &= D + \beta g^2(v). \end{aligned} \tag{6.8}$$

where $f(v)$, $g(v)$, D and β are defined by Eqs. (6.4) and (6.6). Additional details of this derivation are in the references cited.

Given some initial condition, $P(v,0)$, the distribution $P(v,t)$ varies in time as deduced with Eq. (6.7) and attains a steady distribution at infinite time for which $\partial P(v,t)/\partial t = 0$ and denoted by $P_0(v)$. For most of the applications to be discussed, the reduced speed, $x = \sqrt{mv^2/2k_BT_b}$ is used and generally $x \in (-\infty, \infty)$. From Eq. (6.7), this equilibrium probability density is

$$P_0(v) = \frac{1}{B(v)}\exp\left(-\int_{-\infty}^{v}\frac{A(v')}{B(v')}dv'\right), \tag{6.9}$$

and is not in general a Maxwellian.

6.1.2 *Spectral Solution of the Ornstein-Uhlenbeck Fokker-Planck Equation*

The equilibrium distribution analogous to Eq. (6.9) for the Brownian motion Fokker-Planck equation, Eq. (6.3), is defined by

$$\left[vP_0(v) + \frac{k_BT_b}{m}\frac{\partial P_0(v)}{\partial v}\right] = 0,$$

and the steady state distribution of Eq. (6.3) is a Maxwellian,

$$P_0(v) = \sqrt{\frac{m}{2\pi k_BT_b}}e^{-mv^2/2k_BT_b}. \tag{6.10}$$

normalized such that

$$\int_{-\infty}^{\infty} P_0(v)dv = 1.$$

We consider an initial condition whereby all the particles start with a specific speed v_0 that is

$$P(v, 0) = \delta(v - v_0). \tag{6.11}$$

The solution of this Fokker-Planck equation is readily determined with the transformation to a strict diffusion equation where the diffusion coefficient is $D = \mu k_B T_b/m$. We redefine the variables so as to remove the term in $\partial P/\partial v$ in Eq. (6.3) in a manner analogous to the transformation of the Fokker-Planck equation to a Schrödinger equation discussed in Sect. 6.3.2. We make the change of variable $u = ve^{\nu t}$ and set $P(v, t) = e^{\nu t} Q(u, t)$. With these substitutions, the Fokker-Planck equation can be written in terms of $Q(u, t)$, that is

$$\frac{\partial Q(u, t)}{\partial t} = De^{2\nu t} \frac{\partial^2 Q(u, t)}{\partial u^2}. \tag{6.12}$$

With the change in the time variable to $\tau = (e^{2\nu t} - 1)/\nu$, we transform the Fokker-Planck equation to the diffusion equation, that is

$$\frac{\partial Q(u, \tau)}{\partial \tau} = D \frac{\partial^2 Q(u, \tau)}{\partial u^2}. \tag{6.13}$$

This equation could be considered as a Fokker-Planck equation without drift which is referred to as a Weiner process (Risken 1996; Gillespie 1996).

We have solved the diffusion equation with a Fourier transform method in Chap. 4, Sect. 4.6.5 and the solution of Eq. (6.13) is

$$Q(u, \tau) = \frac{1}{\sqrt{4\pi D\tau}} e^{-(u-u_0)^2/4D\tau}. \tag{6.14}$$

With this result, the solution to the Ornstein–Uhlenbeck, Eq. (6.13), in the reduced speed, $x = \sqrt{mv^2/2k_B T_b}$, is

$$P(x, t) = \left[\frac{1}{\pi(1 - e^{-2\nu t})}\right]^{1/2} \exp\left[-\frac{(x - x_0 e^{-\nu t})^2}{(1 - e^{-2\nu t})}\right]. \tag{6.15}$$

A spectral solution of Eq. (6.3) can be expressed in Hermite polynomials in x by substituting $P(x, t) = e^{-x^2} g(x, t)$ into Eq. (6.3) written in terms of x. The result is the differential equation

$$\frac{\partial g(x,t)}{\partial t} = \nu e^{x^2} \frac{\partial}{\partial x}\left[e^{-x^2} \frac{\partial g(x,t)}{\partial x} \right],$$
$$= \nu \left[-2x \frac{\partial g}{\partial x} + \frac{\partial^2 g}{\partial x^2} \right]. \tag{6.16}$$

With the expansion in Hermite polynomials

$$g(x,t) = \sum_{n=0}^{\infty} c_n(t) H_n(x), \tag{6.17}$$

Eq. (6.16) can be written as

$$\sum_{n=0}^{\infty} H_n(x) \frac{dc_n}{dt} = \nu \sum_{n=0}^{\infty} c_n(t) \left[-2x H_n'(x) + H_n''(x) \right]. \tag{6.18}$$

With the relation $-2x H_n' + H_n'' = -2n H_n$, the time dependence of the coefficients is given by

$$\frac{dc_n(t)}{dt} = -2n\nu c_n(t). \tag{6.19}$$

With the expansion of the initial condition in the Hermite polynomials, the spectral solution is given by

$$P(x,t) = e^{-x^2} \sum_{n=0}^{\infty} \frac{1}{2^n n! \sqrt{\pi}} H_n(x_0) H_n(x) e^{-2n\nu t}. \tag{6.20}$$

Equations (6.15) and (6.20) can be used to study the rate of convergence of the expansion in Hermite polynomials (Wei et al. 1997). A study of the use of orthogonal expansions for the solution of Fokker-Planck equations was reported by Cukier et al. (1973). An eigenfunction analysis of the three-dimensional Ornstein-Uhlenbeck process with expansions in associated Laguerre polynomials and spherical harmonics was reported recently by Wilkinson and Pumir (2011).

6.1.3 *Rayleigh and Lorentz Fokker-Planck Equations from the Boltzmann Equation; The Kramers-Moyal Expansion*

In Chap. 3 (Eq. (3.49)) and Chap. 5 (Eq. (5.110)), we discussed the Wigner-Wilkins kernel (Wigner 1943; Wigner and Wilkins 1944; Hoare and Kaplinsky 1970; Hoare 1971) for the linear Boltzmann integral operator for a hard sphere cross section. This

Boltzmann equation models the relaxation of an ensemble of test particles of mass m dilutely dispersed in a second gas of particles of mass M which is taken to be at equilibrium with a Maxwellian distribution at temperature T_b.

The hard sphere collision operator in the Boltzmann equation for a binary gas mixture can be approximated by Fokker-Planck equations in the mass ratio limits $\gamma = M/m \to \infty$ (the "Lorentz" limit) or $\gamma \to 0$ (the "Rayleigh" limit), respectively as shown by Andersen and Shuler (1964). The derivation is based on the expansion of the kernel in the small energy transfer on collision for these disparate mass ratios. The integral operator is expanded up to second order in the small energy transfer and this transformation of the integral equation to a Fokker-Planck equation is known as the Kramers-Moyal expansion (Risken 1996; Knessl et al. 1984; van Kampen 2007).

For the disparate mass ratio limit, $\gamma \to 0$, the Rayleigh Fokker-Planck equation is

$$\frac{\partial P(y,t)}{\partial t} = \frac{\partial}{\partial y}\left[(y-3)P(y,t) + \frac{\partial}{\partial y}[yP(y,t)]\right], \tag{6.21}$$

where $y = mv^2/k_BT_b$ is the reduced energy and t is in units of τ given by $1/\tau = K_R = \frac{16}{3}Mmn_b\sigma_0\sqrt{2k_BT_b/\pi M}$. For $\gamma \to \infty$, the Lorentz Fokker-Planck equation is

$$\frac{\partial P(x,t)}{\partial t} = \frac{1}{4}\frac{\partial}{\partial x}\left[(2x^2-3)P(x,t) + \frac{\partial}{\partial x}[xP(x,t)]\right], \tag{6.22}$$

where $x = \sqrt{mv^2/2k_BT_b}$ is the reduced speed and $1/\tau = K_L = 2\sqrt{m/M}n_b\sigma_0$ $\sqrt{2k_BT_b/M}$. The hard sphere cross section is denoted by σ_0 and n_b is the density of the background gas. A spectral solution of the Rayleigh Fokker-Planck equation in terms of Hermite polynomials is described in the next section. There is no known spectral solution of the Lorentz Fokker-Planck equation in terms of classical polynomials.

6.1.4 Spectral Solution of the Rayleigh Fokker-Planck Equation

We consider an analysis similar to the one in Sect. 6.1.2. If we set $P(y,t) = P_0(y)g(y,t)$ where $P_0(y) = (2/\sqrt{\pi})\sqrt{y}e^{-y}$ in dimensionless units and we get the differential equation

$$\frac{\partial g(y,t)}{\partial t} = \frac{1}{P_0(y)}\frac{\partial}{\partial y}\left[yP_0(y)\frac{\partial g(y,t)}{\partial y}\right]. \tag{6.23}$$

The evaluation of the partial derivative in the square bracket gives

$$\frac{\partial g(y,t)}{\partial t} = y\frac{\partial^2 g(y,t)}{\partial y^2} + (\frac{3}{2}-y)\frac{\partial g(y,t)}{\partial y}. \tag{6.24}$$

The differential operator on the right hand side is related to the eigenvalue problem for the associated Laguerre polynomials, $L_n^{(\frac{1}{2})}(y)$, that is

$$y\frac{d^2L_n^{(\frac{1}{2})}(y)}{dy^2} + (\frac{3}{2} - y)\frac{dL_n^{(\frac{1}{2})}(y)}{dy} = -ny. \tag{6.25}$$

Thus, the spectral solution is represented by the expansion in the associated Laguerre polynomials

$$g(y,t) = \sum_{n=0}^{\infty} c_n L_n^{(\frac{1}{2})}(y)e^{-nt}, \tag{6.26}$$

where the coefficients for a δ-function initial condition, $P(y,0) = \delta(y - y_0)$, are

$$c_n = \frac{\Gamma(n+1)}{\Gamma(n+\frac{3}{2})} L_n^{(\frac{1}{2})}(y_0). \tag{6.27}$$

Analogous to the expansion of the Ornstein-Uhlenbeck Fokker-Planck equation in Hermite polynomials, the solution of Eq. (6.21) can be expanded in Laguerre polynomials, that is

$$P(y,t) = \sqrt{y}e^{-y} \sum_{n=0}^{\infty} \frac{\Gamma(n+1)}{\Gamma(n+3/2)} L_n^{(\frac{1}{2})}(y_0) L_n^{(\frac{1}{2})}(y)e^{-nt}. \tag{6.28}$$

Andersen and Shuler (1964) summed this series and found the analytic result,

$$P(y,t) = \frac{e^{t/2}}{2\sqrt{\pi y_0(1-e^{-t})}} \left\{ \exp\left[-\frac{(\sqrt{y} - \sqrt{y_0 e^{-t}})^2}{1-e^{-t}} \right] - \exp\left[-\frac{(\sqrt{y} + \sqrt{y_0 e^{-t}})^2}{1-e^{-t}} \right] \right\}, \tag{6.29}$$

analogous to Eq. (6.15) for the Ornstein-Uhlenbeck equation. This provides another opportunity to study the rate of convergence of the Laguerre expansions.

For an initial Maxwellian distribution at temperature $T(0) > T_b$, the expansion in Laguerre polynomials can be summed in closed form (Andersen and Shuler 1964) to give

$$P(y,t) = \frac{2}{\sqrt{\pi}} \left[\frac{T_b}{T(t)} \right]^{3/2} \sqrt{y} \exp[-\frac{T_b}{T(t)} y], \tag{6.30}$$

which is a Maxwellian distribution with the time dependent temperature $T(t)$. Equation (6.30) also defines the intial Maxwellian at $T(0)$. An important property of

this Fokker-Planck equation is that if the initial distribution function is a Maxwellian at some temperature $T(0) > T_b$, the time dependent distribution remains Maxwellian with a time dependent temperature. This property of the Rayleigh Fokker-Planck equation is referred to as canonical invariance (Andersen et al. 1964; Andersen and Shuler 1964). This is a consequence of the fact that for this Rayleigh Fokker-Planck equation the moments of the distribution function in the Laguerre basis set are uncoupled and the temperature relaxation is a pure exponential given by

$$\frac{T(t) - T_b}{T(0) - T_b} = e^{-t}. \tag{6.31}$$

6.2 Numerical Methods for the Solution of the Fokker-Planck Equation

We have expressed the spectral solutions of the Ornstein-Uhlenbeck Fokker-Planck equation in Hermite polynomials and of the Rayleigh Fokker-Planck equation in Laguerre polynomials. Analogous pseudospectral solutions can also be derived which provide identical numerical results. We present in the next section a formalism for the use of nonclassical basis functions for the solution of the general Fokker-Planck equation in Eq. (6.7) with arbitrary drift and diffusion coefficients, $A(v)$ and $B(v)$, respectively. In Sect. 6.2.2, an equivalent pseudospectral formalism is presented.

6.2.1 Spectral Methods with Nonclassical Basis Functions

We consider a solution of the Fokker-Planck equation with a spectral method and with a basis set analogous to the solution of the Ornstein-Uhlenbeck equation in Sect. 6.1.2. The polynomial basis set is defined with the steady distribution $P_0(x)$ as the weight function. If we set $P(x,t) = P_0(x)g(x,t)$ in the Fokker-Planck equation, Eq. (6.7), where $P_0(x)$ is given by Eq. (6.9), then the equation for $g(x,t)$ becomes

$$\begin{aligned}\frac{\partial g(x,t)}{\partial t} &= \frac{1}{P_0(x)}\frac{\partial}{\partial x}\left[B(x)P_0(x)\frac{\partial g(x,t)}{\partial x}\right], \quad x \in [0,\infty)\\ &= -A(x)\frac{\partial g(x,t)}{\partial x} + B(x)\frac{\partial^2 g(x,t)}{\partial x^2},\\ &= -Lg(x,t),\end{aligned} \tag{6.32}$$

where the definition of $P_0(x)$ has been used. The term in square brackets in Eq. (6.32) can be considered as a flux. With the form of the operator, L, in the first line of

Eq. (6.32), L is self-adjoint with respect to $P_0(x)$ as the weight function provided that the zero flux boundary condition

$$P_0(x)B(x)\frac{\partial g(x)}{\partial x}\bigg|_0^\infty = 0, \tag{6.33}$$

is imposed. The linear time dependent Fokker-Planck equation, Eq. (6.32), admits a solution in terms of the eigenfunctions, $\psi_n(x)$, and eigenvalues, λ_n, defined by

$$L\psi_n(x) = \lambda_n\psi_n(x), \tag{6.34}$$

and the solution can be written as

$$P(x,t) = P_0(x)\sum_{n=0}^{\infty} a_n e^{-\lambda_n t}\psi_n(x), \tag{6.35}$$

where the a_n coefficients are determined from the initial distribution, $P(x,0)$. The self-adjoint property of L can be verified by calculating the matrix element $\langle\phi_1|L|\phi_2\rangle$ with L defined as in Eq. (6.32). With an integration by parts, it is easily shown that $\langle\phi_1|L|\phi_2\rangle = \langle\phi_2|L|\phi_1\rangle$ provided Eq. (6.33) is satisfied.

The eigenvalues and eigenfunctions are determined with a Galerkin spectral method and nonclassical basis sets and we use the basis set $\{S_n(x)\}$ orthonormal with $P_0(x)$ as weight function, that is

$$\int_0^\infty P_0(x)S_n(x)S_m(x)dx = \delta_{nm}. \tag{6.36}$$

The set $\{S_n(x)\}$, introduced in this chapter, is used to denote a general basis set of nonclassical polynomials orthonormal with respect to different equilibrium density functions, $P_0(x)$, defined by a specific physical problem. The matrix elements of the Fokker-Planck operator L in this basis set are given by

$$\begin{aligned} L_{nm}^{(sp)} &= \int_0^\infty P_0(x)S_n(x)LS_m(x)dx \\ &= -\int_0^\infty P_0(x)S_n(x)\frac{1}{P_0(x)}\frac{d}{dx}\left[P_0(x)B(x)\frac{dS_m(x)}{dx}\right]dx, \end{aligned} \tag{6.37}$$

where the superscript (sp) denotes the polynomial spectral representation. With an integration by parts, we get the symmetric matrix representation of the Fokker-Planck operator,

$$\boxed{L_{nm}^{(sp)} = -\int_0^\infty P_0(x)B(x)S_n'(x)S_m'(x)dx, \qquad (n,m) = 0,1,\ldots,N-1} \tag{6.38}$$

where zero flux boundary conditions are satisfied, Eq. (6.33). We highlight this important result showing the self-adjoint property of the Fokker-Planck equation subject to zero flux boundary conditions. The eigenvalues, λ_n, and eigenfunctions, $\psi_n(x)$, are determined with a numerical diagonalization of the matrix $\mathbf{L}^{(sp)}$ of dimension N. Although we have not demonstrated this explicitly here, the numerical results will show that the coefficients of the expansion $\psi_n(x)$ in the $S_n(x)$ basis set are linear variational parameters. Thus, the variational theorem is applicable and this spectral method will provide an upper bound to the eigenvalues for each N and converge from above. The time dependent solution of the Fokker-Planck equation is given by Eq. (6.35).

We will use L to denote several different Fokker-Planck operators in the sections that follow and each is defined at the outset. Otherwise the notation would become excessive.

6.2.2 *Pseudospectral Methods with Nonclassical Quadratures*

We introduce the basis set $R_n(x)$ orthonormal with respect to $w(x)$ defined by

$$R_n(x) = \sqrt{\frac{P_0(x)}{w(x)}}S_n(x), \tag{6.39}$$

and evaluate the derivative $S'(x) \equiv dS(x)/dx$,

$$S_n'(x) = \sqrt{\frac{w}{P_0}}\left(\frac{w'}{2w} - \frac{P_0'}{2P_0}\right)R_n(x) + \sqrt{\frac{w}{P_0}}R_n'(x). \tag{6.40}$$

Thus, the matrix elements of the Fokker-Planck operator, Eq. (6.38), are given by

$$L_{nm}^{(sp)} = -\int_0^\infty w(x)B(x)\left[R_n'(x) + h(x)R_n(x)\right]\left[R_m'(x) + h(x)R_m(x)\right]dx, \tag{6.41}$$

where

$$\boxed{h(x) = \frac{w'(x)}{2w(x)} - \frac{P_0'(x)}{2P_0(x)},} \tag{6.42}$$

and is a measure of the departure of $w(x)$ from $P_0(x)$. This result is highlighted as it shows that an optimal choice of weight function might be $w(x) = P_0(x)$ giving $h(x) = 0$.

The matrix elements are evaluated with the quadrature based on the weight function $w(x)$, that is

$$L_{nm}^{(sp)} = -\sum_{k=1}^{N} w_k B(x_k)[R_n'(x_k) + h(x_k)R_n(x_k)][R_m'(x_k) + h(x_k)R_m(x_k)], \quad (6.43)$$

where x_k and w_k are the quadrature points and weights associated with the polynomials orthogonal with respect to the weight function, $w(x) = P_0(x)$. To express this spectral representation in the equivalent physical space representation, we transform

$$L_{ij}^{(ps)} = \sum_{m=0}^{N-1}\sum_{n=0}^{N-1} T_{in} L_{nm}^{(sp)} T_{jm}, \quad (6.44)$$

where the superscript (ps) denotes the discrete pseudospectral representation and the transformation matrix between physical and spectral space is defined as in Chap. 3, namely

$$T_{in} = \sqrt{w_i} R_n(x_i).$$

We need only consider the first transformation with the sum over n as the second over m is similar. With the definition of T_{in}, the term in $R_n(x_k)$ is transformed as

$$\begin{aligned} h(x_k)\sum_{n=0}^{N-1} T_{in} R_n(x_k) &= h(x_k)\sum_{n=0}^{N-1} \sqrt{w_i} R_n(x_i) R_n(x_k), \\ &= \frac{h(x_k)}{\sqrt{w_k}}\delta_{ik}. \end{aligned} \quad (6.45)$$

The transformation of $R_n'(x_k)$ employs the derivative matrix operator giving

$$\begin{aligned} \sum_{n=0}^{N-1} T_{in} R_n'(x_k) &= \sum_{n=0}^{N-1} \sqrt{w_i} R_n(x_i) \sum_{\ell=1}^{N} D_{k\ell}\sqrt{\frac{w_\ell}{w_k}} R_n(x_\ell), \\ &= \sum_{\ell=1}^{N} D_{k\ell}\sqrt{\frac{w_i w_\ell}{w_k}} \sum_{n=0}^{N-1} R_n(x_i) R_n(x_\ell), \\ &= \sum_{\ell=1}^{N} D_{k\ell}\sqrt{\frac{w_i w_\ell}{w_k}} \frac{\delta_{i\ell}}{w_i}, \\ &= \frac{D_{ki}}{\sqrt{w_k}}. \end{aligned} \quad (6.46)$$

The transformation with T_{jm} yields similar results and we find the discrete pseudospectral representation

$$\boxed{L_{ij}^{(ps)} = -\sum_{k=1}^{N} B(x_k)[D_{ki} + h(x_k)\delta_{ki}][D_{kj} + h(x_k)\delta_{kj}], \quad (i, j) = 1, 2, \ldots, N.} \tag{6.47}$$

This result is also highlighted because for the quadrature defined with the stationary distribution, $w(x) = P_0(x)$, for which $h(x_k) = 0$, the representation of L_{ij} has the simpler form,

$$L_{ij}^{(ps)} = -\sum_{k=1}^{N} B(x_k) D_{ki} D_{kj}. \tag{6.48}$$

The representation of the Fokker-Planck operator given by Eq. (6.48) is straightforward to program in MATLAB for different choices of the basis set and associated quadrature points and weights. The derivative matrix operator, D_{ki}, is calculated as discussed in Chap. 3, Eqs. (3.138) and (3.139).

The pseudospectral solution of the Ornstein–Uhlenbeck Fokker-Planck equation is equivalent to the solution of the Schrödinger equation for the quantum harmonic oscillator. The drift coefficient, $B(x) = 1$, (Eq. 6.16), and $P_0(x) = w(x) = e^{-x^2}$, $x \in (-\infty, \infty)$, so that the derivative matrix operator, D_{ki}, is defined in terms of the Hermite polynomials as discussed in Chap. 4. The eigenvalues of the self-adjoint representation of the Fokker-Planck operator $\mathbf{L}^{(ps)}$ (Eq. 6.48) are $\lambda_n = n$ and the eigenfunctions are the Hermite polynomials.

For the Rayleigh Fokker-Planck equation $B(y) = y$, and with the Gauss Laguerre quadrature weights and points defined with $P_0(y) = w(y) = \sqrt{y}e^{-y}$, $y \in [0, \infty)$, the eigenvalues of $\mathbf{L}^{(ps)}$ are $\lambda_n = n$ and the eigenfunctions are the Laguerre polynomials. This is consistent with the spectral solutions given by Eqs. (6.20) and (6.28).

6.2.3 *The Chang-Cooper Finite Difference Method of Solution of the Fokker-Planck Equation*

The finite difference algorithm by Chang and Cooper (1970) has found numerous applications for the solution of the Fokker-Planck equation in many different applications (Larsen et al. 1985; Park and Petrosian 1996; Buet and Dellacherie 2010; Abolhassani and Matte 2012).

The self-adjoint form of the Fokker-Planck equation, Eq. (6.32), was shown to be consistent with zero flux at the boundaries, Eq. (6.33). This boundary condition is also related to particle conservation

$$\frac{\partial}{\partial t}\int_0^\infty P_0(x)g(x,t)dx = P_0(x)B(x)\frac{\partial g(x,t)}{\partial x}\Big|_{x=0}^{\infty} = 0. \tag{6.49}$$

Any useful discretization would have to ensure particle conservation which yields, $\lambda_0 = 0$.

We discretize the speed variable according to $0 = x_1 < x_2 < x_3 \cdots < x_N = x_{max}$ with $x_{i+1} = x_i + \Delta x$, and $\Delta x = x_{max}/(N-1)$ where x_{max} is the speed point chosen large enough so that the flux boundary condition is satisfied. We also introduce a shifted grid at the midpoint defined by $x_{i+1/2} = x_i + \Delta x/2$. With a centered difference for the derivative,

$$\frac{\partial g(x,t)}{\partial x}|_{x_{i+1/2}} \approx \frac{g(x_{i+1},t) - g(x_i,t)}{\Delta x}, \tag{6.50}$$

the finite difference representation of the eigenvalue problem is,

$$\sum_{j=1}^{N} L_{ij}\phi_n(x_j) = \lambda_n \phi_n(x_i), \tag{6.51}$$

where

$$Ł_{ii} = \frac{1}{(\Delta x)^2}\frac{x_i^2 P_0(x_i)B_i + x_{i+1}^2 P_0(x_{i+1})B_{i+1}}{x_{i+1/2}^2 P_0(x_{i+1/2})}, \quad i = 1,\ldots,N, \tag{6.52}$$

$$Ł_{i,i-1} = -\frac{1}{(\Delta x)^2}\frac{x_i^2 P_0(x_i)B_i}{x_{i+1/2}^2 P_0(x_{i+1/2})}, \quad i = 2,\ldots,N, \tag{6.53}$$

$$Ł_{i,i+1} = -\frac{1}{(\Delta x)^2}\frac{x_{i+1}^2 P_0(x_{i+1})B_{i+1}}{x_{i+1/2}^2 P_0(x_{i+1/2})}, \quad i = 1,\ldots,N-1, \tag{6.54}$$

with the understanding that the first term in the fraction on the right hand side of Eq. (6.52) vanishes for $i = 1$ and the second term vanishes for $i = N$ in order to enforce the boundary conditions.

We use a forward Euler difference algorithm for the time derivative, that is

$$\frac{\partial g(x_i,t)}{\partial t} = \frac{g_i^{(n+1)} - g_i^{(n)}}{\Delta t}, \tag{6.55}$$

where $t = n\Delta t$ and $g_i^{(n)} = g(x_{i+1/2}, n\Delta t)$. The Chang-Cooper finite difference algorithm for the Fokker-Planck equation is

$$g_i^{(n+1)} = g_i^{(n)} + \Delta t \frac{x_{i+1}^2 P_0(x_{i+1}) B_{i+1}[g_{i+1}^{(n+1)} - g_i^{(n+1)}] - x_i^2 P_0(x_i) B_i[g_i^{(n+1)} - g_{i-1}^{(n+1)}]}{(\Delta x)^2 x_{i+1/2}^2 P_0(x_{i+1/2})}. \tag{6.56}$$

This result can be rewritten compactly as the matrix equation

$$\sum_{j=1}^{N} V_{ij} g_j^{(n+1)} = g_i^{(n)}, \tag{6.57}$$

where the matrix $\mathbf{V}$ is tridiagonal with elements

$$\begin{aligned} V_{i,i} &= 1 + \Delta t L_{i,i}, \quad i = 1, \ldots, N, \\ V_{i,i-1} &= \Delta t L_{i,i-1}, \quad i = 2, \ldots, N, \\ V_{i,i+1} &= \Delta t L_{i,i+1}, \quad i = 1, \ldots, N-1 \end{aligned} \tag{6.58}$$

At each time step, the updated values $g_i^{(n+1)}$ are obtained with the inversion of Eq. (6.57).

The Chang-Cooper finite difference scheme, as a discrete representation of L, does not give rapidly convergent eigenvalues and eigenfunctions (Leung et al. 1998). However, with the algorithm Eq. (6.56), the probability density function remains positive, entropy increases with time and a Maxwellian is recovered at equilibrium (Buet and Dellacherie 2010). We use this algorithm in Sect. 6.4.2 to solve the Fokker-Planck equation for a model that involves heating of a plasma by wave-particle interactions.

6.3 Electron Thermalization; The Lorentz Fokker-Planck Equation Revisited

The degradation or thermalization of energetic electrons in atomic and molecular moderators is an important aspect of radiation chemistry and physics (Mozumder 1999; Robson 2006), plasma processing of semiconductor devices (Petrović et al. 2009), the physics of the aurora (Stamnes 1980; Basu et al. 1993; Solomon 2001; Shematovich et al. 2008) fundamental aspects of the approach to equilibrium (Trunec et al. 2003; Sospedra-Alfonso and Shizgal 2011) and thermalization in condensed matter (Sakai 2007; White et al. 2010).

The electron anisotropic nonequilibrium distribution functions are often expanded in the direct product of the spherical harmonics in (θ, ϕ) and the Sonine–Laguerre polynomials for the reduced speed or reduced energy dependence (Kumar et al. 1980; Robson and Ness 1986; Robson 2006; White and Robson 2011; Abolhassani and Matte 2012). This methodology requires the matrix elements of the collision operator

in the Boltzmann equation as discussed in Chap. 5. There have also been solutions of the electron Boltzmann equation with a B spline representation (Pitchford and Phelps 1982) as well as with Monte Carlo methods (Koura 1983; Solomon 2001; Shematovich et al. 2008).

For molecular moderators such as N_2, O_2 and CH_4, inelastic collisions that involve changes in the rotational and/or vibrational states of the moderator (Pitchford and Phelps 1982; Kowari et al. 1992) and electron attachment to electronegative gases such as SF_6 and CCl_4 must be included (Kowari and Shizgal 1996; Kowari et al. 1998).

The relaxation of electrons of moderate energy in atomic moderators for which only elastic collisions need be included (Mozumder 1981; Knierim et al. 1982; Risken and Voigtlaender 1984; McMahon and Shizgal 1985; Shizgal and McMahon 1985) is presented in this section. In atomic moderators, there have been two notable phenomena exhibited, namely the transient negative mobility (Shizgal and McMahon 1985; Dyatko et al. 2001; Dyatko 2007) and the negative differential conductivity effect in gas mixtures (Shizgal 1990) previously thought to occur only for polyatomic gases with internal degrees of freedom.

Owing to the small electron mass m_e to moderator mass M ratio, the Boltzmann collision operator can be replaced by the Fokker-Planck operator corresponding to the Lorentz limit discussed in Sect. (6.1.3). The Boltzmann equation or the Fokker-Planck equation have been used in the study of electron thermalization in rare gases (Lin et al. 1979; Knierim et al. 1982; McMahon and Shizgal 1985; Shizgal and McMahon 1985). The physics of the problem is defined by the energy dependent momentum transfer cross section $\sigma_{mt}(v)$ for electron-atom collisions and the strength of the applied electric field, E. The electric field results in a drift of the electrons with a mobility determined by the electron-atom cross section.

To account for the electron drift in the applied electric field, there is a small anisotropy of the electron velocity distribution function which is expressed by the expansion in Legendre polynomials, that is,

$$f(\mathbf{v}, t') = \sum_{\ell=0}^{\infty} f_\ell(v, t') P_\ell(\cos\theta), \tag{6.59}$$

where θ is the angle between $\mathbf{v}$ and the polar axis taken in the direction of the electric field. Owing to the small mass ratio, m_e/M, the anisotropy of the distribution remains small and only the terms in $\ell = 0$ and $\ell = 1$ in Eq. (6.59) need to be retained. This is referred to as the "two-term" approximation (Hagelaar and Pitchford 2005). The coupled equations for the first two terms, f_0 and f_1, are

$$\begin{aligned} \frac{\partial f_0}{\partial t'} + \frac{eE}{3m_e}\left(\frac{\partial}{\partial v} + \frac{2}{v}\right) f_1 &= \frac{m_e}{Mv^2}\frac{\partial}{\partial v}\left[v^3\gamma(v)\left(1 + \frac{k_B T_b}{m_e v}\frac{\partial}{\partial v}\right)\right] f_0, \\ \frac{\partial f_1}{\partial t'} + \frac{eE}{m_e}\frac{\partial f_0}{\partial v} &= -\gamma(v) f_1, \end{aligned} \tag{6.60}$$

where $\gamma(v) = N_b v \sigma_{mt}(v)$ and N_b is the density of the moderator. There is an initial fast transient that we ignore and thus we set $\partial f_1/\partial t' = 0$. This aspect of relaxation in the Lorentz limit was illustrated in Chap. 3; see Fig. 5.15.

We also define the reduced speed $x = v\sqrt{m_e/2k_B T_s}$ with an arbitrary scaling temperature T_s and dimensionless time $t = t'/\tau$ where

$$\tau = \left[\frac{nm_e\sigma_0}{2M}\sqrt{\frac{2k_B T_b}{m_e}}\right]^{-1}. \tag{6.61}$$

A representative hard sphere cross section is denoted by σ_0. We also consider a scaling of the speed variable in anticipation of the use of a quadrature based solution of the Fokker-Planck equation so that we define $s^2 = T_s/T_b$. With these definitions and the steady state value of f_1 given by

$$f_1 = -\frac{eE}{\gamma m_e}\frac{\partial f_0}{\partial v}, \tag{6.62}$$

we have the Fokker-Planck equation for f_0, that is

$$\frac{\partial f_0}{\partial t} = \frac{s}{x^2}\frac{\partial}{\partial x}\left[2x^4\hat{\sigma}(x)f_0 + \frac{x^2}{s^2}B(x)\frac{\partial f_o}{\partial x}\right], \tag{6.63}$$

where

$$B(x) = x\hat{\sigma}x) + \frac{(\alpha/s)^2}{x\hat{\sigma}(x)}, \tag{6.64}$$

and the field strength parameter is

$$\alpha^2 = \frac{M}{6m_e}\left[\frac{eE}{n\sigma_0 k_B T_b}\right]^2. \tag{6.65}$$

In Eq. (6.63), $\hat{\sigma}(x) = \sigma_{mt}(x)/\sigma_0$ is a dimensionless cross section written as a function of reduced speed. The steady state distribution is from Eq. (6.63) given by

$$f_0(x,\infty) = D(x) = C\exp\left[-2s^2\int_0^x \frac{(x')^2\hat{\sigma}(x')}{B(x')}dx'\right]. \tag{6.66}$$

The steady solution, $D(x)$ given by Eq. (6.66), is precisely $P_0(x)$ in Sect. 6.2.1. The distribution, $D(x)$, is referred to as the Davydov distribution which reduces to a Maxwellian in the absence of an electric field. If we set $f(x,t) = D(x)g(x,t)$, the equation for $g(x,t)$ is given by

$$\frac{\partial g}{\partial t} = \frac{s}{D(x)x^2}\frac{\partial}{\partial x}\left[\frac{x^2}{s}B(x)D(x)\frac{\partial g}{\partial x}\right] = -Lg, \quad x \in [0,\infty). \tag{6.67}$$

The linear operator on the right hand side of Eq. (6.67) that we have denoted by L is self adjoint with $D(x)$ as weight function with zero flux boundary conditions, that is,

$$x^2 D(x)B(x)\frac{\partial g(x,t)}{\partial x}\Big|_{x=0}^{x=\infty} = 0. \tag{6.68}$$

We are interested in the eigenvalue problem defined by

$$L\psi_n(x) = \lambda_n \psi_n(x). \tag{6.69}$$

6.3.1 Hard Sphere Cross Section and Zero Electric Field, $E = 0$

If there is no external electric field and the cross section is a hard sphere $\sigma(x) = \sigma_0$, then $B(x) = x$ and the equilibrium distribution is the Maxwellian $P_0(x) = x^2\exp(-x^2)$. We consider a calculation of the eigenvalue spectrum of this Fokker-Planck operator with the Maxwell polynomials orthonormal with respect to the weight function $w(x) = x^2\exp(-x^2)$. The "traditional" method of solution of the Boltzmann equation involves the representation of the collision operator in the Sonine-Laguerre polynomials (Knierim et al. 1982) denoted by $L_{nm}^{(SL)}$.

The calculation of this matrix representation of the collision operator in the Boltzmann equation defined by $L_{nm}^{(SL)} = \langle L_n^{(\frac{1}{2})}|L|L_m^{(\frac{1}{2})}\rangle$ with weight function $w(y) = \sqrt{y}e^{-y}$ is straightforward but algebraically tedious (Shizgal and Fitzpatrick 1974) and the final expressions obtained can lead to considerable round-off errors in the numerical calculation of the matrix elements. In the Lorentz limit, the result is simpler and we have that

$$L_{nm}^{(SL)} = -2\sqrt{\pi}A\frac{m_e}{M}\sqrt{\frac{m!n!}{\Gamma(n+\frac{3}{2})\Gamma(m+\frac{3}{2})}}\sum_{r=1}^{min(n,m+1)} r(r+1)N(n-r)N(m-r) \tag{6.70}$$

where $N(\ell) = \Gamma(\ell-\frac{1}{2})/(2\ell!\sqrt{\pi})$ and $A = 2n_b\pi d^2\sqrt{2k_BT_b/m_e}$. The matrix $\mathbf{L}^{(SL)}$ in the Sonine-Laguerre representation is a full matrix.

Our main objective is to compare the convergence of the eigenvalues of the Boltzmann collision operator as calculated with the representation given by Eq. (6.70) and a pseudospectral method of solution based on the non-classical polynomials orthogonal with respect to weight function $w(x) = P_0(x) = x^2\exp(-x^2)$.

The matrix representation of the Lorentz Fokker-Planck operator in the Maxwell polynomials, $M_n(x)$, $p = 2$, orthonormal with respect to a weight function $w(x) = x^2 e^{-x^2}$ is defined by $L_{nm}^{(MP)} = \langle M_n | L | M_m \rangle$ where the scalar product is with respect to $w(x)$. Lo and Shizgal (2006) derived the explicit tridiagonal form of this spectral representation as

$$L_{mn}^{(MP)} = \begin{cases} (n-1)\alpha_{n-1} + \sum_{k=0}^{n-2} \alpha_k, & m = n > 1, \\ 2(n-1)\sqrt{\beta_n}, & m = n+1, \\ 2(m-1)\sqrt{\beta_m}, & m = n-1, \\ 0, & \text{otherwise.} \end{cases} \tag{6.71}$$

where α_n and β_n are the coefficients in the three term recurrence relation discussed in Chap. 2. It should be clear that the transformation of $L_{nm}^{(MP)}$ with the transformation $T_{in} = \sqrt{w_i} M_n(x_i)$, yields the discrete pseudospectral (ps) representation $L_{ij}^{(ps)}$ given by

$$L_{ij}^{(ps)} = -\sum_{k=1}^{N} x_k D_{ki} D_{kj}, \tag{6.72}$$

where in Eq. (6.48), $B(x_k) = x_k$. An equivalent pseudospectral representation can also be calculated for the Sonine-Laguerre quadratures.

A comparison of the convergence of the eigenvalues of the Fokker-Planck operator for a hard sphere cross section versus the size of the basis set N is shown in Table 6.1. It is clear that the convergence of the eigenvalues is much faster with the Maxwell polynomials as basis functions. The first nonzero eigenvalue, λ_1, requires

Table 6.1 Convergence of the eigenvalues of the hard sphere Lorentz Fokker-Planck equation with the Sonine-Laguerre polynomial basis set (*left*) in comparison with the Maxwell polynomial basis set (*right*)

$w(y) = \sqrt{y}e^{-y}$ (Laguerre)					$w(x) = x^2 e^{-x^2}$ (Maxwell)				
N	λ_1	λ_2	λ_3	λ_5	N	λ_1	λ_2	λ_3	λ_5
1	6.018				1	4.976			
2	5.317	16.35			2	4.716	11.52		
3	5.066	13.85	30.66		3	4.68704	10.40	19.84	
5	4.872	12.10	23.61	68.94	4	4.68378	10.16	17.40	
7	4.797	11.41	21.22	53.80	5	4.68343	10.121	16.68	41.28
10	4.748	10.91	19.56	45.96	6	4.68340	10.1137	16.485	35.55
20	4.7032	10.406	17.75	38.29	7	4.68340	10.1127	16.4401	33.11
30	4.6930	10.267	17.19	35.87	8		10.1125	16.4314	32.05
50	4.6871	10.178	16.79	33.94	9		10.1125	16.4300	31.64
75	4.6851	10.145	16.62	32.97	10			16.4297	31.512
100	4.6840	10.132	16.550	32.50	11			16.4297	31.4765
125	4.6840	10.125	16.512	32.231	12				31.4683
150	4.6839	10.122	16.490	32.056	13				31.4666

Reprinted from (Lo and Shizgal 2006) with permission from the American Institute of Physics

150 Laguerre polynomials for convergence to five significant figures whereas only 6 Maxwell polynomials are required. The higher eigenvalues also converge very quickly with the Maxwell polynomial basis set.

Risken and Voigtlaender (1984) introduced the Maxwell polynomials in the transformation of the Fokker-Planck eigenvalue problem to a Schrödinger equation presented in the following section. They studied the relaxation of neutrons in a heavy gas moderator with the assumption that the Lorentz Fokker-Planck equation is applicable. They report eigenvalues in agreement with the results listed in Table 6.1 calculated with a continued fraction method (Risken and Till 1996).

The pseudospectral method of solution of the Lorentz Fokker-Planck equation is applicable also to realistic energy dependent momentum transfer cross sections (McMahon and Shizgal 1985) and also with a nonzero electric field (Shizgal and McMahon 1985). In these applications, the nonclassical polynomial basis sets that are used for the eigenvalue problem are orthonormal with respect to $P_0(x)$ parametrized by the momentum transfer cross section and the electric field strength, Eq. (6.66). The method was also applied to the relaxation of positrons in He and Ne (Shizgal and Ness 1987), for an oscillatory electric field (Viehland et al. 1988) and in systems with an admixture of a strongly electron attaching gas such as SF_6 and CCl_4 (Shizgal 1988). A review of this subject was presented by Shizgal et al. (1989).

6.3.2 *Transformation of the Fokker-Planck Eigenvalue Problem to a Schrödinger Equation; Supersymmetric Quantum Mechanics*

The eigenvalue problem of the Fokker-Planck equation is

$$A(x)\frac{d\psi_n}{dx} - B(x)\frac{d^2\psi_n}{dx^2} = \lambda_n \psi_n. \tag{6.73}$$

We transform the independent variable x to a new variable z defined by

$$z = \int^x \frac{1}{\sqrt{B(x')}} dx',$$

so that

$$\frac{dz}{dx} = \frac{1}{\sqrt{B}} \qquad \text{and} \qquad \frac{d}{dx} = \frac{1}{\sqrt{B}}\frac{d}{dz},$$

giving

$$\frac{A}{\sqrt{B}}\frac{d\psi_n}{dz} - \sqrt{B}\left(-\frac{B'}{2B^{3/2}}\frac{d\psi_n}{dz} + \frac{1}{\sqrt{B}}\frac{d^2\psi_n}{dz^2}\right) = \lambda_n \psi_n.$$

where the prime, ($B' \equiv dB[x(z)]/dz$), denotes differentiation with respect to z. The eigenvalue equation in the new variable z is

$$-\frac{d^2\psi_n}{dz^2} + \left(\frac{A}{\sqrt{B}} + \frac{B'}{2B}\right)\frac{d\psi_n}{dz} = \lambda_n \psi_n. \tag{6.74}$$

A function $C(z)$ is defined by

$$\psi_n(z) = e^{C(z)}\phi_n(z),$$

where the functions $\phi_n(z)$ will be shown to satisfy a Schrödinger equation. With $\psi_n'(z) \equiv d\psi_n(z)/dz$, we have that

$$\psi_n' = C' e^C \phi_n + e^C \phi_n',$$

and

$$\psi_n'' = C'' e^C \phi_n + (C')^2 e^C \phi_n + 2C' e^C \phi_n' + e^C \phi_n''.$$

The Fokker-Planck eigenvalue equation, Eq. (6.74), is rewritten in terms of $\phi_n(z)$ as

$$-\left[C''\phi_n + (C')^2\phi_n + 2C'\phi_n' + \phi_n''\right] + \left(\frac{A}{\sqrt{B}} + \frac{B'}{2B}\right)(C'\phi_n + \phi_n') = \lambda_n \phi_n. \tag{6.75}$$

We set the coefficient of ϕ_n' to zero and get the defining equation for $C(z)$, that is,

$$\frac{dC(z)}{dz} = \frac{1}{2}\left(\frac{A}{\sqrt{B}} + \frac{B'}{2B}\right), \tag{6.76}$$

which when integrated gives

$$C(z) = \frac{1}{2}\int^z \frac{A(z')}{\sqrt{B(z')}}dz' + \frac{1}{4}\ln B(z). \tag{6.77}$$

With these definitions, the partial differential equation, Eq. (6.75), for $\phi_n(z)$ is the Schrödinger equation

$$-\frac{d^2\phi_n}{dz^2} + V(z)\phi_n(z) = \lambda_n \phi_n(z), \tag{6.78}$$

where Eq. (6.76) has been used and the coefficient of ϕ_n in Eq. (6.75) is the potential $V(z)$, given by

$$V(z) = (C'(z))^2 - C''(z). \tag{6.79}$$

The orthonormality of the eigenfunctions $\psi_n(x)$ is defined in terms of $P_0(x)$ and given by

$$\int_0^\infty P_0(x)\psi_n(x)\psi_m(x)dx = \delta_{nm},$$

$$\int_0^\infty P_0[x(z)]e^{C(z)}\phi_n(z)e^{C(z)}\phi_m(z)\sqrt{B(x(z))}dz = \delta_{nm}, \tag{6.80}$$

which is consistent with the normalization

$$\int_0^\infty \phi_n(z)\phi_m(z)dz = \delta_{nm}, \tag{6.81}$$

so that

$$P_0[x(z)]e^{2C(z)}\sqrt{B[x(z)]} = 1, \tag{6.82}$$

which is consistent with the definition of $C(z)$. Moreover, if we set $W(z) = 2C'(z)$ we have that

$$\boxed{V(z) = \frac{W(z)^2}{4} - \frac{W(z)'}{2},} \tag{6.83}$$

and

$$W(z) = \frac{A}{\sqrt{B}} + \frac{B'}{2B}. \tag{6.84}$$

Thus the equilibrium solution of the Fokker-Planck equation can be expressed as

$$P_0(x) = \exp[-\frac{1}{2}\int^x W[z(x')]dx'], \tag{6.85}$$

and is the ground state of the Fokker-Planck equation with $\lambda_0 = 0$ as can be easily verified by differentiating $P_0(x)$ twice.

The function $W(z)$ is the "superpotential" of supersymmetric quantum mechanics. We have derived the formal relationship between the Fokker-Planck equation and the Schrödinger equation (Comtet et al. 1985; Cooper et al. 1995; Risken and Till 1996; Feizi et al. 2011). This close relationship between these two large classes of problems has been exploited to advantage in the study of nucleation (Demeio and Shizgal 1993a), electron relaxation in molecular gases (Demeio and Shizgal 1993b), relaxation in plasmas (Shizgal 1992) and other applications (Gomez-Ullate et al. 2009).

6.3.3 Pseudospectral Representation of the Schrödinger Equation; Supersymmetric Quantum Mechanics

The spectral representation of the Hamiltonian in the Schrödinger equation, Eq. (6.78), for a basis set $\{S_n(y)\}$ orthonormal with unit weight function is

$$H_{nm}^{(sp)} = -\int_0^\infty S_n(y) S_m''(y) dy + \int_0^\infty S_n(y) V(y) S_m(y) dy. \tag{6.86}$$

We integrate the first integral by parts so that

$$H_{nm}^{(sp)} = \int_0^\infty S_n'(y) S_m'(y) dy + V_{nm}, \tag{6.87}$$

where the potential matrix element is $V_{nm} = \int S_n(y) V(y) S_m(y) dy$. Define a second polynomial set $\{F_n\}$ orthogonal with weight function $w(y)$, that is,

$$S_n(y) = \sqrt{w(y)} F_n(y), \tag{6.88}$$

where the weight function is defined as $w(y) = \exp(-\int W(y')dy')$ analogous to the equilibrium distribution for the Fokker-Planck equation, Eq. (6.85). Equation (6.87) can then be rewritten as,

$$H_{nm}^{(sp)} = \int w[F_m' + \frac{w'}{2w} F_m][F_n' + \frac{w'}{2w} F_n] dy + V_{nm}. \tag{6.89}$$

If one of the cross terms, $F_m' F_n$, in the integrand above is integrated by parts we find that,

$$H_{nm}^{(sp)} = \int w F_n' F_m' dy + [V_{nm} - \tilde{V}_{nm}], \tag{6.90}$$

where $\tilde{V}_{nm}$ are the matrix elements of the potential

$$\tilde{V}(y) = \frac{1}{4} W^2(y) - \frac{1}{2} W'(y), \tag{6.91}$$

defined in terms of the "superpotential", $W(y)$, in supersymmetric quantum mechanics. We transform the spectral representation $H_{nm}^{(sp)}$ to the discrete representation with the transformation $\mathbf{T}$, that is,

$$H_{ij}^{(ps)} = \sum_{n=0}^{N-1} \sum_{m=0}^{N-1} T_{in} H_{nm}^{(sp)} T_{jm}, \tag{6.92}$$

to give the final desired result, namely

$$\boxed{H_{ij}^{(ps)} = \sum_{k=1}^{N} D_{ki} D_{kj} + [V(y_i) - \tilde{V}(y_i)]\delta_{ij},} \tag{6.93}$$

If the potential of interest can be written as in Eq. (6.91), then a useful weight function for the definition of the basis set is given by the equilibrium distribution function or the ground state wave function, Eq. (6.85). For this choice, $\tilde{V}(y) = V(y)$, and the pseudospectral representation of the Hamiltonian reduces to

$$H_{ij}^{(ps)} = \sum_{k=1}^{N} D_{ki} D_{kj}. \tag{6.94}$$

This approach has been described in detail by Shizgal and Chen (1996) and Lo and Shizgal (2006).

6.4 Relaxation and Wave-Particle Heating in Space Plasmas

The Fokker-Planck equation plays a dominant role in plasma physics (Chandrasekhar 1942; Spitzer 1962; Hinton 1983; Shoub 1987) and stellar astrophysics (Spitzer and Härm 1958; Binney and Tremaine 2008; Lemou and Chavanis 2010). We consider as was done in Chap. 5, the kinetic theory of a test particle of mass m and charge Z dilutely dispersed in a large excess of a second species of mass M and charge Z_b at equilibrium with temperature T_b and number density N_b. The Coulomb differential scattering cross section for collisions between the charged particles interacting via a Coulomb potential is given by

$$\sigma(g, \theta) = \left(\frac{Z_b Z e^2}{2\mu g^2}\right)^2 \frac{1}{\sin^4(\theta/2)}. \tag{6.95}$$

The cross section varies inversely as the fourth power of the relative velocity, g, and diverges for small scattering angle, θ.

The Coulomb Fokker-Planck equation finds numerous applications in space science and in particular for the modelling of the solar and polar winds. The solar wind consists primarily of protons and electrons that escape the solar gravitational field. The polar wind (Lie-Svendsen and Rees 1996; Pierrard and Lemaire 1998) is analogous to the solar wind (Parker 1965; Vocks 2002) and represents the escape of ions from the ionosphere along open magnetic field lines at high latitudes (Marsch 2006; Echim et al. 2011).

6.4.1 Pseudospectral Solution of the Coulomb Fokker-Planck and Associated Schrödinger Equations; The Approach to Equilibrium and the Continuous Spectrum

The Fokker-Planck equation for Coulomb collisions is derived from the Boltzmann equation with the differential cross section, Eq. (6.95), with the assumption of small energy transfers in individual binary collisions between charged particles. The small energy transfer collisions are those with large impact parameters. Consistent with this approximation, the small angle singularity in the momentum transfer differential cross section is eliminated by restricting the scattering angle such that $\theta > \theta_{min}$ where $\sin^2(\theta_{min}/2) = [1 + \Lambda]^{-1}$, where $\Lambda = \lambda_D/b_0$; λ_D is the Debye length and $b_0 = ZZ_b e^2/2k_B T_b$, the impact parameter that corresponds to the scattering angle $\theta = \pi/2$ (Spitzer 1962; Mitchner and Kruger 1973; Hinton 1983).

The Fokker-Planck equation derived from the Boltzmann equation as discussed in the previous paragraph is

$$\frac{\partial f(v,t')}{\partial t'} = \frac{A}{v^2}\frac{\partial}{\partial v}\left[G(v)\left(1 + \frac{kT_b}{mv}\frac{\partial}{\partial v}\right)\right] f(v,t'), \tag{6.96}$$

where $A = (4\pi N_b e^4 Z^2 Z_b^2/mM)\ln\Lambda$ and the diffusion coefficient is

$$G(v) = \text{erf}(\sqrt{\frac{Mv^2}{2kT_b}}) - \sqrt{\frac{2Mv^2}{\pi kT_b}}\exp(-\frac{Mv^2}{2kT_b}), \tag{6.97}$$

as discussed elsewhere (Karney 1986; Shizgal 2004; Chavanis 2006).

The steady state distribution from Eq. (6.96) is a Maxwellian. A dimensionless time $t' = t/\tau$ is defined with $\tau = ([2A/3\sqrt{\pi}][M/2k_B T_b]^{3/2})^{-1}$ and the reduced speed $x = v\sqrt{m/2k_B T_s}$ where the temperature parameter $T_s = s^2 T_b$. The parameter s is the quadrature scaling parameter introduced in Chap. 3. With these definitions, the Fokker-Planck equation is

$$\frac{\partial f(x,t)}{\partial t} = \frac{2}{s^3 x^2}\frac{\partial}{\partial x}\left[G_1(sx)\left(1 + \frac{1}{2xs^2}\frac{\partial}{\partial x}\right)\right] f(x,t), \tag{6.98}$$

where $G_1(sx) = h(\gamma)G(v)$, $\gamma = \sqrt{M/m}$ and $h(\gamma) = 3\sqrt{\pi}/4\gamma^{3/2}$.

If we set $f(x,t) = e^{-s^2x^2} g(x,t)$, the Fokker-Planck equation is

$$\frac{\partial g}{\partial t} = \frac{1}{s^2}\left[A(x)\frac{\partial g}{\partial x} - B(x)\frac{\partial^2 g}{\partial x^2}\right] = Lg, \tag{6.99}$$

with $B(x) = G_1(sx)/(sx)^3$. The drift coefficient in terms of $B(x)$ is

$$A(x) = 2s^2 x B(x) - \frac{2B(x)}{x} - \frac{dB(x)}{dx}. \tag{6.100}$$

We are concerned with the eigenvalue problem

$$L\psi_n(x) = -\lambda_n \psi_n(x),$$

with L defined with Eq. (6.99). The physical space pseudospectral representation of this Fokker-Planck operator is

$$L_{ij}^{(ps)} = \frac{1}{s^2} \sum_{k=1}^{N} B(x_k)[D_{ki} + x_k(s^2 - 1)\delta_{ki}][D_{kj} + x_k(s^2 - 1)\delta_{kj}]. \tag{6.101}$$

If the scaling parameter, $s = 1$, Eq. (6.101) reduces to Eq. (6.48).

The eigenvalues are determined with the numerical diagonalization of the matrix $\mathbf{L}^{(ps)}$ of dimension N. The convergence of the lower order eigenvalues is shown in Table 6.2 and the rapid convergence is clear.

We transform the Fokker-Planck eigenvalue equation to a Schrödinger equation as discussed in Sect. 6.3.3 and derive, after some algebra, the potential in x, that is

$$V_-(x) = \frac{G_1(x)}{x}\left(1 - \frac{9}{16x^4}\right) - 3\left[1 + \frac{\gamma^2}{2} - \frac{3}{8x^2}\right]e^{-\gamma^2 x^2} - \frac{9x}{16G_1(x)}e^{-2\gamma^2 x^2}. \tag{6.102}$$

The potentials are shown in Fig. 6.1 for two mass ratios, $M/m = 0.01$ and 0.04, and the eigenvalues (bound states) are indicated with the horizontal lines. There are a finite number of discrete eigenvalues and the number of states diminishes with increasing mass ratio. Since the potential barrier is finite, the eigenstates are not true bound states (Corngold 1981) and could be referred to as "quasi-bound" states. The only bound state is the ground state with $\lambda_0 = 0$. However, it is readily verified that

Table 6.2 Convergence of the eigenvalues of the pseudospectral representation of the Coulomb Fokker-Planck operator, Eq. (6.101), for mass ratio, $\gamma = 0.3$

N	λ_1	λ_2	λ_3	λ_4	λ_5	λ_6	λ_7
4	3.82049	7.522947	18.6937				
6	3.82023	7.35052	10.7565	16.6796	47.3754		
8	3.82023	7.34943	10.5866	13.7437	18.4730	30.7286	96.2670
10		7.34943	10.5828	13.5261	16.4786	20.7524	20.3964
20				13.5139	16.1314	18.4301	20.3807
30				13.5139	16.1341	18.4301	20.3897
40						18.4301	20.3807
SWKB	3.82031	7.34954	10.5831	13.5144	16.1348	18.4313	20.3829
WKB	3.82834	7.35710	10.5900	13.5208	16.1407	18.4366	20.3875

Reproduced from Shizgal (1992) with permission from Taylor and Francis

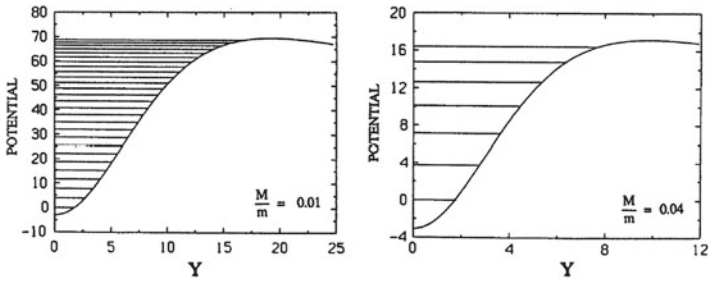

Fig. 6.1 Potential, $V_-(y)$, in the Schrödinger equation corresponding to the Coulomb Fokker-Planck equation for mass ratios $M/m = 0.01$ and 0.04. There are a finite number of eigenstates which are strictly not discrete. Reproduced from Shizgal (1991) with permission from Beylich A.E.: Rarefied gas dynamics. In: Proceedings of the 17th International Symposium on Rarefied Gas Dynamics, Wiley-VCH Verlag GmbH and Co. KGaA. pp. 22–29, (1991)

in the Rayleigh limit, $\gamma = 0$, $V_-(x) = x^2 - 3$ and the eigenvalues are all discrete and given by $\lambda_n = 4n$, the harmonic oscillator eigenvalues.

The converged eigenvalues in the table are compared with the semiclassical Wentzel-Kramers-Brillouin (WKB) eigenvalues (Miller and Good 1953), namely

$$\int_{x_1}^{x_2} \sqrt{\lambda_n - V_-(x)}dx = \left(n + \frac{1}{2}\right)\pi, \tag{6.103}$$

and the corresponding supersymmetric, SWKB, eigenvalues (Fricke et al. 1988)

$$\int_{x_1'}^{x_2'} \sqrt{\lambda_n - W^2(x)}dx = n\pi, \tag{6.104}$$

where the integral limits are the classical turning points. The agreement with the SWKB and WKB approximations is very good.

We expand the solution in the eigenfunctions of L and the time dependence of the average energy is

$$\frac{E(t')}{E_{th}} = \sum_{k=0}^{\infty} c_k e^{-\lambda_k t'}, \tag{6.105}$$

where $E_{th} = 3k_B T_b/2$ is the thermal energy and the coefficients are

$$c_k = \frac{2}{3}s^5 a_k \int_0^{\infty} e^{-s^2x^2}\psi_k(x)x^4 dx. \tag{6.106}$$

The coefficients a_k are the expansion coefficients of the intial condition

$$g(x,0) = \sum_{k=0}^{\infty} a_k \phi_k(x).$$

The 7 eigenvalues for $\gamma = 0.3$ are shown in Table 6.2 as the horizontal lines in the potential functions $V_-(x)$ and $W^2(x)$ in Fig. 6.2. The additional eigenvalue in $V_-(y)$ is $\lambda_0 = 0$. The eigenfunctions $\psi_4(x)$ and $\psi_6(x)$ are also shown in Fig. 6.2 with the WKB eigenfunctions denoted with the symbols. Two examples of continuum eiegenfunctions are shown in Fig. 6.3. The symbols that coincide with the solid curves are the results with the WKB approximation. These numerical eigenfunctions are L^2 square integrable with the discrete quadrature (Reinhardt 1979) defining the norm.

The relaxation of the temperature is given by $T(t') = 2E(t')/3k_B$ with $E(t')$ as in Eq. (6.105). The time variation of $T(t')/T_b$ is shown in Fig. 6.4 for four mass ratios includes the sum over discrete and continuous eigenvalues and is convergent. For mass ratio $M/m = 0.4$, there are no bound states and the discrete sum is over the continuous spectrum.

In Chap. 5, we discussed the properties of the discrete and continuous portions of the eigenvalue spectra of the Boltzmann integral collision operators. It is these spectral properties that determine the time dependent approach to equilibrium (Sospedra-Alfonso and Shizgal 2013). For the Boltzmann equation, there is always a discrete

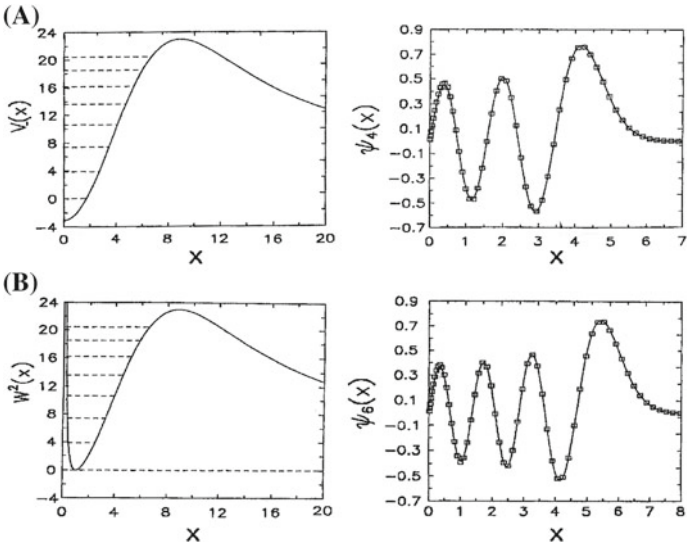

Fig. 6.2 (*Left hand graphs*) **(A)** The potential $V_-(y)$ in the Schrödinger potential; **(B)** The super potential $W^2(y)$ with a minimum value of 0. The bound states are shown with the *dashed horizontal lines*. (*Right hand graphs*) Eigenfunctions of the Fokker-Planck equation **(A)** $\psi_4(x)$ and **(B)** $\psi_6(x)$. The symbols are the WKB approximations (Miller and Good 1953). Reproduced from Shizgal (1992) with permission from Taylor and Francis

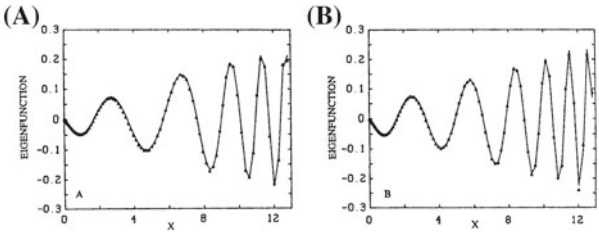

Fig. 6.3 The continuum eigenfunction of the Fokker-Planck collision operator for Coulomb collisions (symbols) in comparison with the WKB approximation (*solid curve*) with $T_b = 300\,\mathrm{K}$, $s = 0.6042$ and $\gamma = 0.04$; **(A)** $\lambda = 5.855$ and **(B)** $\lambda = 7.603$. Reproduced from Shizgal (1992) with permission Beylich A.E.: Rarefied gas dynamics. In: Proceedings of the 17th International Symposium on Rarefied Gas Dynamics, Wiley-VCH Verlag GmbH and Co. KGaA. pp. 22–29, (1991)

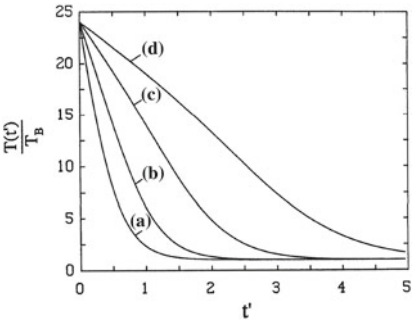

Fig. 6.4 Temperature relaxation for $T(0)/T_b = 24$ and $\gamma = a\,0.2, b\,0.3, c\,0.4$ and $d\,0.5$. Reproduced from Shizgal (1991) with permission Beylich A.E.: Rarefied gas dynamics. In: Proceedings of the 17th International Symposium on Rarefied Gas Dynamics, Wiley-VCH Verlag GmbH and Co. KGaA. pp. 22–29, (1991)

spectrum whereas for the Coulomb Fokker-Planck equation we have demonstrated that the spectrum can be completely continuous, except for $\lambda_0 = 0$. The approach to equilibrium is an exponential if there is at least one discrete eigenvalue, that is "the spectral gap" as discussed in Chap. 5. For mass ratios for which there are no discrete "quasi-bound" states, the approach to equilibrium can be a complicated non-exponential function of time (Corngold 1981). This may be the case for curve d in Fig. 6.4.

We consider the variation of the energy coefficients in the energy relaxation, Eq. (6.105), versus the numerical continuous eigenvalues. This variation of $c(\lambda)$ versus λ is shown in Fig. 6.5 for different scaling parameters. The discrete values of λ_k and c_k (or λ and $c(\lambda)$) in the continuum vary with a change in the scaling parameter, s, or with a change in the number of quadrature points, N, but the variation of $c(\lambda)$ versus λ is on the same curve as shown in Fig. 6.5. As a consequence, the pseudospectral solution of the Fokker-Planck equation provides a converged solution even though the continuum has not been treated rigorously. However, the analytic form of the time variation of the average energy, equivalently the temperature, very close to equilibrium (Corngold 1981; Shizgal 1991) has not been confirmed.

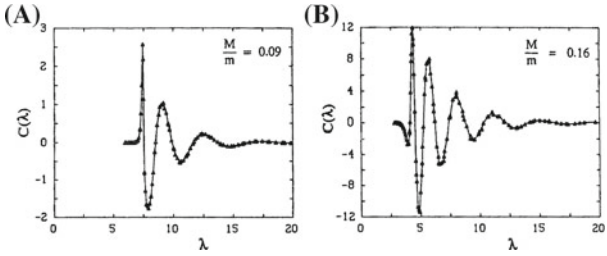

Fig. 6.5 Variation of the coefficients, $c(\lambda)$ (in units of 10^3) for the temperature relaxation versus the continuous eigenvalue, λ. $T(0)/T_b = 24$. The symbols are the numerical results for 4 different values of the scaling parameter. Reproduced from Shizgal (1991) with permission Beylich A.E.: Rarefied gas dynamics. In: Proceedings of the 17th International Symposium on Rarefied Gas Dynamics, Wiley-VCH Verlag GmbH and Co. KGaA. pp. 22–29, (1991)

6.4.2 *Fokker-Planck Equation for Wave Particle Heating of Ions; Kappa Distributions, and Tsallis Nonextensive Entropy*

Tsallis (1995) derived the Kappa distribution

$$f_\kappa(x) = C_\kappa \left[\frac{1}{1+\frac{x^2}{\kappa+1}}\right]^{\kappa+1}, \tag{6.107}$$

in the development of a new form of entropy functional for problems in statistical mechanics. In Eq. (6.107), $C_\kappa = 2\pi\Gamma(\kappa+1)/[\sqrt{\pi(\kappa+1)}]^3\Gamma(\kappa-\frac{1}{2})$ is a normalization such that $4\pi\int_0^\infty f_\kappa(x)x^2dx = 1$. In the limit, $\kappa \to \infty$, the Kappa distribution tends to a Maxwellian. The Tsallis nonextensive entropy formalism is a controversial topic (Nauenberg 2003; Tsallis 2004; Lutsko and Boon 2011).

In Chap. 4, we discussed the expansion of the Kappa distribution function, in Laguerre polynomials, Eq. (4.60). We demonstrated that the expansion in Laguerre polynomials is a divergent asymptotic series as the decay of $f_\kappa(x)$ as $x \to \infty$ is slower than that of the Laguerre weight function, $w(x) = \sqrt{x}e^{-x}$; see Fig. 4.9 (Mintzer 1965; Leblanc and Hubert 1997). It is clear that the normalization C_κ does not exist for $\kappa \to 1/2$. The average kinetic energy, that is the average of $mv^2/2$ with $f_\kappa(x)$, defines the nonequilibrium "temperature"

$$\frac{T_\kappa}{T_b} = \frac{\kappa+1}{\kappa-\frac{3}{2}}, \tag{6.108}$$

which also diverges for $\kappa \to 3/2$. A nonphysical feature of the Kappa distribution is that the nth moment diverges for $\kappa \to (n+1)/2$ (Treumann et al. 2004; Shizgal 2007). For this reason, Magnus and Pierrard (2008) could not generate the Gaussian quadrature weights and points for the Kappa distribution and used instead modified weight functions.

In space physics, the Kappa distribution has been employed to explain the nature of energetic distributions in space physics (Meyer-Vernet 2001; Livadiotis and McComas 2009), the heating of the solar chromosphere (Scudder 1994), the escape of charged particles from the solar atmosphere and from the high latitude terrestrial ionosphere known as the solar and polar winds, respectively (Pierrard et al. 2004; Pierrard and Lazar 2010). There is an ongoing effort in space physics to better understand the complex mechanism for the energization of ions and electrons by plasma waves (Schulz and Lanzerotti 1974; Stix 1992; Gary 1993).

One approach is based on a Fokker-Planck equation where the wave-particle interactions are modelled with a second diffusion operator (Nicholson 1983) that is

$$\frac{\partial f(x,t)}{\partial t} = \sqrt{\frac{m}{M}}\left(\frac{1}{x^2}\frac{\partial}{\partial x}\left[D_1(v_{th}x)(1+\frac{1}{2x}\frac{\partial}{\partial x})\right]f(x,t) + \frac{\alpha v_{th}}{2}\frac{1}{x^2}\frac{\partial}{\partial x}\left[x^2 D_2(v_{th}x)\frac{\partial}{\partial x}f(x,t)\right]\right), \tag{6.109}$$

where in the second differential operator term the parameter α is an adjustable parameter that controls the strength of the wave-particle interactions relative to the Coulomb collision rate. It is clear that for $\alpha = 0$, the steady state distribution is a Maxwellian. Equation (6.109) has been written in dimensionless time, $t = t'/t_0$, where $t_0 = [2N\sigma_{eff}\sqrt{2kT_b/M}]^{-1}$ and $\sigma_{eff} = [4\pi N Z^2 Z_b^2 e^4 \ln\Lambda]/(2kT_b)^2$.

The steady distribution obtained by setting $\partial f/\partial t = 0$ in Eq. (6.109) is given by

$$\frac{df_{ss}(x)}{f_{ss}(x)} = -\left[\frac{2x}{1+\alpha v_{th}x^3\frac{D_2(v_{th}x)}{\hat{D}_1(z)}}\right]dx, \tag{6.110}$$

where

$$\hat{D}_1(z) = \mathrm{erf}(z) - \frac{2z}{\sqrt{\pi}}e^{-z^2}, \tag{6.111}$$

with $z = \sqrt{\gamma}x$, $\gamma = M/m$. As a consequence of the wave-particle interaction diffusion term, the steady state solution of Eq. (6.109), $f_{ss}(v)$, is no longer a Maxwellian and depends on the ratio of the strength of the wave-particle diffusion term relative to the strength of Coulomb collisional relaxation, that is on α, as well as the mass ratio M/m. The velocity dependence of this steady-state distribution function depends on both $\hat{D}_1(z)$ and $D_2(v_{th}x)$.

The choice of the wave-particle diffusion coefficient has been discussed in the literature (Crew and Chang 1985; Stix 1992; Ma and Summers 1999; Vocks 2002; Shizgal 2007). There is at present no theoretical model for the occurrence of a Kappa distribution except for the works of Ma and Summers (1999) and Hasegawa et al. (1985). We consider the wave-particle diffusion coefficient to be of the form $D_2(v_{th}x) = 1/(v_{th}x)$ following on the work of Ma and Summers (1999). To reproduce the result obtained by them, one has to choose $D_2(v_{th}x) = 1/(v_{th}x)$ and

$v \gg v_{th}$, that is $\gamma \to \infty$ in which case $\hat{D}_1(z) \to 1$. Thus the mass dependence and the behaviour $\hat{D}_1(z) \approx z^{-3}$ as $z \to 0$ are not retained by setting $\hat{D}_1(z) \equiv 1$.

The steady state distribution function that is obtained in this limit is

$$\frac{df_\kappa(x)}{f_\kappa(x)} = -\left[\frac{2x}{1+\alpha x^2}\right] dx, \tag{6.112}$$

and when integrated leads to the Kappa distribution, Eq. (6.107). In this way, the adjustable κ parameter in exospheric models is interpreted in terms of the strength of wave-particle interactions and $\kappa = (1-\alpha)/\alpha$.

The steady state distribution, $f_{ss}(x)$, the Kappa distribution, $f_\kappa(x)$ and the Maxwellian are compared in Fig. 6.6 for two mass ratios and the arbitrary choice $\alpha = 1/8$. The steady state distribution has a more extended high energy tail than either the Kappa distribution or the Maxwellian. The mass ratios chosen correspond to O^+ and Fe^+ in the solar atmosphere. For the larger mass ratio the tail of the steady distribution is more extended than for the smaller mass consistent with the observed heating of the heavy minor ions in the solar atmosphere.

For this application, we use the Chang-Cooper finite difference algorithm described in Sect. 6.2.3 to integrate the Fokker-Planck equation given by Eq. (6.109) with an initial Maxwellian distribution. With this numerical method, there is no reference to the eigenvalue spectrum of the operator in Eq. (6.109) as we have done for all the other applications. The solutions converge provided that the grid spacing in the finite difference reduced speed discretization and the time step are sufficiently small. The evolution of the distribution functions showing the heating of the tail of the distributions is shown in Fig. 6.7a, b for $m/M = 16$ and 55.85, respectively. The increase in the temperature is shown in Fig. 6.7c for several heavy ions in the solar atmosphere. This heating is consistent with observations that the temperature of the

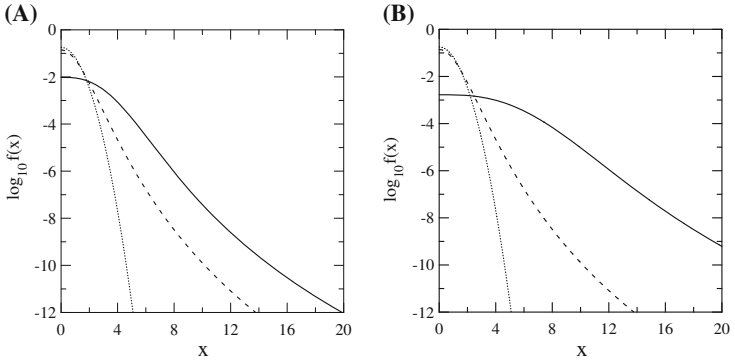

Fig. 6.6 Comparison of the Maxwellian (*dotted curve*), Kappa (*dashed curve*) and steady, $f_{st}(x)$ (*solid curve*) distributions. The diffusion coefficient for wave-particle interactions is $\hat{D}_2(x) = 1/x$, the mass ratio m/M and α are **(A)** 16, 1/8 **(B)** 55.845, 1/8. For the Kappa distribution, $\kappa = (1-\alpha)/\alpha$. Reprinted from Shizgal (2007) with permission from Springer

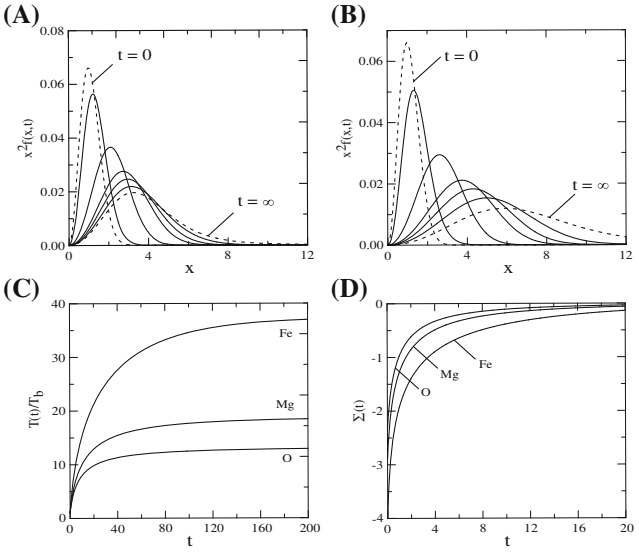

Fig. 6.7 Approach to a steady state distribution, $f_{ss}(x)$, with an initial Maxwellian and the inclusion of wave-particle energization; $\alpha = 0.25$ and $\hat{D}_2(x) = 1/x$. Successive distributions are at reduced times equal to 0.4, 2, 6, 10 and 20 for m/M equal to **(A)** 16 and **(B)** 55.85. **(C)** The heating of the gas is shown as $T(t)/T_b$ and **(D)** the Kulback entropy increases with time. The mass ratio, m/M, is equal to (O) 16, (Mg) 24.3 and (Fe) 55.85. Reprinted from (Shizgal 2007) with permission from Springer

minor ions in the solar atmosphere increases with mass (Pierrard et al. 2004).

In Fig. 6.7d, we show the monotonic increase in the Kullback–Leibler entropy functional defined by

$$\Sigma(t) = 4\pi \int x^2 f(x,t) \ln \frac{f(x,t)}{f_{ss}(x)} dx. \tag{6.113}$$

This final result demonstrates that the usual notions of entropy rationalizes the generation of a non-equilibrium distribution which is neither a Maxwellian nor a Kappa distribution. The nonextensive entropy formalism of Tsallis (1995) is not required as previously suggested (Collier 2004; Leubner and Vörös 2005) and references therein. A pseudospectral solution of the Fokker–Planck operator equation, Eq. (6.109), is of considerable interest, especially with concern to the properties of the eigenvalue spectrum of the operator with wave-particle interactions ($\alpha \neq 0$).

6.5 Fokker-Planck or Smoluchowski Equation for Bistable Potentials

Potentials $U(y)$, where y denotes a coordinate for internal rotation in a molecule about some symmetry axis, are known for many molecules including for example butane, C_4H_{10}, (Ryckaert and Bellemans 1978; Montgomery et al. 1979; Blackmore and Shizgal 1985b; Pastor and Karplus 1989; Travis and Searles 2006), hydrogen peroxide, HOOH, (Koput et al. 2001; Lin and Guo 2003; Lynch et al. 2004; Le et al. 2009) and chlorine peroxide, ClOOCl (Gomes and Pacios 1996). The cis-trans isomerization kinetics for such molecules can be modelled with a Fokker-Planck or Smoluchowski[5] equation of the form

$$\frac{\partial P(y,t)}{\partial t} = \frac{\partial}{\partial y}\left[U(y)P(y,t) + \frac{\partial B(y)P(y,t)}{\partial y}\right] = LP(y,t), \quad y \in (-\infty,\infty), \tag{6.114}$$

where y is a reaction coordinate.

A simple model for the isomerization kinetics used by many researchers (Larson and Kostin 1978; Bernstein and Brown 1984; Voigtlaender and Risken 1985; Blackmore and Shizgal 1985a, b; Cartling 1987; Drozdov 1999; Drozdov and Tucker 2001; Felderhof 2008) is defined with the drift and diffusion coefficients given by

$$U(y) = y^3 - y, \qquad B(y) = \epsilon. \tag{6.115}$$

This model potential is bimodal with two minima at $y = \pm 1$. The steady distribution is

$$P_0(y) = C\exp[-\frac{y^4}{4\epsilon} + \frac{y^2}{2\epsilon}], \tag{6.116}$$

and has two sharp maxima at $y = \pm 1$, especially for ϵ small as shown in Fig. 6.8. The constant C is a normalization. The model is also referred to as the quartic potential because of the form of $P_0(y)$. This type of Fokker-Planck equation with two stable states also has application to climate models (Nicolis and Nicolis 1981; Nicolis 1982; Shizgal and Chen 1997) and laser physics (Blackmore et al. 1986; Shizgal and Chen 1997). The recent work by (Blaise et al. 2012) provides an extensive bibliography on diffusion in a double well potential.

We study the time evolution of this system in terms of the eigenfunction expansion discussed in Sect. 6.2. The eigenvalues and eigenfunctions can be calculated numerically with the diagonalization of the spectral matrix representation of the linear

[5] Marian Smoluchowski (1872–1917) was a Polish physicist who was responsible for the development of fundamental concepts in statistical physics, kinetic theory and Brownian motion. His name is associated with integral equations for coagulation and a Fokker-Planck equation for chemical reactions.

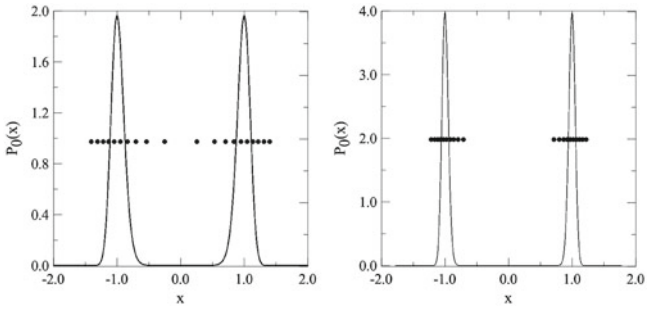

Fig. 6.8 Steady state bimodal distribution $P_0(x) = C\exp[-\frac{1}{\epsilon}(x^4/4 - x^2/2)]$ for $\epsilon = 0.02$ on the *left* and $\epsilon = 0.005$ on the *right*. The distribution of quadrature points with $N = 20$ is also shown

Fokker-Planck operator, L, defined by Eq. (6.114), that is

$$L_{mn}^{(sp)} = \int_{-\infty}^{\infty} w(y) B_n(y) L B_m(y) dy, \tag{6.117}$$

where the nonclassical polynomials, $B_n(y)$, are orthonormal with respect to the weight function, $w(y) = P_0(y)$, that is

$$\int_{-\infty}^{\infty} \exp\left[-\frac{1}{\epsilon}\left(\frac{y^4}{4} - \frac{y^2}{2}\right)\right] B_n(y) B_m(y) dx = \delta_{nm}, \tag{6.118}$$

as discussed in Chap. 2, Sect. 2.5.2.

Since $w(y)$ is even and the integrals are evaluated over $(-\infty, \infty)$, the recurrence coefficients, $\alpha_n = 0$. The polynomials $B_n(y)$ are even when n is an even number and odd when n is an odd number. After some detailed algebraic manipulations presented in Appendix B of Lo and Shizgal (2006), the symmetric matrix representation of the Fokker-Planck operator is given by

$$L_{mn}^{(sp)} = \begin{cases} -(\beta_2 + \beta_1 - 1), & m = n = 2, \\ (n-1)(\beta_n + \beta_{n-1} - 1) + 2\sum_{k=1}^{n-2} \beta_k, & m = n > 2, \\ (n-1)\sqrt{\beta_{n+1}\beta_n}, & m = n + 2, \\ (m-1)\sqrt{\beta_{m+1}\beta_m}, & m = n - 2, \\ 0 & \text{otherwise}, \end{cases} \tag{6.119}$$

where β_n are the recurrence coefficients in the three term recurrence relation discussed in Chap. 2. The eigenvalue problem is $L\psi_n(y) = -\lambda_n \psi_n(y)$, with L as defined by Eq. (6.114).

This matrix representation of the Fokker-Planck operator for the bimodal model is pentadiagonal where the off-diagonal elements for $m \neq n \pm 2$ are zero. As a

consequence, the eigenfunctions are odd or even and there is no coupling between them. Thus, the matrix representation $L_{nm}^{(sp)}$ can be split into two separate matrices, $\mathbf{L}^{even}$ with even n and m and $\mathbf{L}^{odd}$ with odd n and m. The spectrum of the Fokker-Planck operator is composed of a set of singlet and nearly degenerate triplets. With $B(y_i) = \epsilon$, the pseudospectral discrete matrix representation of the Fokker-Planck operator is given by Eq. (6.48)

$$L_{ij}^{(ps)} = -\epsilon \sum_{k=1}^{N} D_{ki} D_{kj}, \tag{6.120}$$

and yields the same eigenvalues and eigenfunctions as obtained with the spectral representation. However, $L_{ij}^{(ps)}$, is a full matrix and the symmetry properties of the problem as determined from the structure of $L_{nm}^{(sp)}$ are not apparent. As demonstrated in Chap. 2, the quadrature points are distributed nonuniformly within the domain, as shown in Fig. 6.8 for two choices of ϵ. Therefore, the pseudospectral approach is more flexible than the polynomial based spectral method as different weight functions can be easily used to improve the convergence. The matrix elements for such nonclassical basis functions may be difficult to calculate analytically as given by Eq. (6.119).

The convergence of the lower order eigenvalues for $\epsilon = 0.01$ is shown in Table 6.3 versus the number of quadrature grid points, N, for three different grids as defined by the weight functions shown in the table. As can be seen, the first nonzero eigenvalue λ_1 is extremely small relative to the other eigenvalues. The reciprocal of this eigenvalue represents the isomerization rate as discussed later. The three eigenvalues $\lambda_3 - \lambda_5$ are nearly degenerate and converge at different rates. The first set of results are obtained with the grid defined by $w_a(y) = P_0(y),\ \ y \in (-\infty, \infty)$.

The convergence can be improved by taking advantage of the symmetry of the eigenstates and calculating the even and odd eigenvalues with different weight functions, $w_b^{(e)}(y)$ and $w_b^{(o)}(y)$, $y \in [0, \infty)$, as shown in the middle of the table. The convergence requires about half the number of quadrature points as with $w_a(y) = P_0(y)$ over the whole interval. The bottom portion of the table shows the convergence with the uniform grid for the Sinc collocation method (SCM) (Wei 1999; Amore 2006) as well as a comparison with the limited results by Dekker and van Kampen (1979).

The convergence of the eigenvalues for $\epsilon = 0.001$ is shown in Table 6.4 and a third weight function is chosen in order to accelerate the convergence. The weight function is $w_c(y) = P_0(y) + \exp(-\frac{y^2}{2\epsilon})$ where the added exponential term yields quadrature points in the middle of the interval near the origin. The convergence of the eigenvalues is extremely rapid relative to the Sinc collocation method with a uniform grid.

The distribution of quadrature points relative to the bimodal potential is shown in Fig. 6.9 for three values of ϵ. The distribution of grid points is uniform for all three values with the SCM. The quadrature points labelled QDM (a) are densely distributed over the region of the outermost potential wells. The acronym QDM is for the Quadrature Discretization Method which is the pseudspectral representation given by Eq. (6.120). The quadrature points for QDM (b) are defined over the interval

$x \in [0, \infty)$ and are more densely distributed near the origin. The points for QDM (c) are distributed densely about the origin. The rate of convergence of the eigenvalues in Tables 6.3 and 6.4 is consistent with the distribution of the quadrature points for these different weight functions.

The structure of the eigenvalue spectrum is made clearer by considering the transformation to a Schrödinger equation and one finds the potential

$$V(y) = \frac{y^2(y^2-1)^2}{4\epsilon} - \frac{1}{2}(3y^2-1), \tag{6.121}$$

which has three minima at

$$y^0 = 0, \quad y^{\pm} = \pm\sqrt{\left[\frac{2}{3} + \sqrt{\frac{1}{9} + 2\epsilon}\right]}. \tag{6.122}$$

Table 6.3 Convergence of the eigenvalues of the Fokker-Planck operator with the bistable potential, $U(y) = y^3 - y$; $\epsilon = 0.01$

N	λ_1	λ_2	λ_3	λ_4	λ_5
$w_a(y) = \exp[-(\frac{y^4}{4\epsilon} - \frac{y^2}{2\epsilon})]/\exp(1/4\epsilon)$; $y \in (-\infty, \infty)$					
12	5.0833 (−8)		1.866176	1.865861	
24	3.6651 (−11)		1.865757	1.865753	
36	7.0354 (−12)	1.388230	1.865752	1.865758	2.664871
48	6.1809E-12	0.994289	1.865735	1.865754	1.956370
60	6.15499 (−12)	0.968472	1.865337		1.869329
72	6.15466 (−12)	0.967870	1.864560		1.866993
84	6.15465 (−12)	0.967865	1.864542		1.866975
$w_b^{(e)}(y) = w_a(y)$; $w_b^{(o)}(y) = y^2 w_a(y)$; $y \in [0, \infty)$					
12	6.4259 (−12)	1.256087	1.865747	1.865757	2.113341
15	6.1656 (−12)	0.990778	1.865720	1.865754	1.913825
18	6.1405 (−12)	0.969092	1.865601		1.875631
24	6.1424 (−12)	0.967879	1.864549		1.866982
27	6.1436 (−12)	0.967865	1.864542		1.866975
30	6.1427 (−12)	0.967864			
Sinc collocation method $x_{max} = 2.2$					
12	7.4085 (−1)	1.076821	3.336192	3.321671	1.574892
24	3.3865 (−3)	0.967915	1.931199	1.930972	1.865051
36	−4.8093 (−5)	0.967864	1.864066	1.864927	1.866629
48	1.7533 (−8)		1.864542	1.865754	1.866975
60	7.9956 (−12)				
DvK[a]		0.968	1.862		1.867

Reprinted from Lo and Shizgal (2006) with permission of the American Institute of Physics
[a] Dekker and van Kampen (1979)

Table 6.4 Convergence of the eigenvalues of the Fokker-Planck operator with the bistable potential, $U(x) = x^3 - x$; $\epsilon = 0.001$

N	λ_2	λ_3	λ_4	λ_5
$w_c(y) = \exp[-(\frac{y^4}{4\epsilon} - \frac{y^2}{2\epsilon})]/\exp(\frac{1}{4\epsilon}) + \exp(-\frac{y^2}{2\epsilon})$				
6	0.9980526	2.0000470	2.0200067	2.0694590
12	0.9969809	1.9878205	1.9880010	1.9881554
18	0.9969817	1.9878873	1.9878903	1.9878937
24		1.9878896	1.9878896	1.9878893
30				1.9878896
Sinc collocation method $x_{max} = 1.2$				
12	3.4140030	21.7611343	21.7517512	3.4979300
24	1.2875835	8.5716393	8.5704015	1.6476678
36	1.0279928	4.1568953	4.1569000	1.7776398
48	0.9984717	2.5344712	2.5345542	1.9649680
60	0.9970079	2.0928734	2.0928574	1.9872886
72	0.9969819	1.9995592	1.9995565	1.9878842
84	0.9969817	1.9884160	1.9884156	1.9878896
96		1.9878838	1.9878838	
108		1.9878884	1.9878884	
120		1.9878896	1.9878896	

Reprinted from Lo and Shizgal (2006) with permission of the American Institute of Physics

In the limit $\epsilon \to 0$, the potential barriers between the two minima become larger and the potentials near the minima are quadratic, that is,

$$\lim_{\epsilon\to 0} V^{\pm}(y) \to \frac{(y - y^{\pm})^2}{\epsilon} - 1, \quad y \approx y^{\pm}, \tag{6.123}$$
$$\lim_{\epsilon\to 0} V^{0}(y) \to \frac{y^2}{4\epsilon} + \frac{1}{2} \quad y \approx 0.$$

and the corresponding eigenvalues are

$$\lim_{\epsilon\to 0} \lambda_k^{\pm} \to 2k, \quad k = 0, 1, 2, \ldots \tag{6.124}$$
$$\lim_{\epsilon\to 0} \lambda_k^{0} \to k + 1, \quad k = 0, 1, 2, \ldots$$

Thus in the very small ϵ limit the eigenvalues approach integer values, the zero eigenvalue is doubly degenerate and the remaining even eigenvalues are triply degenerate.

The importance of the distribution of grid points is illustrated in Fig. 6.9 where the grid points are shown in relation to the potentials in the Schrödinger equation. For $\epsilon = 0.1$ in Fig. 6.9a, the grid points are well distributed in the two wells of the potential. For $\epsilon = 0.01$, the potential has a minimum near the origin and $w_a(y) = P_0(y)$ does not properly capture the eigenfunction in this region whereas the quadrature

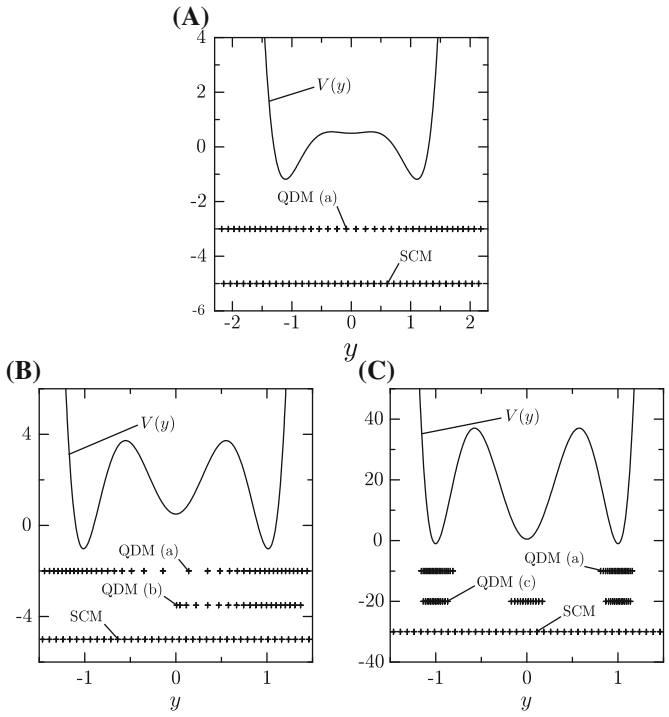

Fig. 6.9 The bimodal potential, $V(y)$, for ϵ equal to **(A)** 0.1, **(B)** 0.01 and **(C)** 0.001. The quadrature points with weight functions $w_a(y) = \exp[-(\frac{y^4}{4\epsilon} - \frac{y^2}{2\epsilon})]/\exp(1/4\epsilon)$; $y \in (-\infty, \infty)$, $w_b^{(e)}(y) = w_a(y) \quad y \in [0, \infty)$; $w_b^{(o)}(y) = y^2 w_a(y)$; $y \in [0, \infty)$ and $w_c(y) = \exp[-(\frac{y^4}{4\epsilon} - \frac{y^2}{2\epsilon}]\exp(\frac{1}{4\epsilon}) + \exp(-\frac{y^2}{2\epsilon})$ are shown. Reprinted from Lo and Shizgal (2006) with permission of the American Institute of Physics

over the positive interval defined with $w_b(y), \quad y \in [0, \infty)$ has more quadrature points close to the origin than does $w_a(y), \quad y \in (-\infty, \infty)$. For $\epsilon = 0.001$, we use a weight function centred about the origin together with $w_a(y)$. These results illustrate the flexibility of a pseudospectral method based on nonclassical weight functions that accelerate the convergence.

The variation of the eigenvalues versus ϵ is shown in Fig. 6.10. The top graph illustrates the very rapid decrease of λ_1 with decreasing ϵ. This eigenvalue represents the slowest mode and the reciprocal can be identified with the long time isomerization rate coefficient. The division of the other eigenvalues into singlet and triplet states is shown in the bottom graph with the triplet states converging to integer values for $\epsilon \to 0$. The objective of such modelling is to determine the nonequilibrium isomerization rate coefficient.

The cis-trans isomerization of n-butane has been studied by numerous researchers (Ryckaert and Bellemans 1978; Montgomery et al. 1979; Pastor and Karplus 1989; Shizgal et al. 1991; Travis and Searles 2006) with a particular potential reported by Montgomery et al. (1979) and also used by Marechal and Moreau (1984).

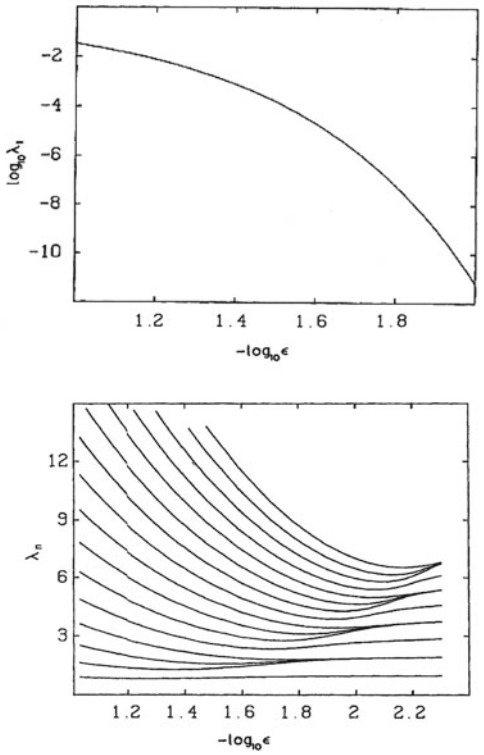

Fig. 6.10 Eigenvalue spectrum of the Fokker-Planck operator for the bistable potential; (*Top graph*) Variation of the smallest nonzero λ_1 eigenvalue versus ϵ. (*Bottom graph*) Variation of the higher eigenvalues showing the splitting into singlet and triplet states. Reprinted from Blackmore and Shizgal (1985a); Copyright 1985 by the American Physical Society

The solution of the time dependent Fokker-Planck equation for an initial delta function, $\delta(y - y_0)$, with all of the particles in one well at y_0 is given by

$$P(y,t) = \sum_{n=0}^{\infty} \psi_n(y_0)\psi_n(y)e^{-\lambda_n t}, \tag{6.125}$$

where λ_n are the eigenvalues of the Smoluchowski operator, L, in Eq. (6.114). The eigenvalues are calculated with the pseudospectral method with quadrature points and weights defined with the equilibrium density, $P_0(y)$ and the associated discrete derivative operator in physical space (Blackmore and Shizgal 1985a).

The number density of isomers in the potential well on the right for $y \in [0, \infty)$ is denoted by $N_A(t)$ and the isomerization rate equation is defined by

$$\frac{dN_A(t)}{dt} = -k(t)\left[N_A^{eq} - N_A(t)\right]. \tag{6.126}$$

where the nonequilibrium time dependent rate coefficient is determined from the time dependent reactive flux over the barrier. From a correlation function formalism (Montgomery et al. 1979; Marechal and Moreau 1984; Blackmore and Shizgal 1985a), the time dependent nonequilibrium rate coefficient can be written in the form

$$k(t) = \sum_{n=0}^{\infty} A_n e^{-\lambda_n t}, \tag{6.127}$$

with the A_n coefficients given by

$$A_n = \lambda_n \left[\int_0^{\infty} \psi_n(y) dy \right]^2, \tag{6.128}$$

and determined numerically with the nonclassical quadrature points. The details of this calculation were provided by Blackmore and Shizgal (1985a).

The nonequilibrium rate coefficient is compared with the transition state theory estimate given by

$$k_{tst} = S(0)\sqrt{\frac{k_B T_b}{2\pi m}}, \tag{6.129}$$

where

$$S(y) = \frac{e^{-U(y)/k_B T_b}}{\int_{-\infty}^{\infty} e^{-U(y)/k_B T_b} dy}.$$

The time dependent rate coefficient for butane isomerization in the potential reported by Montgomery et al. (1979) is summarized in Fig. 6.11. The time dependent rate coefficient given by Eq. (6.127) relative to the equilibrium transition state theory (tst) rate coefficient, Eq. (6.129), is shown in the figure as the solid curves *(a)* and *(b)*. The curve labelled *(b)* is for the potential as reported and the one labelled *(a)* is for an harmonic fit to this potential. The curve denoted by MM and MCB are the results by Marechal and Moreau (1984) and the simulations by Montgomery et al. (1979), respectively. There are many reactive systems and diffusion processes that are modelled with the Smoluchowski equation (Szabo et al. 1980; Bagchi et al. 1983; Chavanis 2006; Felderhof 2008) including protein folding (Bicout and Szabo 2000), dielectric relaxation (Coffey et al. 2009) and a Smoluchowski equation with a capture term (Spendier et al. 2013) that overlaps in some respects the studies of the nonequilibrium reactive system in Sect. 5.4.4.

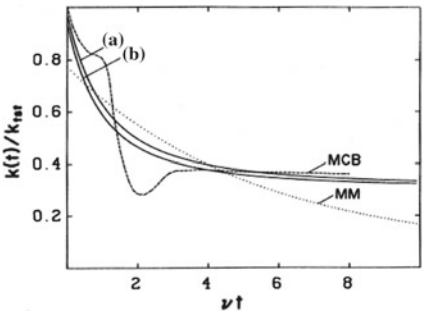

Fig. 6.11 The time dependent nonequilibrium rate coefficient for butane isomerization with the potential reported by Montgomery et al. (1979) *(b)* and with an harmonic fit to the potential *(a)*. The *dashed curve* (MM) is the result by Marechal and Moreau (1984) and the *dotted curve* (MCB) is the result by Montgomery et al. (1979). The collision frequency $\nu = 3 \times 10^{12}$ sec^{-1}. Reprinted with permission from Blackmore and Shizgal (1985a); Copyright 1985 by the American Institute of Physics

6.6 Kramers Equation and Nonequilibrium Chemical Kinetics; A Spectral Solution

It has been long recognized that reactive processes for gaseous systems proceed with the perturbation of the species velocity distribution functions from Maxwellian (Ross and Mazur 1961; Shizgal and Karplus 1970; Shizgal and Napier 1996; Kustova and Giordano 2011; Dziekan et al. 2012). These analyses of the departure from Maxwellian are based on the Boltzmann equation. The fundamental quantities that define the Boltzmann equation are the cross sections for elastic and reactive collisional processes. We considered spectral methods of solution of the chemical kinetic Boltzmann equation in Chap. 5, Sect. 5.4.4. The theoretical description of the kinetics of isomerization reactions presented in Sect. 6.5 based on the Fokker-Planck or equivalently the Smoluchowski equation in position space assumed a Maxwellian distribution function of the particles in velocity space.

The Kramers equation (Kramers 1940) for the distribution function, $f(r, v, t)$, of a test particle at position r and velocity v, at time t in the potential $U(r)$ is given by

$$\frac{\partial f}{\partial t} - v\frac{\partial f}{\partial r} - \frac{F}{m}\frac{\partial f}{\partial v} = \nu\frac{\partial}{\partial v}\left(v + \frac{k_B T_b}{m}\frac{\partial}{\partial v}\right) f. \tag{6.130}$$

The equation is comparable to the Boltzmann equation in Chap. 5, Eq. (5.30) with a drift term on the left hand side and a collision term on the right hand side. The force $F = -\partial U(r)/\partial r$ is derivable from an internal potential $U(r)$. The collision term is a particular choice which can be recognized as the Ornstein-Uhlenbeck Fokker-Planck operator in Sect. 6.1.2. The strength of the collision operator is denoted by the collision frequency ν. Kramers equation is generally used to model isomerization reactions in liquids for which the potential is the internal molecular torsional potential

about a symmetry axis in a molecule with cis-trans isomers. The frequency ν is related to the viscosity of the background liquid in which the isomerization rate is measured. There exists experimental data of the isomerization rates versus the viscosity of the liquid. The magnitude of ν reflects the strength of the coupling of the nonequilibrium system with the surroundings at equilibrium. When ν is large, the coupling is strong and the velocity distribution function approaches the equilibrium Maxwellian distribution at the heat bath temperature, T_b.

We continue the analogy of Kramers equation with the Boltzmann equation and relate the problem to rarefied gas dynamical problems where instead of ν we have the Knudsen number, 1/Kn, playing a similar role. In the small Kn collision dominated regime, departures from equilibrium are small and pertubation type methods such as the Chapman-Enskog method work remarkably well. The other extreme is the almost fully collisionless situation when Kn is very large and the Boltzmann equation can be solved with Liouville's theorem. It is the intermediate situation when Kn ≈ 1 that is the most difficult to treat theoretically.

A review of the many different applications of Kramers equation in chemistry and physics is beyond the scope of this book. The reader is directed to the excellent review by Hänggi et al. (1990) that provides a large bibliography up to about 1990. Another good overview is the book by Risken and Till (1996). A more recent summary was provided by Pollak and Talkner (2005). References 1–40 in the introduction section of the paper by Voigtlaender and Risken (1985) refers to a large number of applications of the Kramers equation. Numerical methods for the efficient solution of the Kramers equation are of considerable importance (Berezhkovskii et al. 1996; Bicout et al. 2001; Schindler et al. 2005; Bi and Chakraborty 2009; Coffey et al. 2009; Müller et al. 2012).

In this section we describe a particular pseudospectral method of solution of the Kramers equation with the symmetric bistable double Morse potential introduced by Garrity and Skinner (1983) given by

$$U(r) = \frac{U_m}{[1 - e^{-br_0}]^4}\left[1 - e^{-b(r_0+r)}\right]^2\left[1 - e^{-b(r_0-r)}\right]^2, \tag{6.131}$$

where r is an internal spatial coordinate, r_0 and $-r_0$ are the positions of the minima and br_0 is a parameter which controls the width of the barrier of height U_m that separates cis-trans isomers, as in the previous section. The potential is shown for two values of br_0 in Fig. 6.12.

The "collision" operator on the right hand side of Eq. (6.130) that describes the coupling of the system with the surrounding heat bath is the Ornstein-Uhlenbeck Brownian motion Fokker-Planck operator discussed in Sect. 6.1.2. This is not the only choice for the operator that couples the reactive system with the surrounding heat bath. Garrity and Skinner (1983) used the Bhatnagar–Gross–Krook (Bhatnagar et al. 1954) model of the Boltzmann collision operator. The correspondence between the Boltzmann equation and the Kramers equation was made in the paper by Skinner and Wolynes (1980) and they proposed alternate collision operators in the Kramers equation that couple the reactive system with the heat bath.

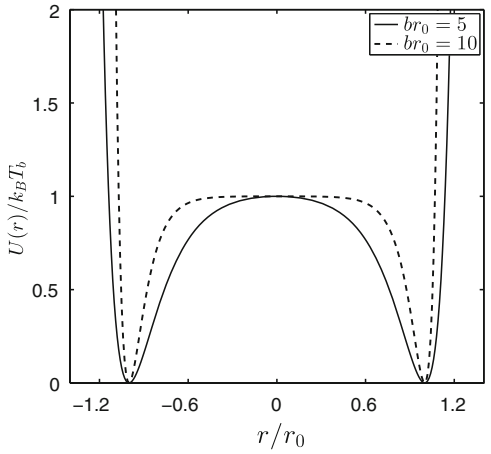

Fig. 6.12 The model bimodal double Morse potential (Garrity and Skinner 1983)

In the high collision frequency limit, $\nu \rightarrow \infty$, the Kramers equation can be transformed to the Smoluchowski equation (Risken 1996; Gardiner 2003) for the distribution in r. This transformation involves the integration over the Maxwellian velocity distribution for the probability density in position (Blackmore 1985)

$$P(r,t) = \int_{-\infty}^{\infty} f(r,v,t)dv, \tag{6.132}$$

and the result is the Smoluchowski equation

$$\frac{\partial P}{\partial t} = L_S P, \tag{6.133}$$

where L_S is defined by,

$$L_S P = \frac{1}{\nu m}\frac{\partial U^{'}(r)P}{\partial r} + D\frac{\partial^2 P}{\partial r^2}, \tag{6.134}$$

and $D = k_B T_b/m\nu$ is the diffusion coefficient as treated in the previous section.

The theoretical maximum reaction rate is the transition state theory (tst) estimate. The extent of the nonequilibrium reactive effects is determined by the magnitude of the coupling of the reactive system with the heat bath. If the coupling is strong, the nonequilibrium effects are small and conversely if the coupling is weak, the nonequilibrium effects can be large. This is similar to the treatment in Chap. 5 with the chemical kinetic Boltzmann equation where the elastic cross section controls the coupling with the heat bath.

The collision frequency ν plays the same role in Kramers equation as does 1/Kn in gas kinetic theory. We are interested in the solution of Kramers equation over the whole range of friction coefficient. In the large collision frequency limit, the Kramers equation is approximated by the Smoluchowski equation.

The Kramers equation in dimensionless variables, $x = v\sqrt{m/2kT}$, $\rho = r/r_0$, and $t' = t\nu/2$, is

$$\begin{aligned}\frac{\partial P(x,\rho,t)}{\partial t'} &= \frac{\partial}{\partial x}\left[\frac{\partial}{\partial x} + 2x\right]P(x,\rho,t) - \frac{1}{\nu}\left[2\nu\frac{\partial}{\partial \rho} - V(\rho)\frac{\partial}{\partial x}\right]P(x,\rho,t)\\ &= L_K P(x,\rho,t),\end{aligned} \tag{6.135}$$

where $\gamma = \sqrt{mr_0^2\nu^2/2kT}$ is the friction coefficient and

$$V[\rho(r)] = -\frac{1}{kT}\frac{dU(r)}{dr}. \tag{6.136}$$

We expand the probability density in the eigenfunctions of the Kramers operator, L_K. The eigenfunctions and eigenvalues can be complex as the Kramers operator is not Hermitian. We expand the eigenfunctions in Hermite polynomials in velocity v and in the eigenfunctions of the Smoluchowski operator in the spatial coordinate ρ. The Hermite polynomials are the eigenfunctions of the Ornstein-Uhlenbeck "collision" operator as discussed in Sect. 6.1.2.

The system is initially prepared to be entirely in one of the potential wells, that is

$$P(x,\rho,0) = \begin{cases} P_0(x,\rho), & \rho > 0,\\ 0, & \text{otherwise,}\end{cases} \tag{6.137}$$

where the equilibrium distribution is

$$P_0(x,\rho) = Ne^{-x^2}\exp\left(\int^{\rho} V(\rho')d\rho'\right), \tag{6.138}$$

and N is a normalization constant.

We expand $P(x,\rho,t)$ in the eigenfunctions of L_K,

$$P(x,\rho,t') = \sum_{n=0}^{\infty} a_n e^{-\lambda_n t'}\Psi_n(x,\rho), \tag{6.139}$$

where

$$L_K\Psi_n(x,\rho) = -\lambda_n\Psi_n(x,\rho). \tag{6.140}$$

The expansion coefficients, a_n, are determined by the initial condition,

$$a_n = \int_{-\infty}^{\infty}\int_{-\infty}^{\infty} P(x,\rho,0)\Psi_n^*(x,\rho)/P_0(x,\rho)dxd\rho,$$
$$= \int_{0}^{\infty}\int_{-\infty}^{\infty} \Psi_n^*(x,\rho)dxd\rho. \tag{6.141}$$

With Eq. (6.139), it can be shown (Shizgal et al. 1991) that the time dependent relaxation time is given by

$$\tau^{-1}(t') = \sum_{n=0}^{\infty} A_n \exp(-\lambda_n^r t')\left[\lambda_n^r \cos(\lambda_n^i t') + |\lambda_n^i| \sin(|\lambda_n^i| t')\right], \tag{6.142}$$

where $\lambda_n = \lambda_n^r + i\lambda_n^i$ are the complex eigenvalues and

$$A_n = a_n \int_{-\infty}^{\infty}\int_{0}^{\infty} P_n(x,\rho)dxd\rho.$$

For a sufficiently large barrier separating the two minima, λ_1 will be much less than the higher eigenvalues and the relaxation time will tend to the limiting value,

$$\frac{1}{\tau} \to \lambda_1 A_1, \tag{6.143}$$

as $t \to \infty$. This result also requires that A_1 is of the order of unity and the remaining coefficients A_n are very much smaller (Blackmore and Shizgal 1985b).

We compare the results obtained with Eq. (6.143) with the transition state theory (tst) value of the relaxation time

$$\frac{1}{\tau_{tst}} = S(0)\sqrt{kT/2\pi m}, \tag{6.144}$$

where

$$S(r) = e^{-U(r)/kT} / \int_{-\infty}^{\infty} \exp[-U(r')/kT]dr'. \tag{6.145}$$

It is important to note that this result is independent of ν.

The eigenvalue equation for the Kramers operator, $L_K \Psi_n = -\lambda_n \Psi_n$, is written in terms of the eigenfunctions, $\phi_n(x, \rho) = \Psi_n / P_0$ which satisfy the eigenvalue problem,

$$\tilde{L}_K \phi_n = [\frac{\partial}{\partial x} - 2x]\frac{\partial}{\partial x}\phi_n - \frac{1}{\gamma}[2x\frac{\partial}{\partial \rho} - V(\rho)\frac{\partial}{\partial x}]\phi_n = -\lambda_n \phi_n. \tag{6.146}$$

Since the first operator in x alone is diagonal in the Hermite polynomials, $H_j(x)$ (normalized to unity), we consider the expansion

$$\phi_n(x, \rho) = \sum_{j=0}^{\infty} c_j(\rho) H_j(x), \tag{6.147}$$

in Eq. (6.146) and find that the coefficients satisfy the set of operator equations (Brinkmann 1956; Risken and Till 1996; Blackmore and Shizgal 1985b; Shizgal et al. 1991),

$$\sum_{j=0}^{\infty}\left(2j\delta_{jk} + \frac{\sqrt{2j}}{\gamma}\left[\frac{\partial}{\partial x}\delta_{j,k-1} + (\frac{\partial}{\partial \rho} - V(\rho))\delta_{j,k+1}\right]\right) c_j(\rho) = \lambda_n c_k(x). \tag{6.148}$$

Equation (6.148) is a tri-diagonal system of coupled differential operator equations in the spatial variable (Brinkmann 1956; Risken and Till 1996).
The eigenfunctions, $S_\ell(x)$, of the Smoluchowski operator, $\tilde{L}_S$, defined by,

$$\tilde{L}_S S_\ell(\rho) = -\frac{1}{\gamma^2}\left[\phi(\rho) - \frac{\partial}{\partial \rho}\right]\frac{\partial}{\partial \rho} = -\lambda_\ell^S S_\ell(\rho), \tag{6.149}$$

are used as nonclassical basis functions to expand

$$c_j(\rho) = \sum_{\ell=0}^{\infty} d_{j\ell} S_\ell(\rho). \tag{6.150}$$

The set of eigenvalue differential operator equations, Eq. (6.148), reduces to the matrix eigenvalue equation

$$\sum_{k'=0}^{\infty}\sum_{\ell'=0}^{\infty}\left(2k\delta_{k,k'}\delta_{\ell,\ell'} - \sqrt{2(k+1)}\delta_{k',k+1}G_{\ell',\ell}/\gamma + \sqrt{2k}\delta_{k',k-1}G_{\ell,\ell'}/\gamma\right) d_{k',\ell'} = \lambda d_{k,\ell}. \tag{6.151}$$

The quantities

$$G_{\ell,\ell'} = \int_{-\infty}^{\infty} v(\rho) S_\ell(\rho) \frac{dS_{\ell'}(\rho)}{d\rho} d\rho, \tag{6.152}$$

are the matrix elements of the derivative operator over the spatial variable with the eigenfunctions of the Smoluchowski operator, where the weight function is $v(\rho) = \exp(-\int^{\rho} V(\rho')d\rho')$. These eigenfunctions form the nonclassical basis set for the solution of the Kramers equation.

The eigenfunctions of the Smoluchowsi operator which define the $G_{\ell,\ell'}$ matrix elements are determined with the pseudospectral solution of the Smoluchowski equation as discussed in Sect. 6.5. This particular numerical approach permits the efficient numerical evaluation of the derivative of the eigenfunctions with the derivative matrix operator, **D**, and the evaluation of the matrix elements with the associated quadrature. These matrix elements are evaluated with the derivative operator and quadrature as

$$\boxed{G_{\ell\ell'} = \sum_{m=1}^{M} w_m \frac{v(x_m)}{w(x_m)} S_\ell(x_m) \sum_{m'=1}^{M} D_{mm'} S_{\ell'}(x_m),} \tag{6.153}$$

where

$$w(x) = \exp[-U_m(x^4 - 2x^2)/(k_B T_b)],$$

defines the quadrature points, x_m and weights, w_m. Thus we make use of both the pseudospectral derivative evaluation and the Gaussian quadrature, both for the nonclassical Smoluchoski eigenfunctions as basis functions. It is useful to mention that the matrix elements $G_{\ell\ell'}$ are the representations of the derivative operator in the basis set of Smoluchowski eigenfunctions.

A detailed consideration of the form of Eq. (6.151) shows that the characteristic polynomial which determines the eigenvalues factors into two polynomials, with eigenvalues that correspond to even and odd eigenfunctions (Voigtlaender and Risken 1985), and the dimensionality of the eigenvalue problem is reduced. The reaction rate, which is given by λ_1, is of primary interest. Consequently, the eigenfunction corresponding to this eigenvalue must satisfy the conditions, $P_1(x, -\rho) = -P_1(x, \rho)$ and $P_1(-x, \rho) = P_1(x, \rho)$. Since the overall parity is odd, the eigenvalue λ_1 can be determined by restricting the calculation to the space of odd eigenfunctions.

Table 6.5 shows the convergence of λ_1 versus the number of Hermite polynomials M and the number of Smoluchowski eigenfunctions N for $br_0 = 4$. The convergence of this eigenvalue is very rapid for large γ as expected in view of the use of the Smoluchowski eigenfunctions as basis functions. We show the results only for an even number of Smoluchoswki basis functions, N even. The results for N odd are nonphysical as λ_1 increases with N. This feature of the matrix representation of the Kramers operator has been interpreted and discussed in detail by Shizgal et al. (1991).

Table 6.5 Convergence of λ_1 of the Kramers operator in units of 10^{-2} ($\sqrt{k_B T_b/2m}/r_0$); $br_0 = 4$; $U_m/k_B T_b = 5$

N/M	4	10	16	22
$\gamma = 2$				
4	1.876			
10	2.256	2.043		
16	2.268	2.050	2.049	
22	2.267	2.049		
$\gamma = 1$				
4	2.295	2.158		
10	2.968	2.317	2.119	
16	3.020	2.118	2.159	2.157
22	3.022	2.172	2.154	2.153
$\gamma = 0.4$				
4	3.202	2.525		
10	2.572	1.529	1.377	1.359
16	2.669	1.637	1.506	1.478
22	2.679	1.623	1.497	1.470
$\gamma = 0.1$				
4	4.742	1.474		
10	2.003	0.6823	0.470	0.448
16	2.099	0.828	0.665	0.599
22	2.110	0.790	0.634	0.574

Reproduced from (Shizgal et al. 1991) with permission Beylich A.E.: Rarefied gas dynamics. In: Proceedings of the 17th International Symposium on Rarefied Gas Dynamics, Wiley-VCH Verlag GmbH and Co. KGaA. pp. 85–92, (1991)

The variation of the relaxation rate relative to the transition state estimate is shown in Fig. 6.13 versus the friction coefficient. The present method of calculation of these isomerization rates gives reliable estimates down to $\gamma = 0.05 - 0.1$. This variation of the reaction rate with γ with a maximum at some intermediate γ is referred to as the "turnover" problem that has been investigated experimentally and theoretically since the publication of Kramers paper (Kramers 1940). It is the turnover of the graph in the Figure that has been difficult to calculate. With increasing γ, the convergence becomes more rapid.

There have been and continue to be many experimental studies of the isomerization rates in different solvents with different viscosities. The viscosity is related to the friction coefficient, γ, and thus the turnover in Fig. 6.13 has been verified experimentally (Pollak et al. 1989; Anna and Kubarych 2010; Pollak and Ianconescu 2014).

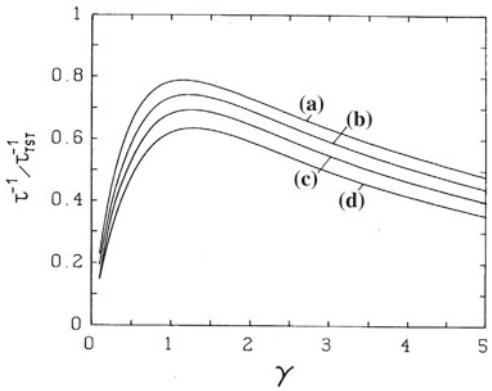

Fig. 6.13 The ratio $\tau^{-1}/\tau_{TST}^{-1}$ versus the friction coefficient γ demonstrates the classic "turnover problem". The value of br_0 is equal to *(a)* 0, *(b)* 2, *(c)* 3 and *(d)* 4. Reproduced from (Shizgal et al. 1991) with permission Beylich A.E.: Rarefied gas dynamics. In: Proceedings of the 17th International Symposium on Rarefied Gas Dynamics, Wiley-VCH Verlag GmbH and Co. KGaA. pp. 85–92, (1991)

6.7 Sturm-Liouville Problems and the Schrödinger Equation

The Sturm-Liouville problem (Pryce 1993; Al-Gwaiz 2008) refers to the solution, either analytically or numerically, of the eigenvalue problem

$$L\psi_n(x) = \lambda_n w(x)\psi_n(x), \tag{6.154}$$

where $w(x) > 0$ is a weight function and L is the second order differential operator, defined by

$$Lf(x) = \frac{d}{dx}\left[p(x)\frac{df(x)}{dx}\right] + q(x)f(x). \tag{6.155}$$

It is useful to notice that this operator is in the form of a diffusion equation where $p(x)$ is a diffusion coefficient in a Fokker-Planck equation and $q(x)$ is a gain or loss term. We assume that $p(x) > 0$, $dp(x)/dx$, $q(x)$ and $w(x) > 0$ are real valued and piecewise continuous. Any linear second order differential equation can be written in this form. The eigenfunction, $\psi_n(x)$, defined on the interval $[a, b]$ is subject to two homogeneous boundary conditions which are linear combinations of the value of the function and derivative at the two interval end points and are of the form

$$\begin{aligned} A_1\psi_n(a) + B_1\psi_n'(a) &= 0, \\ A_2\psi_n(b) + B_2\psi_n'(b) &= 0, \end{aligned} \tag{6.156}$$

where for $A_k = 0$ we have a Neumann boundary condition and if $B_k = 0$ we have a Dirichlet boundary condition.

In Sect. 6.2.1 we demonstrated the self-adjoint property of the Fokker-Planck operators subject to zero flux boundary conditions. The linear operator defined by the Sturm-Liouville problem is self-adjoint with respect to the boundary conditions, Eq. (6.156).

With the transformation of the independent variable from x to y,

$$y = \int \sqrt{w(x)/p(x)}dx, \tag{6.157}$$

and the transformation of the dependent variable $\psi_n(x)$ to $\phi_n(y)$ of the form

$$\psi_n(x) = m(x)\phi_n[y(x)], \tag{6.158}$$

where $m(x) = [p(x)w(x)]^{-1/4}$, the Sturm-Liouville equation can be written in so-called Liouville normal form which is identical to a Schrödinger equation of the form

$$-\frac{d^2\phi_n(y)}{dy^2} + V(y)\phi_n(y) = \lambda_n\phi_n(y), \tag{6.159}$$

where the potential function $V(y)$ is

$$V(y) = \frac{q[x(y)]}{w[x(y)]} + m[x(y)]\frac{d^2}{dy^2}\left(\frac{1}{m[x(y)]}\right). \tag{6.160}$$

as derived by Pryce (1993).

6.7.1 Classical Polynomials as Eigenfunctions of the Sturm-Liouville and Schrödinger Equations

The classical polynomials discussed in this chapter (and other orthogonal polynomials) satisfy a Sturm-Liouville eigenvalue problem related to an associated Schrödinger equation. Many of the details of these relationships can be found in standard textbooks so we here outline the main results and the reader is referred to other references for a complete development. We presented a preliminary discussion in Sect. 3.9.3.

6.7.2 Legendre Polynomials; Quantized Rotational States of a Rigid Rotor

The rigid rotor model for a diatomic molecule has a fixed internuclear distance at r_e and it is only the orientation of $\mathbf{r} = (r_e, \theta, \phi)$ in terms of the spherical coordinates

that is of concern. The dependence on the azimuthal angle ϕ does not influence the rotational energy and thus only the dependence on θ is considered. The Schrödinger equation is

$$-\frac{\hbar^2}{2I}\left[\frac{1}{\sin\theta}\frac{d}{d\theta}(\sin\theta\frac{d\psi(\theta)}{d\theta})\right] = E\psi(\theta), \tag{6.161}$$

where E is quantized, I is the moment of inertia and the differential operator in θ is from the form of ∇^2 in spherical polar coordinates. With the substitution $x = \cos\theta$, Eq. (6.161) can be expressed as

$$H\psi_\ell(x) = -\frac{d}{dx}\left[(1-x^2)\frac{d\psi_\ell(x)}{dx}\right] = \lambda_\ell\psi_\ell(x), \tag{6.162}$$

where H is the dimensionless Hamiltonian, $E_\ell = \lambda_\ell\frac{\hbar^2}{2I}$ is the energy eigenvalue and

$$\lambda_\ell = \ell(\ell+1). \tag{6.163}$$

These rigid rotor energy eigenvalues are precisely the eigenvalues of the total angular momentum operator L^2. There are two aspects that are important to note. The differential operator in Eq. (6.163) is of the Sturm-Liouville type and the differential operator on the left hand side is self-adjoint on the interval $x \in [-1, 1]$. The eigenvalue equation, Eq. (6.163), is the defining equation for the Legendre polynomials, that is

$$\frac{d}{dx}\left[(1-x^2)\frac{dP_\ell(x)}{dx}\right] = -\ell(\ell+1)P_\ell(x). \tag{6.164}$$

Thus, the solution of this problem is $\psi_\ell(x) \equiv P_\ell(x)$. We have found the basis for which the Hamiltonian is diagonal $H_{\ell,\ell'} = \ell(\ell+1)\delta_{\ell,\ell'}$. This is the physical space representation. The discrete space representation can be obtained with the transformation $T_{\ell j}$ defined in terms of the Legendre polynomials $P_\ell(x)$, that is

$$H_{ij}^{(ps)} = \sum_{\ell=0}^{N-1}\sum_{\ell'=0}^{N-1} T_{i\ell}H_{\ell\ell'}T_{\ell' i}. \tag{6.165}$$

With the transformation, $T_{i\ell} = \sqrt{w_i}P_\ell(x_i)$, one can show that

$$H_{ij}^{(ps)} = \sum_{k=1}^{N}(1-x_k^2)D_{ki}D_{kj}, \tag{6.166}$$

where $\mathbf{D}$ is the derivative matrix operator. The numerical diagonalization of this discrete matrix representation of the Hamiltonian of order N gives N eigenvalues

$\lambda_\ell = \ell(\ell+1)$ exactly. This formalism was introduced in Chap. 3, Sect. 3.9.3, and Fig. 3.26 shows the exact eigenfunction obtained with Eq. (6.166). For Legendre polynomials, $P_\ell(x)$, defined in $x \in [-1, 1]$ with $w(x) = 1$, $p(x) = (1 - x^2)$ and $q(x) = 0$, we find easily from Eq. (6.155) that

$$-(1-x^2)P_\ell^{''}(x) + 2xP_\ell^{'} = \ell(\ell+1)P_\ell(x) \tag{6.167}$$

which is the defining differential equation for Legendre polynomials.

6.7.3 Hermite Polynomials; Quantum Harmonic Oscillator

The Hermite polynomials $H_n(x)$ on $x \in (-\infty, \infty)$, satisfy a Sturm-Liouville problem defined by $w(x) = p(x) = e^{-x^2}$ and $q(x) = 0$ in the general form Eq. (6.155). With these definitions, Eq. (6.155) gives the differential equation

$$H_n^{''}(x) - 2xH_n^{'} = -2nH_n(x). \tag{6.168}$$

This differential equation can be written as a Schrödinger equation in terms of $h_n(x) = e^{-x^2/2}H_n(x)$. Notice that where $H_n(x)$ polynomials are orthogonal with respect to $w(x) = e^{-x^2}$, the basis functions $h_n(x)$ are orthogonal with unit weight function. The defining Schrödinger differential equation for these functions from Eq. (6.168) is

$$-h_n^{''}(x) + x^2 h_n = (2n+1)h_n(x), \tag{6.169}$$

where the term in $h_n^{'}(x)$ does not appear. This is precisely the dimensionless Schrödinger equation for a quantum harmonic oscillator as a simple model for the vibrational states of a non-rotating diatomic molecule.

If the interaction potential between the nuclei of a diatom is $V(r)$ where r is the internuclear separation, the harmonic oscillator model involves the quadratic approximation of the potential at the minimum of the potential, that is,

$$V(r) \approx V(r_e) + \frac{1}{2}\frac{d^2V}{dr^2}\bigg|_{r=r_e}(r - r_e)^2. \tag{6.170}$$

If we define the force constant as $k = \frac{dV}{dr}|_{r=r_e}$ and the displacement from r_e as $x = r - r_e$, the one-dimensional Schrödinger equation is given by

$$-\frac{\hbar^2}{2\mu}\psi_n^{''}(x) + \frac{kx^2}{2}\psi_n(x) = E_n\psi_n(x), \tag{6.171}$$

where $\hbar$ is the Planck constant and $\mu = m_1 m_2/(m_1 + m_2)$ is the reduced mass with m_1 and m_2 the masses of the two nuclei. Comparing Eqs. (6.171) and (6.169), we get the quantized vibrational states given by

$$E_n = (n + \frac{1}{2})\hbar\omega, \tag{6.172}$$

where $\omega = \sqrt{k/\mu}$ is the fundamental frequency of the oscillator.

The harmonic oscillator is a typical benchmark problem for which a variety of different discretizations are compared. One such method is based on the representation of the second derivative operator on $x \in (-\infty, \infty)$ with a uniform grid with spacing Δx. The grid points are thus $x_i = i\Delta x, i = 0, \pm 1, \pm 2, \ldots, \pm N/2$, on the finite interval $[-N\Delta x/2, N\Delta x/2]$. This representation of the second derivative operator

$$D^2_{ij} = \begin{cases} \pi^3/3, & i = j, \\ 2(-1)^{(i-j)}/(i-j)^2, & i \neq j, \end{cases} \tag{6.173}$$

has been reported by Schwartz (1985); Colbert and Miller (1992); Mazziotti (1999); Amore (2006); Baye (2006) and others. The Hamiltonian matrix for the dimensionless quantum harmonic oscillator (Colbert and Miller 1992) is approximated by

$$H_{ij} = \frac{1}{2(\Delta x)^2} \left\{ \begin{matrix} -\pi^3/3, & i = j, \\ -2(-1)^{(i-j)}/(i-j)^2, & i \neq j. \end{matrix} \right\} + \frac{x_i^2}{2}\delta_{ij}. \tag{6.174}$$

The relative accuracy of the approximate harmonic oscillator eigenvalues determined with the diagonalization of the matrix H_{ij} of dimension $N \times N$ given by Eq. (6.174) is shown in Fig. 6.14(A) versus the quantum number n. The lower order eigenstates are well approximated but the error increases with increasing n. The size of the matrix is increased by halving the step size and keeping the interval fixed as

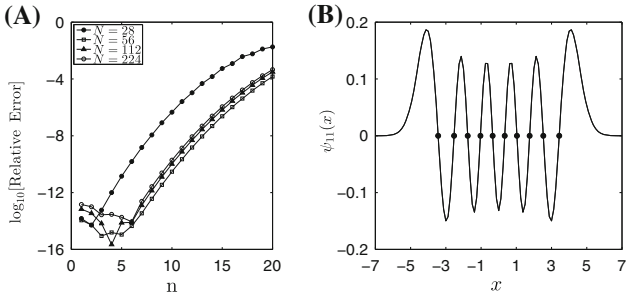

Fig. 6.14 **(A)** Relative accuracy $= 1 - \lambda_n/(n + 1/2)$ for eigenvalues of the quantum harmonic oscillator versus the vibrational quantum number n obtained with the diagonalization of the H_{ij} matrix (Eq. (6.174)) of dimension N; $x \in [-7, 7]$. **(B)** The eigenfunction, $\psi_{11}(x)$, with the 10 Hermite quadrature points shown as the *solid circles*; $N = 112$

shown in the figure and there is not much change for $N = 56$ to $N = 224$. Of interest is the variation of $\psi_{11}(x)$ in Fig. 6.14(B) with $N = 112$. The filled circles are the 10 Hermite quadrature points which coincide rather well with the nodes of the wave function. In order to get a good result for the higher eigenstates the interval has to be made larger.

The optimal basis functions are the Hermite polynomials which are the eigenfunctions of the harmonic oscillator Hamiltonian and the matrix representation of the Hamiltonian in this basis set is diagonal, $\langle n|H|m\rangle = (n+1/2)\delta_{nm}$, and provides the exact result. This result can be derived with the recurrence relations for the Hermite polynomials. This is the spectral solution of this elementary problem.

Baye and Heenen (1986) use a pseudospectral method (a Lagrange mesh method) based on the discrete physical space representation of the second derivative matrix operator in the Hermite polynomial basis

$$H_{ij} = \left\{ \begin{array}{ll} (4N - 1 - 2x_i^2)/12, & i = j, \\ (-1)^{(i-j)}\left[\frac{1}{(x_i - x_j)^2} - \frac{1}{4}\right] & i \neq j. \end{array} \right\} + \frac{x_i^2}{2}\delta_{ij}. \tag{6.175}$$

The diagonalization of this discrete matrix representation gives the eigenvalues $\lambda_n = n+1/2$ to machine accuracy for all but one eigenvalue even though the basis functions used are the exact eigenfunctions of the Hamiltonian. The results of this calculation are summarized in Table 6.6. The four eigenvalues, λ_0 to λ_3, for $N = 6$ to 9 are determined to machine accuracy, although only shown to three significant figures. For each N there is a nonphysical eigenvalue referred to as a"ghost" level (Wei 1997; Willner et al. 2004; Kallush and Kosloff 2006) that are framed in the table. For the harmonic oscillator problem, $\lambda_{ghost} = (3N - 2)/4$, and for $N = 8$ this coincides with an eigenvalue so there are two degenerate eigenvalues. This pattern repeats for $N = 10$ to 13, 14 to 18, etc.

Table 6.6 *Ghost* levels of the quantum harmonic oscillator determined with Eq. (6.175)

n	$\lambda_n = n + \frac{1}{2}$	$N = 6$	$N = 7$	$N = 8$	$N = 9$
01	0.50	0.50	0.50	0.50	0.50
1	1.50	1.50	1.50	1.50	1.50
2	2.50	2.50	2.50	2.50	2.50
3	3.50	3.50	3.50	3.50	3.50
4	4.50	4.00	4.50	4.50	4.50
5	5.50	4.50	4.75	5.50	5.50
6	6.50		5.50	5.50	6.25
7	7.50			6.50	6.50
8	8.70				7.50

The last eigenvalue is replaced with a nonphysical state highlighted by the framed numbers. For $N = 8$, there is a degenerate pair of eigenvalues. $\lambda_5 = \lambda_6 = 5.50$

The reason for the appearance of nonphysical eigenvalues is often attributed to the inexact calculation of the matrix elements of the harmonic potential with the quadrature of order N represented by the diagonal physical space matrix $V(x_i) = (x_i^2/2)\delta_{ij}$. The potential energy matrix elements

$$V_{nm} = \frac{1}{2}\int_{-\infty}^{\infty} e^{-x^2} H_n(x) x^2 H_m(x) dx, \tag{6.176}$$

evaluated with an Nth order quadrature

$$V_{nm}^{(N)} \approx \frac{1}{2}\sum_{i=1}^{N} w_i H_n(x_i) x_i^2 H_m(x_i), \tag{6.177}$$

is not exact. For the element $n = m = N$, the integrand is a polynomial of degree $2N+2$. The quadrature of order N is exact only for polynomials of order up to $2N+1$. We have considered this calculation in detail in Chap. 3, Sect. 3.7.2. The transformation to spectral space of the physical space representation of the multiplicative potential operator with the diagonal matrix $V(x_i)\delta_{ij}$ gives an inaccurate result for the $V_{N,N}$ matrix element. The result with a quadrature of order N in Eq. (6.177) is not correct.

The physical space pseudospectral representation of the harmonic oscillator Hamiltonian based on the Hermite polynomials is

$$H_{ij}^{(ps)} = \frac{1}{2}\sum_{k=1}^{N} D_{ki} D_{kj}. \tag{6.178}$$

where D_{kj} is given by Eq. (3.139). This representation does not have explicit reference to the harmonic potential as does Eq. (6.175). The usual concerns about the accuracy of the quadrature evaluated matrix elements of the potential related to the physical space representation as $V(x_i)\delta_{ij}$ do not play a role (Harris et al. 1965; Dickinson and Certain 1968).

A short MATLAB code constructs the derivative matrix operator $\mathbf{D}$ for the Hermite polynomials. The diagonalization of physical space matrix representation $\frac{1}{2}\mathbf{D}^t \cdot \mathbf{D}$ gives exactly $\lambda_n \equiv n$ relative to the ground state and $\psi_n(x_i) \equiv H_n(x_i)e^{-x^2/2}$. The solid curve in Fig. 6.15 shows the exact $H_{12}(x)e^{-x^2/2}$. The corresponding eigenfunction, $\psi_{12}(x_i)$, from the diagonalization of $\frac{1}{2}\mathbf{D}^t \cdot \mathbf{D}$ with $N = 12$ is shown with the symbols evaluated at the quadrature points. There is exact agreement between the numerical and analytical result.

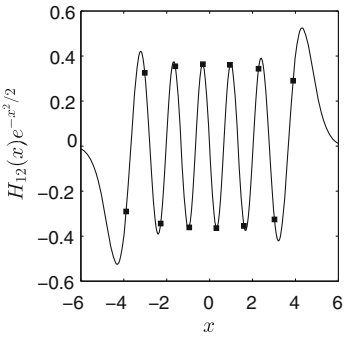

Fig. 6.15 The *solid curve* is the exact Hermite polynomial whereas the symbols represent the values of the 12th eigenfunction of $\mathbf{D}^t \cdot \mathbf{D}$ calculated at 12 quadrature points defined by the Hermite weight function, $w(x) = e^{-x^2}$

6.7.4 The Schrödinger Equation for the Electron Relaxation Problem

We return to the electron relaxation problem discussed in Sect. 6.3 for the hard sphere cross section, $\hat{\sigma} = 1$, and zero electrostaic field, $\alpha = 0$. The Fokker-Planck equation, Eq. (6.63), leads to the eigenvalue problem Eq. (6.73) with $B(x) = x$ and $A(x) = 2x^2 - 3$ (Shizgal 1979). The transformation to the new variable z in Sect. 6.3.2 which is y in this section is defined by

$$y = \int^x \frac{1}{\sqrt{B(x')}} dx' = 2\sqrt{x}.$$

The coefficients in the Fokker-Planck eigenvalue problem are in terms of y,

$$A(y) = \frac{y^4}{2} - 3,$$

and

$$B(y) = \frac{y^2}{4}.$$

The superpotential given by Eq. (6.84) is

$$W(y) = \frac{y^3}{4} - \frac{5}{y}.$$

The potential $V_-(y)$ in the Schrödinger equation

$$-\frac{d^2\psi_n(y)}{dy^2} + V_-(y)\psi_n(y) = \lambda_n\psi_n(y), \tag{6.179}$$

is defined in terms of $W(y)$ in Eq. (6.83) and

$$V_-(y) = \frac{y^6}{64} - y^2 + \frac{15}{4y^2}, \qquad y \in [0, \infty). \tag{6.180}$$

The notation $V_-(y)$ refers to one of the partner potentials in supersymmetric quantum mechanics, the other being $V_+(y)$. We refer the reader to references (Comtet et al. 1985; Cooper et al. 1995, 1987) for further details.

The potential in Eq. (6.180) is shown in Fig. 6.16. The horizontal lines indicate the positions of the eigenvalues calculated as discussed below. At first glance one might consider the basis set of associated Laguerre polynomials or the discrete representation based on the Laguerre quadrature points. However, the optimal polynomial basis set is defined with the weight function equal to the known ground state wave function, that is

$$w(y) = \begin{cases} \exp\left[-\int^y \sqrt{W(y')}dy'\right], \\ y^5 e^{-y^4/16}, \end{cases} \tag{6.181}$$

which gives $V(y) = \tilde{V}(y)$ in Eq. (6.93) and the pseudospectral matrix representation is as in Eq. (6.94) with the physical space derivative operator defined by the weight function Eq. (6.181).

A MATLAB code provides the recurrence coefficients for the polynomials orthogonal with respect to this weight function and the physical space derivative operator. The representation of the Hamitonian for this potential is $\mathbf{H} = \mathbf{D}^t \cdot \mathbf{D}$ given by

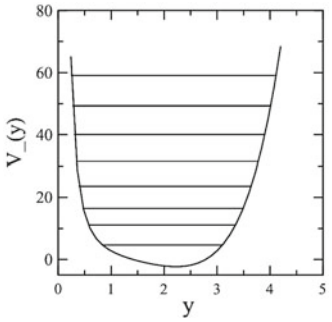

Fig. 6.16 Supersymmetric potential $V_-(y)$, Eq. (6.180), in the Schrödinger equation corresponding to the hard sphere Lorentz Fokker-Planck equation. The *horizontal lines* show the ordering of the eigenvalues in the potential

Table 6.7 Convergence of the eigenvalues of the Schrödinger equation with the potential, Eq. (6.180), with the quadrature defined with the weight function $w(y) = y^5 e^{-y^4/16}$ and the pseudospectral representation $\mathbf{H} = \mathbf{D}^t \cdot \mathbf{D}$, Eq. (6.94)

N	λ_1	λ_2	λ_3	λ_6	λ_{10}	λ_{15}	λ_{20}	λ_{30}
4	4.68598	10.21673	16.86293					
5	4.68346	10.13276	16.83567					
6	4.68340	10.11291	16.48805					
8		10.11257	16.43271	42.95019				
10		10.11252	16.42971	40.95019				
15			16.42968	40.05250	80.91828			
20				40.05238	80.44866	148.9082		
25					80.44794	142.5387	227.5833	
30						142.4463	215.1651	453.450
40							215.1631	397.036
45								388.021
50								387.626
60								387.623
$w(x) = x^2 e^{-x^2}$	4.68340	10.11251	16.42968	40.05238	80.44794	142.44461	215.1631	387.623

The results in the bottom row are the converged eigenvalues for the hard sphere Lorentz Fokker-Planck equation computed with the quadrature defined by $w(x) = x^2 e^{-x^2}$

Eq. (6.94). With the use of this nonclassical basis set and associated quadrature the matrix elements of the potential are not required as with other pseudospectral methods (Harris et al. 1965; Dickinson and Certain 1968).

The convergence of the eigenvalues calculated in this way versus the number of quadrature points is shown in Table 6.7. The convergence is rapid and from above so that the calculation is variational. At each order N an upper bound to the eigenvalue is obtained. There is no occurrence of ghost levels. The bottom row of the table shows the eigenvalues obtained with the solution of the Fokker-Planck eigenvalue problem in complete agreement with the calculations based on the Schrödinger equation. The eigenfunctions corresponding to four eigenvalues are shown in Fig. 6.17. With $N = 80$, the oscillations of these converged eigenfunctions are well resolved.

6.7.5 *Quantum Mechanics for the Vibrational States of a Diatomic Molecule; Morse Potential*

The Morse interatomic potential for a diatomic molecule (Morse 1929) is given by

$$V(r) = D_e \left[1 - e^{-\alpha(y - y_e)} \right]^2, \tag{6.182}$$

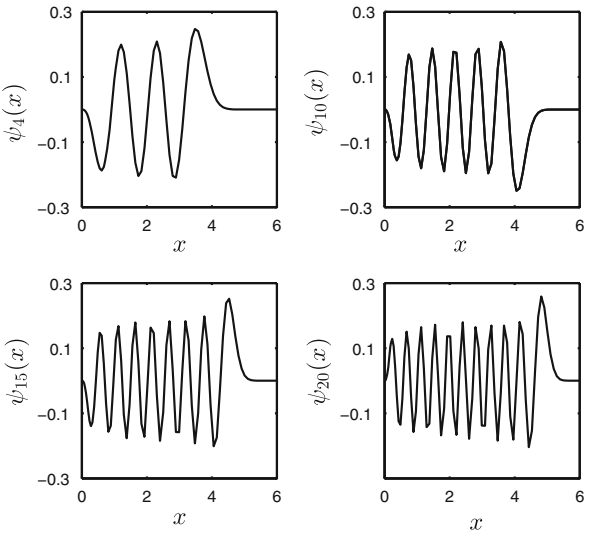

Fig. 6.17 Eigenfunctions of the Schrödinger equation for the potential, $V(y) = \frac{y^6}{64} - y^2 + \frac{15}{y^2}$ that arises from the transformation of the hard sphere Lorentz Fokker-Planck equation to the Schrödinger equation. Eigenfunctions calculated with the diagonalization $\mathbf{H} = \mathbf{D}^t \cdot \mathbf{D}$ with the pseudospectral derivative matrix operator based on the quadrature defined with the weight function $w(y) = y^5 e^{-y^4/16}$, $N = 80$

where D_e is the dissociation energy and α determines the spatial variation relative to the equilibrium position y_e. The exact vibrational eigenvalues with $\hbar = 1$ and reduced mass $\mu = 1$ are

$$\epsilon_n = \left[2\alpha\sqrt{D_e} - \alpha^2\right]n - \alpha^2 n^2, \quad n = 1, 2, \ldots, n_{max}, \tag{6.183}$$

relative to the ground state. There are a finite number of bound states denoted by n_{max}. Table 6.8 lists several diatomic molecules that have been studied by researchers to benchmark numerical methods of solution of the Schrödinger equation. For most of these studies, the interatomic potential is approximated with a Morse potential (Morse 1929). The numerical methods include finite difference methods, pseudospectral methods, methods based on B splines, the Discrete Variable Representation, the Lagrange mesh method, the Fourier grid method, the Sinc interpolation, and the Quadrature Discretization Method. Each method is based on the physical space representation of the derivative operator as determined with an interpolation. The methods are all variants of a pseudospectral method (Gottlieb and Orszag 1977; Francisco 1995; Fornberg 1996; Boyd 2001; Canuto et al. 2006b).

The numerical methods differ primarily with regards to the choice of the basis functions and the application of boundary conditions. Fourier methods are applied on a uniform grid and the number of grid points per wavelength of the eigenfunction is an

Table 6.8 References to numerical solutions of the Schrödinger equation for the vibrational states of diatomic molecules

Molecule	References	Numerical method
HF	Light et al. (1985)	Discrete variable representation
	Hamilton and Light (1986)	Discrete variable representation
	Yang and Peet (1988)	Collocation
	Balint-Kurti and Pulay (1995)	Fourier grid method
	Shizgal and Chen (1996)	Quadrature discretization method
	Guantes and Farantos (1999)	Finite difference
I_2	Braun et al. (1996)	Chebyshev Lanczos
	Shizgal (1997)	Quadrature discretization method
	Wei et al. (1997)	Lagrange interpolation
	Baye and Vincke (1999)	Lagrange mesh method
	Mazziotti (1999)	Spectral difference method
	Wei (2000)	Discrete singular convolution (Sinc)
	Chen and Shizgal (2001)	Quadrature discretization method
	Lo and Shizgal (2008b)	Quadrature discretization method
H_2	Johnson (1977)	Finite difference
	Marston and Balint-Kurti (1989)	Fourier grid method
	Baye (1995)	Lagrange mesh method
H_2^+	ONeil and Reinhardt (1978)	B-spline
	Layton (1993)	Fourier
Cs_2	Kokoouline et al. (1999)	Discrete variable representation
	Willner et al. (2004)	Mapped grid methods
	Lo and Shizgal (2008a)	Quadrature discretization method
	Derevianko et al. (2009)	B-spline
He_2, Ne_2, Ar_2, HeAr, HeNe, etc.	Shizgal (1997)	Quadrature discretization method
He_2, Ne_2, Ar_2	Lo and Shizgal (2006)	Quadrature discretization method

important parameter (Colbert and Miller 1992). Associated with some of the methods is a variational theorem so that the Nth approximation represents an upper bound. For some methods there are nonphysical eigenvalues calculated that are referred to as "ghost" levels (Wei 1997; Kokoouline et al. 1999; Willner et al. 2004).

The Morse potential belongs to the class of potentials in supersymmetric quantum mechanics (Dutt et al. 1988; Cooper et al. 1995). The basis set defined with the weight function

$$w(x) = \exp\left[-2\sqrt{D_e}(x + \frac{e^{-\alpha x}}{\alpha}) + \alpha x \right], \tag{6.184}$$

for which the ground state wavefunction is $\psi_0(x) = \sqrt{w(x)}$ and $V(x) = \tilde{V}(x)$. The pseudospectral representation of the Hamiltonian, Eq. (6.93), reduces to Eq. (6.94).

Table 6.9 Convergence of the eigenvalues in cm^{-1} for the Morse oscillator for HF with $D_e = 49383.407073\,\text{cm}^{-1}$, $\beta = 1.1741 a_0^{-1}$, $x_e = 1.7329 a_0$ and $\mu = 1744.4453572532 m_e$

N	ϵ_2	ϵ_8	ϵ_{14}
4	9819.11761		
6	9805.01756		
8	9805.00714		
10		33041.31574	
12		29960.19345	
14		29067.91526	
16		28925.47987	62676.28749
18		28914.83536	53058.24677
20		28914.43671	48112.83259
25		28914.42738	43025.97932
30			41879.68669
35			41781.77734
40			41780.18827
45			41780.18145
Exact	9805.0714	28914.42738	41780.18143

The quadrature is defined in terms of the weight function, Eq. (6.184) and the eigenvalues determined with the diagonalization of $\mathbf{D}^t \cdot \mathbf{D}$, Eq. (6.94). Reprinted from (Shizgal 1997) with permission from Elsevier

The diagonalization of $\mathbf{D}^t \cdot \mathbf{D}$ gives the eigenvalues and eigenfunctions.

The convergence of the vibrational energies ϵ_2, ϵ_8 and ϵ_{14} for the Morse potential for HF calculated with the quadrature defined with $w(x)$, Eq. (6.184), are shown in Table 6.9 and the rapid convergence of the eigenvalues is evident. It is clear that there is a variational theorem inherent in the method as the convergence of the eigenvalues is from above. For each N, an upper bound to the vibrational state is obtained.

The convergence demonstrated here is faster than reported by other researchers (Balint-Kurti and Pulay 1995; Braun et al. 1996; Hoffman et al. 1998; Baye and Vincke 1999) with different numerical methods. The spectral convergence of the eigenvalues is shown in Fig. 6.18 and several eigenfunctions are shown in Fig. 6.19. Unlike Fourier methods, this high order pseudospectral method with the particular basis set constructed with $w(x) = \psi_0^2(x)$, does not require a particularly dense distribution of quadrature points to accurately calculate the higher order oscillatory vibrational eigenfunctions (Gottlieb and Orszag 1977; Francisco 1995; Fornberg 1996; Boyd 2001; Canuto et al. 2006b).

An important aspect of these benchmark calculations is the total number of bound states for the potential chosen. If the potential supports n_{max} states, the calculation of the lower states up to vibrational quantum number $n \approx 3n_{max}/4$ are relatively easy to calculate in spite of the oscillatory form of the eigenfunctions. It is the vibrational states close to the dissociation limit that are the most difficult to calculate.

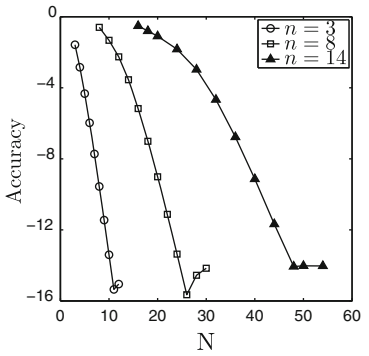

Fig. 6.18 The convergence of the lower order eigenvalues, λ_n, of the Morse potential with diagonalization of $\mathbf{D}^t \cdot \mathbf{D}$; Morse potential for HF with $D_e = 49383.407073\,\mathrm{cm}^{-1}$, $\beta = 1.1741 a_0^{-1}$, $x_e = 1.7329 a_0$ and $\mu = 1744.4453572532 m_e$; Accuracy $= \log_{10} |1 - \lambda_n^{(N)}/\lambda_n^{(exact)}|$

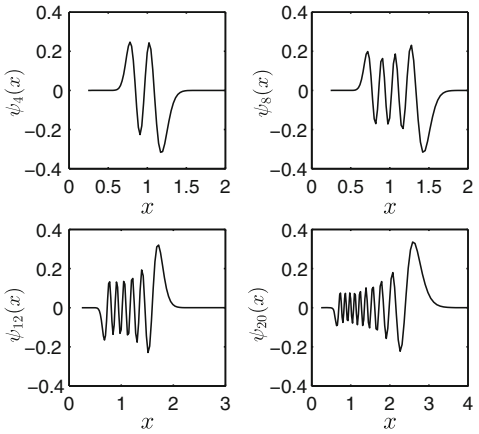

Fig. 6.19 Eigenfunctions determined from the diagonalization of $\mathbf{D}^t \cdot \mathbf{D}$ for selected vibrational states of HF versus x in angstroms

We illustrate this feature with the model Morse potential employed by Pryce (1993) and Weideman (1999)

$$V(x) = 9(1 - e^{-x})^2 - 9,$$

which supports only three bound states,

$$\lambda_n = -n^2 + 5n - \frac{25}{4}, \quad n = 0, 1 \text{ and } 2.$$

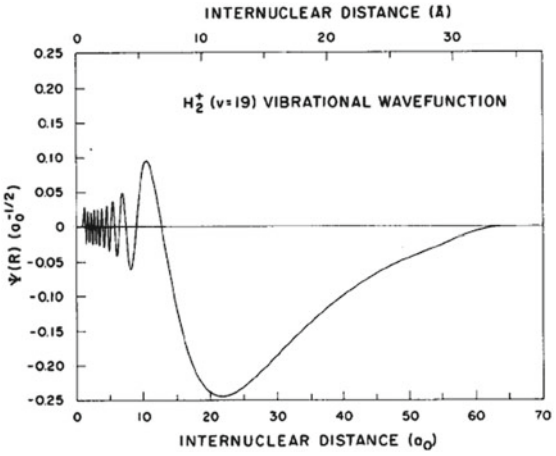

Fig. 6.20 Variational approximation to the $n = 19$ vibrational eigenfunction of H_2^+ with the potential from Wind (1965) with 100 B splines (Shore 1973). Reproduced from ONeil and Reinhardt (1978) with permission of the American Physical Society

The vibrational states are determined with the quadrature based on the weight function

$$w(x) = \exp(-5x + 6e^{-x})$$

for which $V(x) = \tilde{V}(x)$ and pseudospectral representation of the Hamiltonian is $\mathbf{D}^t \cdot \mathbf{D}$. The convergence of the 3 states to 14 significant figures requires 2, 20 and 55 quadrature points (Chen and Shizgal 2001). The numerical difficulty in the accurate calculation of the highest state with only two nodes is the diffuse nature of the eigenfunction just below the dissociation limit. This is illustrated in Fig. 6.20 for a higher order eigenfunction for H_2^+ determined with 100 B splines (ONeil and Reinhardt 1978). The numerical challenge is to capture both the oscillatory behaviour at small internuclear distance as well as the variation on a much larger scale for larger ($r > 20\, a_0$) distances. This behaviour was also demonstrated in Fig. 1 of Meshkov et al. (2008) for the eigenfunctions for a Lennard–Jones potential.

The diatoms, He_2 and Ne_2, with 1 and 3 bound states, respectively, illustrate the same difficulty in the accurate representation of the highest bound state. The potentials for He_2 and Ne_2 were reported by Aziz and Slaman (1991) and Tang and Toennies (2003), respectively. A Morse potential that approximates the true potential (Lo and Shizgal 2008a) is used to define a quadrature based on the weight function, Eq. (6.184). For this realistic potential, $V(y) \neq \tilde{V}(y)$ and the pseudospectral representation of the Hamiltonian given by Eq. (6.93) is diagonalized.

In addition, a mapping, $u = \rho(x)$, is used to redistribute the points so as to best capture the variation of the wave function. Two such mappings are

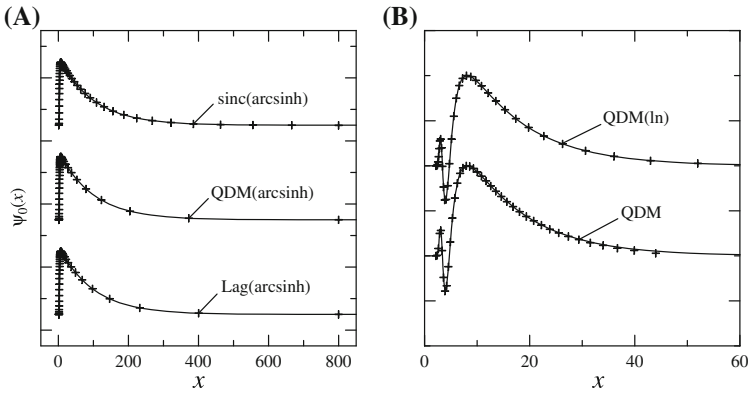

Fig. 6.21 (*Left hand panel*) Single bound state eigenfunction, $\psi_0(x)$, for He_2 with the Aziz and Slaman (1991) interatomic potential. QDM is the quadrature discretization method with a nonclassical weight function with the mapping, Eq. (6.186); Lag refers to the Lagrange mesh method with the same map. (*Right hand panel*) The second excited state eigenfunction, $\psi_2(x)$, for Ne_2 with the Tang and Toennies (2003) potential determined with the QDM, with and without the mapping, Eq. (6.185). Reproduced from Lo and Shizgal (2008a) with permission of the American Institute of Physics

$$\rho(x) = s_1 \ln\left(\frac{x - b_2}{s_2}\right) \tag{6.185}$$

$$\rho(x) = s_1 \sinh^{-1}\left(\frac{x - b_2}{s_2}\right) + b_1, \tag{6.186}$$

where s_1, s_2, b_1 and b_2 are adjustable parameters chosen empirically.

The single ground vibrational state for He_2 and the second excited vibrational state for Ne_2 are shown in Fig. 6.21. The variation of the wave function of the one bound state for He_2 occurs on two different spatial scales. There is a rapid variation near the origin and a very slow decay over a very large distance. The collocation points shown in the figure are distributed nonuniformly on the large interval of interest. The curves labelled QDM are calculated with the quadrature discretization method (Lo and Shizgal 2008a) and the two mappings above. The curves labelled by "Lag" refer to the Lagrange mesh method (Baye 2006).

Pseudospectral methods applied to the entire interval or in subdomains of interest in which case it is referred to as a spectral element method (Deville et al. 2002; Pasquetti and Rapetti 2004) belong to that class of spectral and higher order numerical methods (Azaez et al. 2012). In every application in chemistry, physics and engineering, there are important applications to three and multidimensional problems. The extension from one-dimension to several dimensions generally involves a direct product of several one-dimensional polynomial basis sets. The size of the matrices for such problems increases dramatically with an increase with the number of degrees of freedom especially for the calculation of the rotational–vibrational states of polyatomic molecules (Friesner et al. 1993; Littlejohn et al. 2002; Dawes

and Carrington 2004, 2005; Cassam-Chenaï and Liévin 2012). The numerics is then a problem in linear algebra to find the eigenvalues of a very large matrix.

A reduction in the dimensionality of the problem can be achieved by making use of available symmetries and with other techniques. Also, with a judicious choice of basis functions and/or grid points the number for each vibrational mode can be significantly decreased so as to achieve computational economy. In their case study of the vibrational states of methane, Mielke et al. (2013) introduce the use of optimized vibrational quadratures for the efficient computation of one-dimensional matrix elements. Any reduction in the number of grid points for each degree of freedom could dramatically decrease the dimension of the matrices resulting from the direct product of the different spaces for multidimensional problems. There are ongoing efforts to develop more efficient schemes for the development of sparse grids with algorithms related to cubatures discussed in Chap. 2, Sect. 2.8 (Avila and Carrington 2013; Lauvergnat and Nauts 2014).

6.7.6 *Pseudospectral Solution of the Two Dimensional Schrödinger Equation for the Henon-Heles Potential; Nonclassical Basis Sets*

Quantum problems in two and higher dimensions are often solved with a direct product of the basis sets for each one dimensional variable (Parrish and Hohenstein 2013) (and references therein). The resulting matrix representation of the Hamiltonian for a multidimensional system in either the spectral space or the physical space is the product of matrix representations for each dimension. Consequently the size of the matrices involved can increase very quickly if many basis functions or grid points are required in each dimension. This becomes a computationally challenging problem in order to reduce the dimensionality of the matrices by applying symmetries or particular numerical algorithms to reduce memory requirements and computational speed. The Milne problem (Lindenfeld and Shizgal 1983) and the associated planetary escape problem (Shizgal and Blackmore 1986) discussed in Chap. 5 are examples of problems in kinetic theory in three dimensions.

In this section, we consider the calculation of the eigenvalues of the two dimensional Hamiltonian

$$-\frac{1}{2}\left[\frac{\partial^2\psi_{nm}(x,y)}{\partial x^2}+\frac{\partial^2\psi_{nm}(x,y)}{\partial y^2}\right]+V(x,y)\psi_{nm}(x,y)=\lambda_{nm}\psi_{nm}(x,y), \tag{6.187}$$

where the potential is the Henon-Heles potential

$$V(x,y)=\frac{x^2+y^2}{2}-\lambda x(\frac{x^3}{3}-y^2). \tag{6.188}$$

This potential was introduced by Henon and Heiles (1964) in their study of the motion of a star in the potential of the galaxy and the determination of a third conserved integral of the classical two dimensional motion with this Hamiltonian. The potential, Eq. (6.188), was chosen for its analytic simplicity so as to make the trajectory computations easy and to obtain interesting dynamical results. This system has received considerable attention as a model for classical and quantum chaotic behaviour. For $\lambda = 0$, the problem reduces to two uncoupled harmonic oscillators.

For the two dimensional Schrödinger equation, we choose basis functions

$$\begin{aligned} X_n(x) &= \sqrt{u(x)}G_n(x), \\ Y_n(y) &= \sqrt{v(y)}H_m(y), \end{aligned} \tag{6.189}$$

where $u(x)$ and $v(y)$ are the weight functions and we denote the logarithmic derivatives of the weight functions by

$$\begin{aligned} U(x) &= -\frac{u'(x)}{u(x)}, \\ V(x) &= -\frac{v'(x)}{v(x)}, \end{aligned} \tag{6.190}$$

We extend the pseudospectral analysis of the one-dimensional applications presented in Sect. 6.3.3 to two dimensions by defining the spectral space representation of the Hamiltonian as

$$\begin{aligned} H_{n'm',nm} = \delta_{m'm} \int u(x) G'_{n'}(x) G'_n(x) dx + \delta_{n'n} \\ \int v(y) H'_{m'}(y) H'_m(y) dy + (V_{n'm',nm} - \tilde{V}_{n'm',nm}). \end{aligned} \tag{6.191}$$

The potential matrix elements are $V_{n'm',nm} = \langle X_{n'} Y_{m'} | V(x, y) | X_n Y_m \rangle$ and the matrix elements of the reference potential are

$$\begin{aligned} \tilde{V}_{n'm',nm} = \delta_{m'm} \int \left(\frac{U^2(x)}{4} - \frac{U'(x)}{2} \right) u(x) G_{n'}(x) G_n(x) dx \\ + \delta_{n'n} \int \left(\frac{V^2(y)}{4} - \frac{V'(y)}{2} \right) v(y) H_{m'}(y) H_m(y) dy. \end{aligned} \tag{6.192}$$

We transform this spectral space representation with the appropriate transformation matrices, Eq. (1.24), and obtain the discrete physical space representation

$$H_{ij,k\ell} = \delta_{k\ell} \sum_{k'=0}^{N_x} D_{k'i} D_{k'j} + \delta_{ij} \sum_{k'=0}^{N_y} D_{k'k} D_{k'\ell} + \left[V(x_i, y_j) - \tilde{V}(x_i, y_k) \right], \tag{6.193}$$

where

$$\tilde{V}(x, y) = \left(\frac{U^2(x)}{4} - \frac{U'(x)}{2}\right) + \left(\frac{V^2(y)}{4} - \frac{V'(y)}{2}\right). \tag{6.194}$$

is the usual reference potential in two-dimensions. The pseudospectral representation, Eq. (6.193) is the two-dimensional analog of the one-dimensional representation, Eq. (6.93). The details are similar to the transformations for the Fokker-Planck operator in Sect. 6.2.2.

Two sets of quadratures were used; (1) Hermite quadratures for both dimensions and (2) a quadrature in x based on a nonclassical weight function, $u(x) = \exp[-x^2 + 2\lambda x^3/9]$, chosen empirically and Hermite quadratures in y. With the Hermite quadrature in both dimensions, the lowest order eigenvalues required as few as 8 quadrature

Table 6.10 Eigenvalues of the Henon-Heles potential with $\lambda = \sqrt{0.0125}$ with $u(x) = \exp[-x^2 + 2\lambda x^3/9]$ and $v(y) = \exp(-y^2)$; $N_x = N_y = 32$

n	ℓ	Feit et al. (1982)	Shizgal and Chen (1996)	Echave and Clary (1992)
3	3	3.9825	3.982417	
	−3	3.9859	3.985761	
5	3	5.8672	5.867 015	
	−3	5.8816	5.881 446	
6	6	6.9991	6.998 932	
	−6	6.9996	6.999 387	
7	3	7.6979	7.697 721	
	−3	7.7371	7.736 885	
8	6	8.8116	8.811 327	
	−6	8.8154	8.815 188	
9	3	9.4670	9.466 773	
	−3	9.5526	9.552 382	
9	9	10.0356	10.035 413	
	−9	10.0359	10.035 592	
10	6	10.5727	10.572 480	
	−6	10.5907	10.590 470	
11	3	11.1603	11.160 259	11.160 258
	−3	11.3253	11.325 231	11.325 231
11	9	11.7497	11.749 519	11.749 518
	−9	11.7525	11.752 297	11.752 297
12	6	12.3335	12.333 786	12.333 780
	−6	12.2771	12.277 192	12.277 192
12	12	12.7474	12.748 520	12.748 183
	−12	13.0310	13.032 065	13.032 060
13	3	13.0868	13.086 873	13.086 873
	−3	13.0800	13.081 199	13.081 191

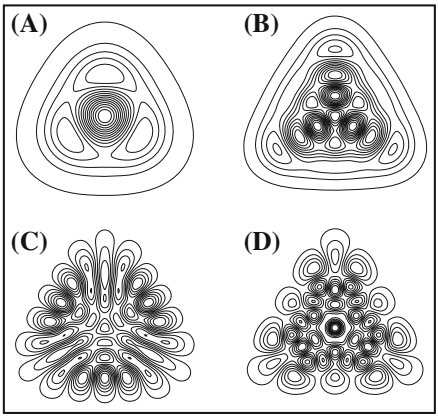

Fig. 6.22 Contour plots of the eigenfunctions of the Schrödinger equation for the Henon-Heles potential with n and ℓ equal to **(A)** 2, 0 **(B)** 6, 0 **(C)** 9, −9 and **(D)** 10, 6; Hermite quadratures were used, $N_x = N_y = 32$; the vertical scale is y and the horizontal scale is x, both in the interval [−7, 7]. Reproduced from Shizgal and Chen (1997) with permission of the American Institute of Physics

points in each variable to get convergence to 5 significant figures and up to 50 quadrature points for the higher states to the same accuracy. The nonclassical weight function provides faster convergence giving 8 significant figure accuracy with 32 quadrature points in each dimension.

The eigenvalues calculated in this way are listed in Table 6.10 in comparison with the previous calculations. Echave and Clary (1992) used Fourier basis functions to solve two one-dimensional reference problems and used the eigenfunctions of these hamiltonians as basis functions for the two-dimensional Henon-Heiles potential. They refer to this method that follows on the earlier work by Hamilton and Light (1986) as the potential optimized discrete variable representation. The results listed in the table are also in agreement with the results by Wei (1999) who used a collocation method referred to as a discrete singular convolution analogous to a Sinc interpolation as used by Amore (2006) and Amore et al. (2009). We discussed the Sinc interpolation in Chap. 2. We list the eigenvalues in the same manner as done by Noid and Marcus (1977). The results are in agreement to the accuracy in the table except for the (12,12) state for which Wei (1999) reports the value of 12.748431. The reason for this discrepancy is not known.

The contour plots of several eigenfunctions are shown in Fig. 6.22 and converged with 50 Hermite basis functions in each variable. The C_{3v} symmetry is evident from the figure and several fine details of the eigenfunctions are recovered. It should be mentioned that this model system with the small value of $\lambda = \sqrt{0.0125}$ is very close to two uncoupled harmonic oscillators in each variable. The convergence of the Hermite polynomial basis set for each dimension for the lower states works as well as it does owing to the small value of λ. It would be of interest to consider larger values and experiment with nonclassical basis sets that might provide faster convergence.

References

Abbott, D.: Overview: unsolved problems of noise and fluctuations. Chaos **11**, 526–538 (2001)

Abolhassani, A.A.H., Matte, J.P.: Multi-temperature representation of electron velocity distribution functions. I. Fits to numerical results. Phys. Plasmas **19**, 102103 (2012)

Al-Gwaiz, M.A.: Sturm-Liouville Theory and Its Applications. Springer, Berlin (2008)

Amore, P.: A variational Sinc collocation method for strong-coupling problems. J. Phys. A: Math. Gen. **39**, L349–L355 (2006)

Amore, P., Fernandez, F.M., Saenz, R.A., Salvo, K.: Collocation on uniform grids. J. Phys. A: Math. Theor. **42**, 115302 (2009)

Andersen, K., Shuler, K.E.: On the relaxation of a hard sphere Rayleigh and Lorentz gas. J. Chem. Phys. **40**, 633–650 (1964)

Andersen, H.C., Oppenheim, I., Shuler, K.E., Weiss, G.H.: Exact condition for the preservation of a canonical distribution in Markovian relaxation process. J. Math. Phys. **5**, 522–536 (1964)

Anna, J.M., Kubarych, K.J.: Watching solvent friction impede ultrafast barrier crossings: a direct test of Kramers theory. J. Chem. Phys. **133**, 174506 (2010)

Avila, G., Carrington Jr, T.: Solving the Schrödinger equation using Smolyak interpolants. J. Chem. Phys. **139**, 134114 (2013)

Azaez, M., El Fekih, H., Hesthaven, J.S.: Spectral and High Order Methods for Partial Differential Equations-ICOSAHOM. Springer, New York (2012)

Aziz, R.A., Slaman, M.J.: An examination of ab initio results for the helium potential energy curve. J. Chem. Phys. **94**, 8047–8053 (1991)

Bagchi, B., Fleming, G.R., Oxtoby, D.W.: Theory of electronic relaxation in solution in the absence of an activation barrier. J. Chem. Phys. **78**, 7375–7385 (1983)

Balint-Kurti, G.G., Pulay, P.: A new grid-based method for the direct computation of excited molecular vibrational-states: test application to formaldehyde. J. Mol. Struct. (Theochem) **341**, 1–11 (1995)

Basu, B., Jasperse, J.R., Strickland, D.J., Daniel, R.E.: Transport-theoretic model for the electron-proton-hydrogen atom aurora. J. Geophys. Res. **98**, 21517–21532 (1993)

Baye, D.: Constant-step Lagrange meshes for central potentials. J. Phys. B: At. Mol. Opt. Phys. **28**, 4399–4412 (1995)

Baye, D.: Lagrange-mesh method for quantum-mechanical problems. Phys. Stat. Sol. B **243**, 1095–1109 (2006)

Baye, D., Heenen, P.H.: Generalized meshes for quantum-mechanical problems. J. Phys. A: Math. Gen. **19**, 2041–2059 (1986)

Baye, D., Vincke, V.: Lagrange meshes from nonclassical orthogonal polynomials. Phys. Rev. E **59**, 7195–7199 (1999)

Berezhkovskii, A.M., Zitserman, V.Yu., Polimenob, A.: Numerical test of Kramers reaction rate theory in two dimensions. J. Chem. Phys. **105**, 6342–6357 (1996)

Bernstein, M., Brown, L.S.: Supersymmetry and the bistable Fokker-Planck equation. Phys. Rev. Lett. **52**, 1933–1935 (1984)

Bhatnagar, P.L., Gross, E.P., Krook, M.: A model for collision processes in gases. I. Small amplitude processes in charged and neutral one-component systems. Phys. Rev. **94**, 511–525 (1954)

Bi, C., Chakraborty, B.: Rheology of granular materials: dynamics in a stress landscape. Philos. Trans. R. Soc. A **367**, 5073–5090 (2009)

Bicout, D.J., Szabo, A.: Entropic barriers, transition states, funnels, and exponential protein folding kinetics: a simple model. Protein Sci. **9**, 452–465 (2000)

Bicout, D.J., Berezhkovskii, A.M., Szabo, A.: Irreversible bimolecular reactions of Langevin particles. J. Chem. Phys. **114**, 2293–2303 (2001)

Binney, J., Tremaine, S.: Galactic Dynamics, 2nd edn. Princeton University Press, New Jersey (2008)

Bird, G.A.: Molecular Gas Dynamics and the Direct Simulation of Gas Flows. Clarendon, Oxford (1994)

Biró, T.S., Jakovác, A.: Power-law tails from multiplicative noise. Phys. Rev. Lett. **94**, 132302 (2005)
Black, F., Scholes, M.: The pricing of options and corporate liabilities. J. Polit. Econ. **81**, 637–654 (1973)
Blackmore, R.S.: (1985) Theoretical studies in stochastic processes. PhD thesis, UBC, http://circle.ubc.ca/handle/2429/25554
Blackmore, R., Shizgal, B.: Discrete ordinate method of solution of Fokker-Planck equations with nonlinear coefficients. Phys. Rev. A **31**, 1855–1868 (1985a)
Blackmore, R., Shizgal, B.: A solution of Kramers equation for the isomerization of n-butane in CCl_4. J. Chem. Phys. **83**, 2934–2941 (1985b)
Blackmore, R., Weinert, U., Shizgal, B.: Discrete ordinate solution of a Fokker-Planck equation in laser physics. Trans. Theory Stat. Phys. **15**, 181–210 (1986)
Blaise, P., Kalmykov, Y.P., Velcescu, A.A.: Extended diffusion in a double well potential: transition from classical to quantum regime. J. Chem. Phys. **137**, 094105 (2012)
Bobylev, A.V., Mossberg, E.: On some properties of linear and linearized Boltzmann collision operators for hard spheres. Kinet. Relat. Models **4**, 521–555 (2008)
Boyd, J.P.: Chebyshev and Fourier Spectral Methods. Dover, New York (2001)
Boyd, T.J.M., Sanderson, J.S.: The Physics of Plasmas. Cambridge University Press, Cambridge (2003)
Braun, M., Sofianos, S.A., Papageorgiou, D.G., Lagaris, I.E.: An efficient Chebyshev-Lanczos method for obtaining eigensolutions of the Schrödinger equation on a grid. J. Comput. Phys. **126**, 315–327 (1996)
Brey, J.J., Casado, J.M., Morillo, M.: Combined effects of additive and multiplicative noise in a Fokker-Planck model. Z. Phys. B—Condens. Matter **66**, 263–269 (1987)
Brinkmann, H.C.: Brownian motion in a field of force and the diffusion theory of chemical reactions. Physica A **22**, 29–34 (1956)
Buet, C., Dellacherie, S.: On the Chang Cooper scheme applied to a linear Fokker Planck equation. Commun. Math. Sci. **8**, 1079–1090 (2010)
Canuto, C., Hussaini, M.Y., Quarteroni, A., Zang, T.A.: Spectral Methods: Fundamentals in Single Domains. Springer, New York (2006b)
Cartling, B.: Kinetics of activated processes from nonstationary solutions of the Fokker-Planck equation for a bistable potential. J. Chem. Phys. **87**, 2638–2648 (1987)
Cassam-Chenaï, P., Liévin, J.: Ab initio calculation of the rotational spectrum of methane vibrational ground state. J. Chem. Phys. **136**, 174309 (2012)
Chandrasekhar, S.: Principles of Stellar Dynamics. Dover, New York (1942)
Chandrasekhar, S.: Brownian motion, dynamical friction, and stellar dynamics. Rev. Mod. Phys. **21**, 383–388 (1949)
Chang, J.C., Cooper, G.: A practical difference scheme for Fokker-Planck equations. J. Comput. Phys. **6**, 1–16 (1970)
Chavanis, P.H.: Relaxation of a test particle in systems with long-range interactions: diffusion coefficient and dynamical friction. Eur. J. Phys. B **52**, 61–82 (2006)
Chen, H., Shizgal, B.D.: A spectral solution of the Sturm-Liouville equation: comparison of classical and nonclassical basis sets. J. Comput. Appl. Math. **136**, 17–35 (2001)
Coffey, W.T., Kalmykov, Y.P., Titov, S.V., Cleary, L.: Quantum effects in the Brownian motion of a particle in a double well potential in the overdamped limit. J. Chem. Phys. **131**, 084101 (2009)
Colbert, D.T., Miller, W.H.: A novel discrete variable representation for quantum-mechanical reactive scattering via the S-Matrix Kohn method. J. Chem. Phys. **96**, 1982–1991 (1992)
Collier, M.R.: Are magnetospheric suprathermal particle distributions (κ functions) inconsistent with maximum entropy considerations. Adv. Space Res. **33**, 2108–2112 (2004)
Comtet, A., Bandrauk, A.D., Campbell, D.K.: Exactness of semiclassical bound-state energies for supersymmetric quantum-mechanics. Phys. Lett. B **150**, 159–162 (1985)
Cooper, F., Ginocchio, J.N., Khare, A.: Relationship between supersymmetry and solvable potentials. Phys. Rev. D **36**, 2458–2473 (1987)

Cooper, F., Khare, A., Sukhatme, U.: Supersymmetry and quantum mechanics. Phys. Rep. **251**, 267–385 (1995)
Corngold, N.: Kinetic equation for a weakly coupled test particle. II. Approach to equilibrium. Phys. Rev. A **24**, 656–666 (1981)
Crew, G.B., Chang, T.S.: Asymptotic theory of ion conic distributions. Phys. Fluids **28**, 2382–2394 (1985)
Cukier, R.I., Lakatos-Lindenberg, K., Shuler, K.E.: Orthogonal polynomial solutions of the Fokker-Planck equation. J. Stat. Phys. **9**, 137–144 (1973)
Dawes, R., Carrington Jr, T.: A multidimensional discrete variable representation basis obtained by simultaneous diagonalization. J. Chem. Phys. **121**, 726–736 (2004)
Dawes, R., Carrington, T.: How to choose one-dimensional basis functions so that a very efficient multidimensional basis may be extracted from a direct product of the one-dimensional functions: energy levels of coupled systems with as many as 16 coordinates. J. Chem. Phys. **122**, 134101 (2005)
Dekker, H., van Kampen, N.G.: Eigenvalues of a diffusion process with a critical point. Phys. Lett. A **73**, 374–376 (1979)
Demeio, L., Shizgal, B.: Time dependent nucleation. II. A semiclassical approach. J. Chem. Phys. **98**, 5713–5719 (1993a)
Demeio, L., Shizgal, B.: A uniform Wentzel-Kramers-Brillouin approach to electron transport in molecular gases. J. Chem. Phys. **99**, 7638–7651 (1993b)
Derevianko, A., Luc-Koenig, E., Masnou-Seeuws, F.: Application of B-splines in determining the eigenspectrum of diatomic molecules: robust numerical description of Halo-state and Feshbach molecules. Can. J. Phys. **87**, 67–74 (2009)
Deville, M.O., Fisher, P.F., Mund, E.H.: High Order Methods for Incompressible Fluid Flow. Cambridge University Press, Cambridge (2002)
Dickinson, A.S., Certain, P.R.: Calculation of matrix elements for one-dimensional quantum-mechanical problems. J. Chem. Phys. **49**, 4209–4211 (1968)
Drozdov, A.N.: Two novel approaches to the Kramers rate problem in the spatial diffusion regime. J. Chem. Phys. **111**, 6481–6491 (1999)
Drozdov, A.N., Tucker, S.C.: An improved reactive flux method for evaluation of rate constants in dissipative systems. J. Chem. Phys. **115**, 9675–9684 (2001)
Dunkel, J., Hänggi, P.: Relativistic Brownian motion. Phys. Rep. **471**, 1–73 (2009)
Dutt, R., Khare, A., Sukhatme, U.P.: Supersymmetry, shape invariance and exactly solvable potentials. Am. J. Phys. **56**, 163–168 (1988)
Dyatko, N.A.: Negative electron conductivity in gases and semiconductors. J. Phys.: Conf. Ser. **71**, 012005 (2007)
Dyatko, N.A., Loffhagen, D., Napartovich, A.P., Winkler, R.: Negative electron mobility in attachment dominated plasmas. Plasma Chem. Plasma Proc. **21**, 421–439 (2001)
Dziekan, P., Lemarchand, A., Nowakowski, B.: Master equation for a bistable chemical system with perturbed particle velocity distribution function. Phys. Rev. **85**, 021128 (2012)
Echave, J., Clary, D.C.: Potential optimized discrete variable representation. Chem. Phys. Lett. **190**, 225–230 (1992)
Echim, M.M., Lemaire, J., Lie-Svendsen, O.: A review on solar wind modeling: kinetic and fluid aspects. Surv. Geophys. **32**, 1–70 (2011)
Einstein, A.: Zur theorie der brownschen bewegung. Ann. Phys. **19**, 371–381 (1906)
Feit, M.D., Fleck Jr, J.A., Steiger, A.: Solution of the Schrödinger equation by a spectral method. J. Comput. Phys. **47**, 412–433 (1982)
Feizi, H., Rajabi, A.A., Shojaei, M.R.: Supersymmetric solution of the Schrödinger equation for the Woods-Saxon potential using the Pekeris approximation. Acta Phys. Pol. B **42**, 2143–2152 (2011)
Felderhof, B.U.: Diffusion in a bistable potential. Phys. A **387**, 5017–5023 (2008)
Fokker, A.D.: Die mittlere energie rotierender elektrischer dipole im strahlungsfeld. Ann. Phys. **348**, 810–820 (1914)

Fornberg, B.: A Practical Guide to Pseudospectral Methods. Cambridge University Press, Cambridge (1996)
Francisco, J.F.: Internal rotational barriers of ClOOCl. J. Chem. Phys. **103**, 8921–8923 (1995)
Frank, T.D.: Kramers-Moyal expansion for stochastic differential equations with single and multiple delays: applications to financial physics and neurophysics. Phys. Lett. A **360**, 552–562 (2007)
Fricke, S.H., Balantekin, A.B., Hatchell, P.J., Uzer, T.: Uniform semiclassical approximation to supersymmetric quantum mechanics. Phys. Rev. A **37**, 2797–2804 (1988)
Friesner, R.A., Bentley, J.A., Menou, M., Leforestier, C.: Adiabatic pseudospectral methods for multidimensional vibrational potentials. J. Chem. Phys. **99**, 324–335 (1993)
Gardiner, C.W.: Handbook of Stochastic Methods. Springer, Berlin (2003)
Garrity, D.K., Skinner, J.L.: Effect of potential shape on isomerization rate constants for the BGK model. Chem. Phys. Lett. **95**, 46–51 (1983)
Gary, S.P.: Theory of Space Plasma Microinstabilities. Cambrigde University Press, Cambridge (1993)
Gillespie, G.T.: Approximating the master equation by Fokker-Planck type equations for single variable chemical systems. J. Chem. Phys. **72**, 5363–5370 (1980)
Gillespie, G.T.: Exact numerical simulation of the Ornstein-Uhlenbeck process and its integral. Phys. Rev. E **54**, 2084–2091 (1996)
Gitterman, M.: Simple treatment of correlated multiplicative and additive noises. J. Phys. A: Math. Gen. **32**, L293–L297 (1999)
Gomes, P.C., Pacios, L.F.: The torsional barrier of ClOOCl. J. Phys. Chem. **100**, 8731–8736 (1996)
Gomez-Ullate, D., Kamran, N., Milson, R.: An extended class of orthogonal polynomials defined by a Sturm-Liouville problem. J. Math. Anal. Appl. **359**, 352–376 (2009)
Gottlieb, D., Orszag, S.: Numerical Analysis of Spectral Methods: Theory and Applications. SIAM, Philadelphia (1977)
Guantes, R., Farantos, S.C.: High order finite difference algorithms for solving the Schrödinger equation. J. Chem. Phys. **111**, 10827–10835 (1999)
Gunther, L., Weaver, D.L.: Monte Carlo simulation of Brownian motion with viscous drag. Am. J. Phys. **46**, 543–545 (1978)
Hagelaar, G.J.M., Pitchford, L.C.: Solving the Boltzmann equation to obtain electron transport coefficients and rate coefficients for fluid models. Plasma Sources Sci. Technol. **14**, 722–733 (2005)
Hamilton, I.P., Light, J.C.: On distributed Gaussian bases for simple model multidimensional vibrational problems. J. Chem. Phys **84**, 306–317 (1986)
Hänggi, P., Talkner, P., Borkovec, M.: Reaction rate theory: fifty years after Kramers. Rev. Mod. Phys. **62**, 251–341 (1990)
Harris, D.O., Engerholm, G.G., Gwinn, W.D.: Calculation of matrix elements for one-dimensional quantum-mechanical problems and the application to anharmonic oscillators. J. Chem. Phys. **43**, 1515–1517 (1965)
Hasegawa, A., Mima, K., Duong-van, M.: Plasma distribution function in a superthermal radiation field. Phys. Rev. Lett. **54**, 2608–2610 (1985)
Henon, M., Heiles, C.: The applicability of the third integral of motion: some numerical experiments. Astron. J. **69**, 73–79 (1964)
Hinton, F.L.: Collisional transport in plasma. In: Galeev, A.A., Sagdeev, R.Z. (eds.) Handbook of Physics, Basic Plasma Physics, pp. 147–197. Elsevier, The Netherlands (1983)
Hoare, M.R.: The linear gas. Adv. Chem. Phys. **20**, 135–214 (1971)
Hoare, M.R., Kaplinsky, C.H.: Linear hard sphere gas: variational eigenvalue spectrum of the energy kernel. J. Chem. Phys. **52**, 3336–3353 (1970)
Hoffman, D.K., Wei, G.W., Zhang, D.S., Kouri, D.J.: Interpolating distributed approximating functionals. Phys. Rev. E **57**, 6152–6160 (1998)
Johnson, B.R.: New numerical methods applied to solving the one dimensional eigenvalue problem. J. Chem. Phys. **67**, 4086–4093 (1977)

Kallush, S., Kosloff, R.: Improved methods for mapped grids: applied to highly excited vibrational states of diatomic molecules. Chem. Phys. Lett. **433**, 221–227 (2006)
Karney, C.F.F.: Fokker-Planck and quasi-linear codes. Comput. Phys. Rep. **4**, 183–244 (1986)
Knessl, C., Mangel, M., Matkowsky, B.J., Schuss, Z., Tier, C.: Solution of Kramers-Moyal equations for problems in chemical physics. J. Chem. Phys. **81**, 1285–1293 (1984)
Knierim, K.D., Waldman, M., Mason, E.A.: Moment theory of electron thermalization in gases. J. Chem. Phys. **77**, 943–950 (1982)
Kokoouline, V., Dulieu, O., Kosloff, R., Masnou-Seeuws, F.: Mapped Fourier methods for long-range molecules: application to perturbations in the $Rb_2(0_u^+)$ photoassociation spectrum. J. Chem. Phys. **110**, 9865–9876 (1999)
Koput, J., Carter, S., Handy, N.C.: Ab initio prediction of the vibrational-rotational energy levels of hydrogen peroxide and its isotopomers. J. Chem. Phys. **115**, 8345–8350 (2001)
Koura, K.: Nonequilibrium electron velocity distribution and temperature in thermalization of low energy electrons in molecular hydrogen. J. Chem. Phys. **79**, 3367–3372 (1983)
Kowari, K., Demeio, L., Shizgal, B.: Electron degradation and thermalization in CH_4 gas. J. Chem. Phys. **97**, 2061–2074 (1992)
Kowari, K., Shizgal, B.: On the existence of a steady electron distribution for systems with electron attachment: Ar-CCl_4 mixtures. Chem. Phys. Lett. **260**, 365–370 (1996)
Kowari, K.-I., Leung, K., Shizgal, B.D.: The coupling of electron thermalization and electron attachment in CCl_4/Ar and CCl_4/Ne mixtures. J. Chem. Phys. **108**, 1587–1600 (1998)
Kramers, H.A.: Brownian motion in a field of force and the diffusion model of chemical reactions. Physica **7**, 284–304 (1940)
Kuczka, J., Hänggi, P., Gadmski, A.: Non-Markovian process driven quadratic noise: Kramers-Moyal expansion and Fokker-Planck modeling. Phys. Rev. E **51**, 2933–2938 (1995)
Kumar, K., Skullerud, H.R., Robson, R.E.: Kinetic theory of charged particle swarms in neutral gases. Aust. J. Phys. **33**, 343–448 (1980)
Kuščer, I., Williams, M.M.R.: Relaxation constants of a uniform hard sphere gas. Phys. Fluids **10**, 1922–1927 (1967)
Kustova, E.V., Giordano, D.: Cross-coupling effects in chemically non-equilibrium viscous compressible flows. Chem. Phys. **379**, 83–91 (2011)
Landau, D.P., Binder, K.: A Guide to Monte Carlo Simulations in Statistical Physics, 3rd edn. Cambridge University Press, Cambridge (2009)
Larsen, E.W., Livermore, C.D., Pomraning, G.C., Sanderson, J.G.: Discretization methods for one-dimensional Fokker-Planck operators. J. Comput. Phys. **61**, 359–390 (1985)
Larson, R.S., Kostin, M.D.: Kramers's theory of chemical kinetics: eigenvalue and eigenfunction analysis. J. Chem. Phys. **69**, 4821–4829 (1978)
Lauvergnat, D., Nauts, A.: Quantum dynamics with sparse grids: a combination of Smolyak scheme and cubature. Application to methanol in full dimensionality. Spectrochim. Acta, A **119**, 18–25 (2014)
Lax, M.: Classical noise IV: Langevin method. Rev. Mod. Phys. **38**, 541–566 (1966)
Layton, E.G.: The Fourier-grid formalism: philosophy and application to scattering problems using R-matrix theory. J. Phys. B: At. Mol. Opt. Phys. **36**, 2501–2522 (1993)
Le, H.M., Huynh, S., Raff, L.: Molecular dissociation of hydrogen peroxide (HOOH) on a neural network ab initio potential surface with a new configuration sampling method involving gradient fitting. J. Chem. Phys. **131**, 014107 (2009)
Leblanc, F., Hubert, D.: A generalized model for the proton expansion in astrophysical winds. I. The velocity distribution function representation. Astrophys. J. **483**, 464–474 (1997)
Lemou, M., Chavanis, P.H.: Escape of stars from gravitational clusters in the Chandrasekhar model. Phys. A **389**, 1021–1040 (2010)
Leubner, M.P., Vörös, Z.: A nonextensive entropy approach to solar wind intermittency. Astrophys. J. **618**, 547–555 (2005)

Leung, K., Shizgal, B.D., Chen, H.: The quadrature discretization method QDM in comparison with other numerical methods of solution of the Fokker-Planck equation for electron thermalization. J. Math. Chem. **24**, 291–319 (1998)

Lie-Svendsen, O., Rees, M.H.: An improved kinetic model for the polar outflow of a minor ion. J. Geophys. Res. **101**, 2415–2433 (1996)

Light, J.C., Hamilton, I.P., Lill, J.V.: Generalized discrete variable approximation in quantum mechanics. J. Chem. Phys. **82**, 1400–1409 (1985)

Lightman, A.P., Shapiro, S.L.: The dynamical evolution of globular clusters. Rev. Mod. Phys. **50**, 437–481 (1978)

Lin, S.Y., Guo, H.: Exact quantum mechanical calculations of rovibrational energy levels of hydrogen peroxide (HOOH). J. Chem. Phys. **119**, 5867–5873 (2003)

Lin, S.R., Robson, R.E., Mason, E.A.: Moment theory of electron drift and diffusion in neutral gases in an electrostatic field. J. Chem. Phys. **71**, 3483–3498 (1979)

Lindenfeld, M.J., Shizgal, B.: The Milne problem: a study of the mass dependence. Phys. Rev. **A27**, 1657–1670 (1983)

Littlejohn, R.G., Cargo, M., Carrington Jr, T., Mitchell, K.A., Poirier, B.: A general framework for discrete variable representation basis sets. J. Chem. Phys. **116**, 8691–8703 (2002)

Livadiotis, G., McComas, D.J.: Beyond Kappa distributions: exploiting Tsallis statistical mechanics in space plasmas. J. Geophys. Res. **114**, A11105 (2009)

Lo, J.Q.-W., Shizgal, B.D.: Spectral convergence of the quadrature discretization method in the solution of the Schrödinger and Fokker-Planck equations: comparison with Sinc methods. J. Chem. Phys. **125**, 194108 (2006)

Lo, J.Q.-W., Shizgal, B.D.: An efficient mapped pseudospectral method for weakly bound states: vibrational states of He_2, Ne_2, Ar_2 and Cs_2. J. Phys. B: At. Mol. Opt. Phys. **41**, 185103 (2008a)

Lo, J.Q.-W., Shizgal, B.D.: Pseudospectral methods of solution of the Schrödinger equation. J. Math. Chem. **44**, 787–801 (2008b)

Lutsko, J.F., Boon, J.P.: Questioning the validity of non-extensive thermodynamics for classical Hamiltonian systems. EPL **95**, 20006 (2011)

Lynch, V.A., Mielke, S.L., Truhlar, D.G.: Accurate vibrational-rotational partition functions and standard-state free energy values for H_2O_2 from Monte Carlo path-integral calculations. J. Chem. Phys. **121**, 5148–5162 (2004)

Ma, C.-Y., Summers, D.: Formation of power-law energy spectra in space plasmas by stochastic acceleration due to Whistler-mode waves. Geophys. Res. Lett. **26**, 1121–1124 (1999)

Magnus, A.P., Pierrard, V.: Formulas for the recurrence coefficients of orthogonal polynomials related to Lorentzian-like weights. J. Comput. Appl. Math. **219**, 431–440 (2008)

Marechal, E., Moreau, M.: On the microscopic kinetic theory of a chemical reaction in the limit of high collision frequency. Mol. Phys. **51**, 133–140 (1984)

Marsch, E.: Kinetic physics of the solar corona and solar wind. Living Rev. Sol. Phys. **3**, 1–100 (2006)

Marston, C.C., Balint-Kurti, G.G.: The Fourier grid Hamiltonian method for bound state eigenvalues and eigenfunctions. J. Chem. Phys. **91**, 3571–3576 (1989)

Mazziotti, D.A.: Spectral difference methods for solving differential equations. Chem. Phys. Lett. **299**, 473–480 (1999)

McMahon, D.R.A., Shizgal, B.: Hot-electron zero-field mobility and diffusion in rare-gas moderators. Phys. Rev. A **31**, 1894–1905 (1985)

Meshkov, V.V., Stolyarov, A.V., Le Roy, R.J.: Adaptive analytical mapping procedure for efficiently solving the radial Schrödinger equation. Phys. Rev. A **78**, 052510 (2008)

Meyer-Vernet, N.: Large scale structure of planetary environments: the importance of not being Maxwellian. Planet. Space Sci. **49**, 247–260 (2001)

Mielke, S.L., Chakraborty, A., Truhlar, D.G.: Vibrational configuration interaction using a tiered multimode scheme and tests of approximate treatments of vibrational angular momentum coupling: a case study for Methane. J. Phys. Chem. A **117**, 7327–7343 (2013)

Miller, S.C., Good Jr, R.H.: A WKB-type approximation to the Schrödinger equation. Phys. Rev. **91**, 174–179 (1953)
Mintzer, D.: Generalized orthogonal polynomial solutions of the Boltzmann equation. Phys. Fluids **8**, 1076–1090 (1965)
Mitchner, M., Kruger, C.H.J.: Partially Ionized Gases. Wiley, New York (1973)
Montgomery, J.A., Chandler, D., Berne, B.J.: Trajectory analysis of a kinetic theory for isomerization dynamics in condensed phases. J. Chem. Phys. **70**, 4056–4066 (1979)
Morse, P.M.: Diatomic molecules according to the wave mechanics II. Vibrational levels. Phys. Rev. **34**, 57–64 (1929)
Mozumder, A.: Electron thermalization in gases. III epithermal electron scavenging in rare gases. J. Chem. Phys. **74**, 6911–6921 (1981)
Mozumder, A.: Fundamentals of Radiation Chemistry. Academic Press, London (1999)
Müller, P.L.G., Hernandez, R., Benito, R.M., Borondo, F.: Detailed study of the direct numerical observation of the Kramers turnover in the LiNC⇌LiCN isomerization rate. J. Chem. Phys. **137**, 204301 (2012)
Nauenberg, M.: Critique of q-entropy for thermal statistics. Phys. Rev. E **67**, 036114 (2003)
Nicholson, D.R.: Introduction to Plasma Theory. Wiley, New York (1983)
Nicolis, C.: Stochastic aspects of climatic transitions—response to a periodic forcing. Tellus **34**, 1–9 (1982)
Nicolis, C., Nicolis, G.: Stochastic aspects of climatic transitions—additive fluctuations. Tellus **33**, 225–234 (1981)
Noid, D.W., Marcus, R.A.: Semiclassical calculation of bound states in a multidimensional system for nearly 1:1 degenerate systems. J. Chem. Phys. **67**, 559–567 (1977)
ONeil, S.V., Reinhardt, W.P.: Photoionization of molecular hydrogen. J. Chem. Phys. **69**, 2126–2142 (1978)
Park, B.T., Petrosian, V.: Fokker-Planck equations of stochastic acceleration: a study of numerical methods. Astrophys. J. Suppl. Ser. **103**, 225–267 (1996)
Parker, E.N.: Dynamical theory of the solar wind. Space Sci. Rev. **4**, 666–708 (1965)
Parrish, R.M., Hohenstein, E.G., Martnez, T.J., Sherrill, C.D.: Discrete variable representation in electronic structure theory: quadrature grids for least-squares tensor hypercontraction. J. Chem. Phys. **138**, 194107 (2013)
Pasquetti, R., Rapetti, F.: Spectral element methods on triangles and quadrilaterals: comparisons and applications. J. Comput. Phys. **198**, 349–362 (2004)
Pastor, R.W., Karplus, M.: Inertial effects in butane stochastic dynamics. J. Chem. Phys. **91**, 211–218 (1989)
Paul, W., Baschnagel, J.: Stochastic Processes; From Physics to Finance, 2nd edn. Springer, Berlin (2013)
Petrović, Z.L., Dujko, S., Marić, D., Malović, G., Nikitović, Ž., Šašič, O., Jovanović, J., Stojanović, V., Radmilović-Radenović, M.: Measurement and interpretation of swarm parameters and their application in plasma modelling. J. Phys. D: Appl. Phys. **42**, 194002 (2009)
Pierrard, V., Lemaire, J.: A collisional model of the polar wind. J. Geophys. Res. **103**, 11701–11709 (1998)
Pierrard, V., Lazar, V.: Kappa distributions; theory and applications in space plasmas. Sol. Phys. **267**, 153–174 (2010)
Pierrard, V., Lamy, H., Lemaire, J.: Exospheric distributions of minor ions in the solar wind. J. Geophys. Res. **109**, A02118 (2004)
Pitchford, L.C., Phelps, A.V.: Comparative calculations of electron-swarm properties in N_2 at moderate E/N values. Phys. Rev. A **25**, 540–554 (1982)
Planck, M.: Ueber einen satz der statistichen dynamik und eine erweiterung in der quantumtheorie. Sitzber. Preuß. Akad. Wiss. pp. 324–341 (1917)
Pollak, E., Talkner, P.: Reaction rate theory: what it was, where is it today, and where is it going? Chaos **15**, 026116 (2005)

Pollak, E., Ianconescu, R.: Finite barrier corrections to the PGH solution of Kramers turnover theory. J. Chem. Phys. **140**, 154108 (2014)
Pollak, E., Grabert, H., Hänggi, P.: Theory of activated rate processes for arbitrary frequency dependent friction: solution of the turnover problem. J. Chem. Phys. **91**, 4073–4087 (1989)
Pope, S.B.: Turbulent Flows. Cambridge University Press, Cambridge (2000)
Pryce, J.D.: Numerical Solution of Sturm-Liouville Problems. Oxford University Press, Oxford (1993)
Reif, F.: Fundamentals of Statistical and Thermal Physics. Waveland Press, Illinois (2008)
Reinhardt, W.P.: L^2 discretization of atomic and molecular electronic continua: moment, quadrature and J-matrix techniques. Comput. Phys. Commun. **17**, 1–21 (1979)
Risken, H.: The Fokker-Planck Equation: Methods of Solution and Applications, 2nd edn. Springer, Berlin (1996)
Risken, H., Voigtlaender, K.: Solutions of the Fokker-Planck equation describing thermalization of neutrons in a heavy gas moderator. Z. Phys. B—Condens. Matter **54**, 253–262 (1984)
Risken, H., Till, F.: The Fokker-Planck equation: Methods of solution and applications, 2nd edn. Springer, Berlin (1996)
Robson, R.E.: Introductory Transport Theory for Charges Particles in Gases. World Scientific, Singapore (2006)
Robson, R.E., Ness, K.F.: Velocity distribution and transport coefficients of electron swarms in gases: spherical-harmonic decomposition of Boltzmann's equation. Phys. Rev. A **33**, 2068–2077 (1986)
Rosenbluth, M., Macdonald, F.W.M., Judd, D.L.: Fokker-Planck equation for an inverse-square force. Phys. Rev. **107**, 1–6 (1957)
Ross, J., Mazur, P.: Some deductions from a formal statistical mechanical theory of chemical kinetics. J. Chem. Phys. **35**, 19–28 (1961)
Ryckaert, J.-P., Bellemans, A.: Molecule dynamics of liquid alkanes. Faraday Discuss. Chem. Soc. **66**, 95–106 (1978)
Sakai, Y.: Quasifree electron transport under electric field in nonpolar simple-structured condensed matters. J. Phys. D: Appl. Phys. **40**, R441–R452 (2007)
Schindler, M., Talkner, P., Hänggi, P.: Escape rates in periodically driven Markov processes. Physica A **351**, 40–50 (2005)
Schulz, M., Lanzerotti, M.L.: Particle Diffusion in the Radiation Belts. Springer, Berlin (1974)
Schwartz, C.: High-accuracy approximation techniques for analytic functions. J. Math. Phys. **26**, 411–415 (1985)
Scudder, J.D.: Ion and electron suprethermal tail strengths in the transition region for the velocity filtration model of the corona. Astrophys. J. **427**, 446–452 (1994)
Shematovich, V.I., Bisikalo, D.V., Gérard, J.-C., Cox, C., Bougher, S.W.: Monte Carlo model of electron transport for the calculation of mars dayglow emissions. J. Geophys. Res. **113**, E02011 (2008)
Shizgal, B.: Eigenvalues of the Lorentz Fokker-Planck equation. J. Chem. Phys. **70**, 1948–1951 (1979)
Shizgal, B.: The coupling of electron thermalisation and electron attachment; SF_6 and $CC1_4$ in rare-gas moderators. J. Phys. B: At. Mol. Opt. Phys. **21**, 1699–1715 (1988)
Shizgal, B.: Negative differential conductivity of electrons in He-Xe and He-Kr mixtures. Chem. Phys. **147**, 271–279 (1990)
Shizgal, B.: Relaxation in ionized gases: the role of the spectrum of the collision operator. In: Beylich, A.E. (ed.) Proceedings of the 17th International Symposium on Rarefied Gas Dynamics, pp. 22–29. VCH Verlagsgesellschaft GmbH, Berlin (1991)
Shizgal, B.: Spectral theory and the approach to equilibrium in a plasma. Trans. Theory Stat. Phys. **21**, 645–665 (1992)
Shizgal, B.D.: The quadrature discretization method (QDM) in the calculation of the rotational-vibrational transitions in rare gas dimers. J. Mol. Struct. (Theochem) **391**, 131–139 (1997)

Shizgal, B.D.: Coulomb collisional processes in space plasmas; relaxation of suprathermal particle distributions. Planet. Space Sci. **52**, 923–933 (2004)
Shizgal, B.D.: Suprathermal particle distributions in space physics: kappa distributions and entropy. Astrophys. Space Sci. **312**, 227–237 (2007)
Shizgal, B., Karplus, M.: Nonequilibrium contributions to the rate of reaction. I. Perturbation of the velocity distribution function. J. Chem. Phys. **52**, 4262–4278 (1970)
Shizgal, B., Fitzpatrick, J.M.: Matrix elements of the linear Boltzmann collision operator for systems of two components at different temperatures. Chem. Phys. **6**, 54–65 (1974)
Shizgal, B., McMahon, D.R.A.: Electric field dependence of transient electron transport properties in rare gas moderators. Phys. Rev. A **32**, 3669–3680 (1985)
Shizgal, B., Blackmore, R.: A collisional kinetic theory of a plane parallel evaporating planetary atmosphere. Planet. Space Sci. **34**, 279–291 (1986)
Shizgal, B., Ness, K.: Thermalisation and annihilation of positrons in helium and neon. J. Phys. B: At. Mol. Phys. **20**, 847–865 (1987)
Shizgal, B., Barrett, J.C.: Time dependent nucleation. J. Chem. Phys. **91**, 6506–6518 (1989)
Shizgal, B.D., Chen, H.: The quadrature discretization method (QDM) in the solution of the Schrödinger equation with nonclassical basis functions. J. Chem. Phys. **104**, 4137–4150 (1996)
Shizgal, B.D., Napier, D.G.: Nonequilibrium effects in reactive systems: the effect of reaction products and the validity of the Chapman-Enskog method. Physica A **223**, 50–86 (1996)
Shizgal, B.D., Chen, H.: The quadrature discretization method in the solution of the Fokker-Planck equation with nonclassical basis functions. J. Chem. Phys. **107**, 8051–8063 (1997)
Shizgal, B., McMahon, D.R.A., Viehland, L.A.: Thermalization of electrons in gases. Radiat. Phys. Chem. **34**, 35–50 (1989)
Shizgal, B., Weinert, U., Blackmore, R.: The QDM in the solution of the Kramers equation for symmetrical potentials. In: Beylich, A.E. (ed.) Proceedings of the 17th International Symposium on Rarefied Gas Dynamics, pp. 85–92. Wiley, Weinheim (1991)
Shore, B.W.: Solving the radial Schrödinger equation by using cubic-spline basis functions. J. Chem. Phys. **58**, 3855–3866 (1973)
Shoub, E.C.: Failure of the Fokker-Planck approximation to the Boltzmann integral for 1/r potentials. Phys. Fluids **30**, 1340–1352 (1987)
Skinner, J,l, Wolynes, P.G.: General kinetic models of activated processes in condensed phases. J. Chem. Phys. **71**, 4913–4927 (1980)
Solomon, S.C.: Auroral particle transport using Monte Carlo and hybrid methods. J. Geophys. Res. **106**, 107–116 (2001)
Sospedra-Alfonso, R., Shizgal, B.D.: Kullback-Leibler entropy in the electron distribution shape relaxation for electron-atom thermalization. Phys. Rev. E **84**, 041202 (2011)
Sospedra-Alfonso, R., Shizgal, B.D.: Energy and shape relaxation in binary atomic systems with realistic quantum cross sections. J. Chem. Phys. **139**, 044113 (2013)
Spendier, K., Sugaya, S., Kenkre, V.M.: Reaction-diffusion theory in the presence of an attractive harmonic potential. Phys. Rev. E **88**, 062142 (2013)
Spitzer, L.J.: Physics of Fully Ionized Gases. Interscience, New York (1962)
Spitzer, L.J.: Physical Processes in the Interstellar Medium. Wiley, New York (1998)
Spitzer, L.J., Härm, R.: Evaporation of stars from open clusters. Astrophys. J. **127**, 544–550 (1958)
Stamnes, K.: Analytic approach to auroral electron transport and energy degradation. Planet. Space Sci. **28**, 427–441 (1980)
Stix, T.H.: Waves in Plasmas. Springer, New York (1992)
Szabo, A., Schulten, K., Schulten, Z.: First passage time approach to diffusion controlled reactions. J. Chem. Phys. **72**, 4350–4357 (1980)
Tang, K.T., Toennies, J.P.: The van der Waals potentials between all the rare gas atoms from He to Rn. J. Chem. Phys. **118**, 4976–4983 (2003)
Travis, K.P., Searles, D.J.: Effect of solvation and confinement on the trans-gauche isomerization reaction in n-butane. J. Chem. Phys. **125**, 164501 (2006)

Treumann, R.A., Jaroschek, C.H., Scholer, M.: Stationary plasma states far from equilibrium. Phys. Plasmas **11**, 1317–1325 (2004)
Trunec, D., Španěl, P., Smith, D.: The influence of electron-electron collisions on electron thermalization in He and Ar afterglow plasmas. Chem. Phys. Lett. **372**, 728–732 (2003)
Tsallis, C.: Non-extensive thermostatics: brief review and comments. Phys. A **221**, 277–290 (1995)
Tsallis, C.: Comment on Critique of q-entropy for thermal statistics. Phys. Rev. E **69**, 038101 (2004)
Uhlenbeck, G.E., Ornstein, L.S.: On the theory of the Brownian motion. Phys. Rev. **36**, 823–841 (1930)
van Kampen, N.G.: Stochastic Processes in Physics and Chemistry, 3rd edn. North Holland, Amsterdam (2007)
Viehland, L.A., Ranganathan, B., Shizgal, S.: Transient microwave conductivity of electrons in helium and argon. J. Chem. Phys. **88**, 362–370 (1988)
Vocks, C.: A kinetic model for ions in the solar corona including wave-particle interactions and Coulomb collisions. Astrophys. J. **568**, 1017–1029 (2002)
Voigtlaender, K., Risken, H.: Solutions of the Fokker-Planck equation for a double-well potential in terms of continued fractions. J. Stat. Phys. **40**, 397–429 (1985)
Wei, H.: Ghost levels and near-variational forms of the discrete variable representation: application to H_2O. J. Chem. Phys. **106**, 6885–6900 (1997)
Wei, G.W.: Discrete singular convolution for the solution of the Fokker Planck equation. J. Chem. Phys. **110**, 8930–8942 (1999)
Wei, G.W.: Solving quantum eigenvalue problems by discrete singular convolution. J. Phys. B: At. Mol. Opt. Phys. **33**, 343–352 (2000)
Wei, G.W., Zhang, D.S., Kouri, D.J., Hoffman, D.K.: Lagrange distributed approximating functionals. Phys. Rev. Lett. **79**, 775–779 (1997)
Weideman, W.A.C.: Spectral methods based on non-classical polynomials. In: Gautschi, G., Golub, G.H., Opfer, G. (eds.) Approximations and Computation of Orthogonal Polynomials, pp. 239–251. birkhauser, Basel (1999)
White, R.D., Dujko, S., Robson, R.E., Petrović, Z.L., McEachran, R.P.: Non-equilibrium transport of positron and electron swarms in gases and liquids. Plasma Sources Sci. Technol. **19**, 034001 (2010)
White, R.D., Robson, R.E.: Multiterm solution of a generalized Boltzmann kinetic equation for electron and positron transport in structured and soft condensed matter. Phys. Rev. E **84**, 031125 (2011)
Wigner, E.P.: A solution of Boltzmann's equation for monoenergetic neutrons in an infinite medium. Technical Report AECD-3125, U.S. Atomic Energy Commission (1943)
Wigner, E.P., Wilkins Jr, J.E.: Effect of temperature of the moderator on the velocity distribution of neutrons with numerical calculations for H as moderator. Technical Report AECD-2275, U.S. Atomic Energy Commission (1944)
Wilkinson, M., Pumir, A.: Spherical Ornstein-Uhlenbeck process. J. Stat. Phys. **145**, 113–142 (2011)
Willner, K., Dulieu, O., Masnou-Seeuws, F.: Mapped grid methods for long-range molecules and cold collisions. J. Chem. Phys. **120**, 548–561 (2004)
Wind, H.: Electron energy for H_2^+ in the ground state. J. Chem. Phys. **42**, 2371–2373 (1965)
Yang, W., Peet, A.C.: The collocation method for bound solutions of the Schrödinger equation. Chem. Phys. Lett. **153**, 98–104 (1988)